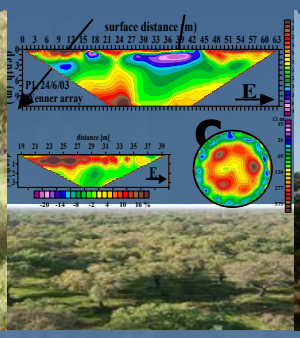

European Commission
Fifth Framework Programme
Energy, Environment and Sustainable Development

WORKSHOP

Water Use of Woody Crops

techniques, issues, modelling and applications on water management

In the frame of the project:

WATERUSE – Evaluation of alternative techniques for determination of water budget components in water – limited, heterogeneous land-use systems

(*Energy, Environment and Sustainable Development Programme*, EVK1-CT-2000-00079 WATERUSE, EU).

www.isa.utl.pt/wateruse

BOOK of ABSTRACTS/PAPERS

20th and 21st
May 2004
Ílhavo, Portugal

Organization:

Ministério da Agricultura, Desenvolvimento Rural e Pescas
IDRHa Instituto de Desenvolvimento Rural e Hidráulica
Instituto Superior de Agronomia
Technical University of Lisbon, Portugal

European Commission

Fifth Framework Programme

Energy, Environment and Sustainable Development

WATERUSE Project

Evaluation of alternative techniques for determination of water budget components in water – limited, heterogeneous land-use systems

Water Use of Woody Crops: techniques, issues, modelling and applications on water management

EXTENDED ABSTRACTS AND PAPERS

Speakers

(in bold: speakers from participant institutions of WATERUSE project)

- **Andrea Pitacco** - Università degli studi di Padova - UPad (I)
- **Carlos Arruda** - Instituto Superior de Agronomia, T University of Lisbon (P),
- **Carlos Pais** - Inst. de Desenvolvimento Rural e Hidráulica - IDRHa (P)
- **Guido D'Urso** - Università di Napoli Federico II - UNap (I)
- **Hamlyn G. Jones**, **Nicole Archer** - University of Dundee - UDun (UK)
- **Isabel Ferreira** - Instituto Superior de Agronomia, T University of Lisbon (P),
- **Isaurindo Oliveira** – Centro Operativo e de Tecnologia do Regadio - COTR (P)
- **Jan Cermak** - Mendel's Univ. of Agric. and Forestry - UMen (CR)
- José Silvestre (INIAP, Ph D Student ISA, P),
- Roland Vogt - Basel University (CH), subcontractor Padova University
- **Said Attia**, **Ulrike Werban** - Albrechts-Univ. zu Kiel - UC-A (DE)
- **Susanne Lorra**, **Andreas Kathage** - GeoHires International Ltd - GHR (DE)
- T. Soares David (collab INIAP-ISA, P),
- **Teresa do Paço**, Instituto Superior de Agronomia, T. University of Lisbon (P).

Instituto Superior de Agronomia – Universidade Técnica de Lisboa (ISA - UTL)
Tapada da Ajuda, 1349-017 Lisboa, PORTUGAL
2004

List of oral contributions

20 th May - Techniques

8:30 - Welcome addresses
Prof. Isabel Ferreira, WATERUSE, Project coordinator, ISA - UTL
Eng. C. Mattamouros Resende, President of IDRHa (Instituto de Desenvolvimento Rural e Hidráulica)
Eng. L. Amorim, Regional Director of DRABL (Agriculture Regional Directorate of Beira Litoral)

Transpiration and evapotranspiration

Chairs: Andrea Pitacco and Carlos Arruda

1 - 9:00 to 9:45 - Introduction - Environmental and physiological control of evapotranspiration (ET) from vegetation - Hamlyn G. Jones

2 - 9:45 to 10:30

a. Sap flow measurements and their scaling up to tree and stand levels - Part A - Jan Cermak (JC) J. Kučera, N. Nadezhdina (NN);

b. Sap flow measurements and their scaling up - Part B - *Granier* method - Isabel Ferreira (IF), T. S. David, J. Silvestre, T. A. Paço, N. Nadezhdina, A. Thomsen, R. M. Silva, A. L. Silva

3 - 11:00 to 11:50

a. Micrometeorological measurement of ET: Part A - Fluxes extra vergine - Roland Vogt (RV) A. Christen, I. Lehner, F. Imbery, A. Pitacco.

b. Micrometeorological measurement of ET: Part B - The role of the canopy in modifying the partitioning of fluxes - Andrea Pitacco (AP), V. Zambetti, R. Vogt

4 - 11:50 to 12:10 - Water stress indicators. Use of sap flow measurements for stress diagnosis - Isabel Ferreira, T. A. Paço, N. Nadezhdina.

12:10 to 12:30 - Questions/ Discussion

Chairs: Guido D' Urso and Carlos Pais

5 - 14:00 to 14:30 - Surface temperature measurement and estimation of evaporation - Hamlyn G. Jones (HGJ) and Nicole Archer (NA)

Soil, roots and water

6 - 14:30 to 15:00 - Soil water measurements - the most usual methods: gravimetric, neutronic, capacitive and time domain reflectometry (TDR) - Carlos Arruda Pacheco (CA)

7 - 15:00 to15:30 - GPR for soil mapping/assessment and roots imaging - Susanne Lorra (SL) and Andreas Kathage (AK)

8 - 15:30 to 16:00 - High resolution hydrogeophysical techniques - Said Attia (SA), Ulrike Werban (UW), R. Meissner, W. Rabbel, A. Ismaeil

Modelling

Chairs: Said Attia and Susanne Lorra

9 - 16:30 to 17:00 - Modelling and simulation of root water uptaking and evapotranspiration for irrigated O*lea europea* - Guido Durso (GD), M. Panico, E. de Marco

10 - 17:00 to 17:20 - Reference ET and crop coefficients: how good is this approach for woody stands? Use of stress coefficients - Isabel Ferreira (IF) and T. A. Paço

11 - 17:20 to 17:50

a. Main biometric parameters and leaf area distribution in an old olive trees and orchard in southern italy - b. Leaf area distribution measurements in solitary growing old trees - J. Čermák, J. Gašpárek, F. de Lorenzi, H.G. Jones.

17:50 to 18:20 - Questions/ Discussion/ Summary

21 st May - Applications on Water Management

Chairs: Hamlyn Jones and Isaurindo Oliveira

12 - 9:00 to 9:30 - General overview on water management - Carlos Pais (CP)
13 - 9:30 to 10:30 - Combination of transpiration & ET techniques
a. Introduction - IF.
b. Application on irrigated peach orchard - Teresa do Paço (TdP), M. I. Ferreira, N. Conceição.
c. Application on vine - José Silvestre (JS) and M. I. Ferreira.
d. Application on kiwi (*Determinação das necessidades de rega em kiwi, na região de Entre-Douro e Minho*) - Rodolfo Silva (RS), M. I. Ferreira, T. A. Paço, A. Veloso, M. Oliveira (also integrated in Project AGRO 288)

14 - 11:00 to 11:40 - Posters session (Chairs: T. S. David and T. A. Paço) - see page 45

15 - 11:40 to 12:30
a. Seasonal trends of transpiration from open *Quercus ilex* stands (*montados*): a comparison between two sites in southern Portugal - Teresa S. David, J. S. David, M. O. Henriques, M. I. Ferreira, S. Cohen.[3], J. S. Pereira.
b. Seasonal changes in water use of evergreen oak woodlands - evapotranspiration and transpiration from a *Quercus suber* stand (*montado*) in the region of Lisbon - M. I. Ferreira and R. M. Silva.
c. Seasonal changes in water use of evergreen oak woodlands - sap flow in roots and stem of *Quercus suber* tree - Nadezhda Nadezhdina, M. I. Ferreira, R. Silva, C. A. Pacheco

Chairs: Jan Cermak and Roland Vogt

16 - 14:00 to 14:30 - Hydrogeophysics of soils and trees - Said A. al Hagrey, Ulrike Werban, R. Meissner, W. Rabbel, A. Ismaeil
17 - 14:30 to 15:00 - Sound tomography for stem investigations providing structural information for stem water/sap flow measurements and analysis - SL/AK
18 - 15:00 to 15:30 - Use of ground airborne and satellite remote sensing for estimating evaporation - NA and H. G. Jones
15:30 to 16:00 - Discussion/ conclusions.
16:30 - 17:00 - Documentary on Techniques and IOP2 (IDRHa)
17:00 - 17:10 - COTR activities - Isaurindo Oliveira

Communications and corresponding Work-packages and Partners

Part WP	1 ISA - UTL	2 IDRHa	3 COTR	4 UDun	5 UMen	6 UC-A	7 UPad	8 GHR	9 UNap
1						**8, 16**			
2	**2b**				**2a,** 2b				
3								**7, 17**	
4	**4**			11	4**, 11**		11		
5				**5, 18**					
7	**13a, b, c, d, 15a, b,** c				**15c**		**3a, 3b**		
8	**10**			1					**9**
9		**19**	**20**						
General	**6**	**12**		**1**					

Note: In bold, first author

Work Packages

WP1 - Development of integrated high-resolution geophysical and hydrological techniques for monitoring water content and water flow in soils
WP2 - Innovative aspects of sap flow measurements by HFD-method
WP3 - Improvements of non destructive techniques (NDT) for analysing stem and root zone structure and water content
WP4 - Integrated whole tree studies: functional and architectural relationships
WP5 - Scaling up of infra-red thermography for estimation of evapotranspiration
WP6 – Establishment of integrated multidisciplinary field sites in Portugal and Italy
WP7 - Use of integrated multidisciplinary field trials to study/describe partitioning of water fluxes in heterogeneous agricultural and semi-natural land use systems
WP8 - Development of a framework for the modelling of water fluxes in heterogeneous landscapes
WP9 - Transfer technology to users and preparation of reports and publications

ABSTRACTS
of oral presentations

1

INTRODUCTION: ENVIRONMENTAL AND PHYSIOLOGICAL CONTROL OF EVAPOTRANSPIRATION (ET) FROM VEGETATION

Hamlyn JONES

Plant Research Group,University of Dundee at SCRI, Invergowrie, Dundee DD2 5DA, Scotland, UK
h.g.jones@dundee.ac.uk

ABSTRACT

This introductory paper will set the scene for the meeting by introducing some of the basic principles underlying evaporation from vegetation canopies, and especially by describing the environmental and physical controls of evaporation. The rate of evaporation (E) depends critically on both plant factors such as stomatal aperture, leaf area index, canopy structure and leaf orientation and on environmental factors such as incoming radiation, atmospheric humidity and windspeed. The interplay of all these factors has been well described by the well-known Penman-Monteith (P-M) evaporation equation which will be described.

The relative importance of plant and environmental factors in the control of the evaporation rate from canopies will be discussed in relation to "environmental coupling" and the so-called "Ω-factor". It will be shown that ET can be described as the sum of an 'imposed' component and an 'equilibrium' component, and the balance between these two depends on the degree of environmental coupling. The importance of this environmental coupling for agricultural and ecological experimentation and measurement and for our understanding of the physiological control of evaporation in different agricultural and natural plant communities and for scheduling of irrigation will be discussed.

The meaning(s) and importance of reference evapotranspiration (ET_0) will also be discussed in relation to its use in irrigation scheduling. Alternative approaches to its estimation will be addressed including the more traditional use of simple evaporation formulae (Blaney-Criddle, Thornthwaite and Priestley-Taylor), the use of evaporation pans and the use of more sophisticated methods.

The presentation will conclude with a brief review of the various approaches available for estimation of actual ET. These will be introduced and compared, as an introduction to the other presentations to this workshop.

2a

SAP FLOW MEASUREMENTS AND THEIR SCALING UP TO TREE AND STAND LEVELS – PART A

J. ČERMÁK[1], J. KUČERA J.[2], N. NADEZHDINA[1]

[1] *Institute of Forest Ecology, Mendel University of Agriculture and Forestry, CZ 61300 Brno, Zemědělská 3, Czech Republic. (corresp. cermak@mendelu.cz).*

[2] *Environmental Measuring Systems, Turistická 5, 62100 Brno, Czech Republic*

Keywords: evaluation of methods, heat balance, heat field deformation, radial pattern of flow, scaling errors

ABSTRACT

Following the pioneering work of Huber early last century, many types of sap flow measurement methods based on very different principles (e.g., thermodynamic, electric, magneto-hydrodynamic, nuclear magnetic resonance, etc.) were described. However, only those based on thermodynamics, are widely used in the field (i.e., forests and orchards) and the measuring devices are commercially available. However, measurement of flow itself represents only the first part in sap flow studies. Additional important items to consider are evaluation of errors, integration of data measured by a certain sensor for the whole stems and spatial variation of flow within trees. Another important issue to consider is the eventual scaling up of data from a series of sample trees to entire stands or even higher levels of biological organization using biometric data, hydrologic models or remote sensing images.

Most frequently applied methods of sap flow measurement are briefly characterised and their goals and weak points underlined. These are: heat pulse velocity (HPV), heat dissipation (HD) and stem heat balance (SHB) methods. Particular attention is paid here to the trunk segment heat balance (THB) and heat field deformation (HFD) methods.

The THB method is very robust and provides reliable data during long-term measurements in trees with diameters over 15 cm in a range of tree species, size and environmental conditions. It has been applied even as a standard when testing other methods. Measured sections are spatially well defined in terms of released heat power, rather wide (4-8 cm) and therefore represent significant parts of stems, especially when more of them are installed around them. It integrates flow in radial direction by technical means, which works well especially in shallow sapwood species. The exact estimation of very low flow (values approaching the fictitious flow) is still difficult since it interferes with the changes of heat loss. There might be some problems with application of THB in stems with very deep sapwood, ill trees with wet heartwood and excessive sap ion content or in some tropical species with sapwood located deep inside stems or those with widely diffused vessels such as palms.

The HFD method is extremely sensitive to very low flows, fast responding (minimum inertia occurs) and has unique capabilities for measuring the real vector of sap flow rate. This includes basipetal flows which occur e.g. during rain events after periods of drought when shoots are absorbing intercepted water or reversed flow in general. Multi-point HFD sensors contain series of

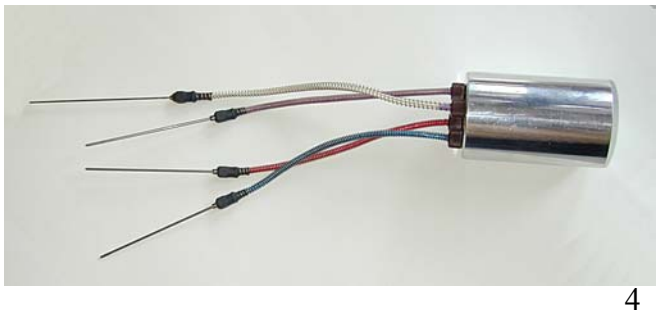

thermocouples and therefore are especially suitable for measurements of radial patterns of flow in stems over a wide range of their diameters. Such a sensor associated with the miniature EMS datalogger is shown in **Figure 1**. Heat energy released in sapwood around the needle heater should be high enough to heat the tangential needle, but low enough to avoid tissue damage. Instalment of especially long needles in deep-sapwood species must be strictly in parallel. Some uncertainties were found during measurements of very high sap flow densities, e.g. those measured just below the crown of tall trees. This is a common problem in most methods working with needle-like heaters.

For both these methods, proper installation of sensors requires basic knowledge of the anatomy and physiology of the conductive systems in sample trees. THB sensors average the radial sap flow profile; multi-point HFD sensors in different depths measure it. Fast growing large stems can grow over sensors during long-term measurements. This changes the relative position of sensors in sapwood and could affect results, if a sufficiently integrating technical system (as in new EMS devices) or multi-point sensors (the only sensors covering radial pattern in all cases) are not applied.

Integrating the radial velocity profile needed for whole tree studies is more important in some methods (especially those using needle-like heaters) and less important in others, where it is overcome by technical arrangements (e.g., internal sectional heating as used by THB). Special caution must be taken in fast growing trees with wide annual rings, when using single-point sensors. Small radial shifts of single-point sensors can cause very different results. An example of sap flow density across "opened" pine tree stem is shown on **Figure 2**.

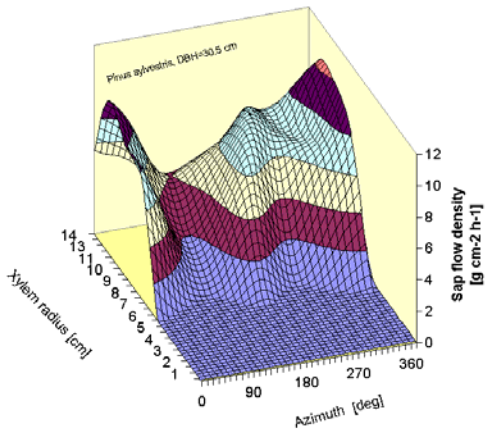

To estimate transpiration of forest stands or orchards on the basis of sap flow measurements in individual trees requires including a series of sample trees of different diameters, depending on the species, tree age, their health state and stand characteristics and also the method applied. Scaling up is usually based on a relationship of sap flow to a selected biometric parameter, e.g. usual forest inventory parameters. Range of sample trees size should cover the actual range of experimental stands. Tree size distribution is also important, because characterisation of a mean tree is problematic in stands with a very wide range of tree sizes. Dominant trees (accounting 1/3 of tree number) account about 2/3 of the total stand water loss, medium trees about ¼ of water loss and suppressed trees only about 5-10%, therefore it is preferable to select sample trees according to special statistical procedure. Scaling up physiological and/or forest inventory parameters from individual trees to forest stands has been generally applied in forestry especially in the case of growth and production.

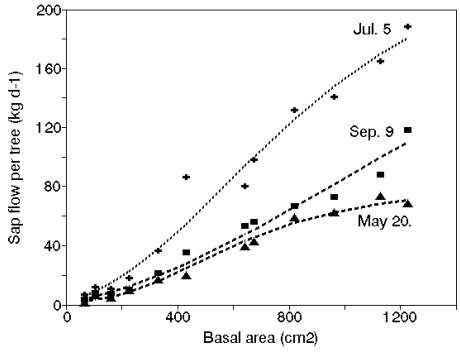

Figure 3. Example of the "scaling curve" on the whole tree level. Relationships between basal area and daily totals of sap flow for the set of 12 sample trees. Three individual days measured under different environmental conditions during the growing season (out of total 180) are shown.

2b

SAP FLOW MEASUREMENTS AND THEIR SCALING UP
PART B – GRANIER METHOD

Mª Isabel F. R. FERREIRA[1], Teresa Soares DAVID[2], José Silvestre[3], Teresa A. PAÇO[1], Nadezhda NADEZHDINA[4], Anton THOMSEN[5], Rodolfo Miranda SILVA[1], Adriano Leovigildo SILVA[1]

[1] *Full Professor, Post-doc research fellow, Ph D student and postgraduate student, at Instituto Superior de Agronomia - UTL, Tapada da Ajuda, 1349-017, Lisboa, Portugal, +351.21.3653476/3335, isabelferreira@isa.utl.pt, tapaco@isa.utl.pt, rodolfo@isa.utl.pt, aleovigildo@isa.utl.pt*

[2] *Researcher , Estação Florestal Nacional, INIAP, Quinta do Marquês, Av. República, 2780-159 Oeiras, Portugal, +351.21.4463737, teresa.david@com.pt*

[3] *Research assistant, Estação Vitivinícola Nacional. Quinta da Almoínha, 2565-191 Dois Portos, Portugal, inia.evn.viti@oninet.pt*

[4] *Researcher, Institute of Forest Ecology, Mendel University of Agriculture and Forestry, Zemedelska 3,61300 Brno,Czech Republic, +42. 0545134181, nadezdan@mendelu.cz*

[5] *Researcher, Danish Institute of Agricultural Sciences, Dept of AgroEcology, anton.thomsen@agrsci.dk*

Keywords: Transpiration, Sap flow, Granier method, Evapotranspiration

---

ABSTRACT

Information on water use of woody crops is scarce because of experimental and modelling limitations related to the size and structure of roots and shoots. The eddy covariance (EC) micrometeorological method is considered relatively reliable and adequate, but it requires large uniform areas. The alternative is the use of sap flow (SF) methods to quantify transpiration (T), which is usually the dominant component of evapotranspiration (ET). Sap flow methods also allow the distinction between T in small plots submitted to different treatments (in relation to water, fertilisers, pruning, etc). The transpiration of woody plants has been studied using a range of sap flow techniques including thermal methods. Between those, the so-called heat dissipation methods (Granier, 1985, 1987, …) have been widely applied because of the relative simplicity of the sensors.

Although heat dissipation sensors are rather simple, their application is not straightforward because of the complexities of sap flow in woody plants, so sap flow is estimated from equations with empirical parameters. The results obtained show that these approaches still need developing and testing to a stage where they can be applied as a routine technique to monitor tree behavior and water consumption in the field. This contribution deals with the so-called Granier technique, including the description of the principle, sensors and its installation, up-scaling, comparison with other techniques, identification of difficulties and solutions to minimize some of the correspondent possible errors. Most of these problems were identified when the comparison with results from other techniques was performed.

The performance of these methods has been verified using other approaches to the estimation of water balance as lysimeters (gravimetric measurements with plants in pots) and eddy covariance, where the sets of results could be compared (Ameglio et al., 1993, Ferreira et al., 1996, Berbigier et al., 1996, Silvestre et al., 1999, Wilson, et al., 2001) and also numerical modelling (Perämäki et al., 2001).

A finite difference simulation model was developed to simulate the heat field around a linear heater and was used here visualise the heat fields for varying flux densities, to estimate the sensitivity to varying wood thermal properties, heater power dissipation, distance between

probes, etc. and to contribute to the analysis of the algorithms used in converting sensor measurement to sap flow estimates. A comparison was made between specified sap flow rates and estimated flow rates using the algorithm proposed by Granier, for a certain range of wood thermal properties. Some results on the scale of a stand and for long term, obtained in the frame of WATERUSE are shown, using the eddy covariance method to measure evapotranspiration, being soil evaporation measured by lysimeters while, for individual plants and short term measurements, a balance was used. The experiments briefly described were carried on for several crops and transpiration rates.

The influence of natural gradients is also shown. It was often obvious a peak by the middle of the morning followed by an apparent relative underestimation about noon when compared with the transpiration patterns obtained with other independent method. As many simultaneous factors seem to influence the thermal gradients in the trunks, it is difficult to solve the problem through an analytical approach. The difference between a heated ΔT sensor and a non-heated one (Ferreira and Zitscher, 1996) seems to be necessary to obtain the corrected thermal gradient, whenever the measurements are performed close to the soil.

The influence of the radial profile on the interpretation of single point measurements is also considered. Some results are shown on the application of the method described in Ferreira et al. (1998) to take this aspect into account.

The method of Granier (1985, 1987), with interesting operational advantages and as a relative inexpensive method, allows to increase the number of sampled trees and to make low cost, long term measurements; when taking the necessary precautions, it is possible to get reliable values of transpiration, at the stand level.

REFERENCES

Ameglio, T.; Archer, P.; Daudet, F-A.; Ferreira, M.I. 1993. Comparaison de trois méthodes de mesure de la transpiration de jeunes arbres. *Agronomie* 13:751-759.

Berbigier, P.; Bonnefond, J.M.; Loustau, D.; Ferreira, M.I.; David, J.S.; Pacheco, C.A.; Pereira, J.S. 1996. Transpiration of a 64-year-old maritime pine stand in Portugal: 2. Evapotranspiration and canopy stomatal conductance measured by an eddy-covariance technique. *Oecologia* 107:43-52.

Ferreira, M.I.; Valancogne, C.; Daudet, F-A.; Ameglio, T.; Michaelsen; J. Pacheco, C. A. 1996. Evapotranspiration and crop water relations in a peach orchard. In: (Camp, C.R.; Sadler, E.J. and Yoder, R.E.; Eds.) *Evapotranspiration and Irrigation Scheduling* (Nov.96, San Antonio, TX), ASAE, pp 60-68.

Ferreira, M.I.; Zitscher, H. 1996. Measurements performed with Granier method in short trunks near the soil. In*:* (Cohen, M.; Edt.) *3rd. Workshop on Measuring Sap Flow in Intact Plants* (Oct. 1996, Sitges, Barcelona), 3pp.

Ferreira, M.I.; Paço, T.A.; Cohen, M.; Oncins, J.A. 1998. Should the radial distribution of sap flow density be considered on the calculation of total sap flow, when using *Granier* sensors? In: (Morison,J.L.; Domimgo, F.; Allen, S. J., eds) *Proced. 4th International Workshop on Field Techniques for Environmental Physiology* (March 1998, Almeria, Spain): poster abstract.

Granier, A. 1985. Une nouvelle méthode pour la mesure du flux de sève brute dans le tronc des arbres. *Ann. Sci. For*., 42: 193-200.

Granier, A. 1987. Mesure du flux de sève brute dans le tronc du Douglas par une nouvelle méthode thermique. Ann. Sci. For., 44: 1-14.

Perämäki, M., T. Vesala and E. Nikinmaa. 2001. Analysing the applicability of the heat balance method for estimating sap flow in boreal forest conditions. Boreal Environment Research 6: 29-43.

Silvestre, J.; Ferreira, I. and Valancogne, C. 1999. Evapotranspiration and water relations from a vineyard in Central Portugal during spring-summer periods. Proc 1st ISHS Workshop on Water Relations of Grapevines (Eds E.H.Ruhl, J. Scmith). Acta Hort. 493: 213-218.

Wilson, K. B.; Hanson, P. J.; Mulholland, P. J.; Baldocchi, D. D. and Wullschleger, S. D. 2001. A comparison of methods for determining forest evapotranspiration and its components: sap flow, soil water budget, eddy covariance and catchment water scale. Agricultural Forest Meteorology 106:153-168.

3a

MICROMETEOROLOGICAL MEASUREMENT OF *ET* PART A: FLUXES EXTRA VERGINE

Roland VOGT[1], Andreas CHRISTEN[1], Irene LEHNER[1],
Florian IMBERY[2], Andrea PITACCO[3]

[1] *Institute of Meteorology, Climatology and Remote Sensing, Dep. of Geoscience, Univ. of Basel, Switzerland, +41.61.2670751*
roland.vogt@unibas.ch

[2] *Meteorological Institute, Univ. of Freiburg, Germany,*

[3] *Department of Environmental Agronomy and Crop Science, Univ. of Padova, Italy*

Keywords: Evapotranspiration, energy balance closure

ABSTRACT

As part of the European project WATERUSE two field studies were carried out in two Mediterranean tree canopies (olives and cork oaks). One main goal was the improvement of parameterisation of the water transfer processes based plant physiological properties. As a subproject we carried out micrometeorological experiments, in order to compare vertical profiles of turbulent exchange properties of the two contrasting rough canopies. A special focus was set on the spatial variability of turbulent heat fluxes inside the canopies.

The first canopy, an olive tree plantation, is located 5 km E of Canosa di Puglia, IT (41°12'N, 16°10'E, 175 m a.s.l.) on approximately level terrain (2° inclined towards NNE). The stand age was 100 years. The distance between the rows was 8.3 m and the tree density was 132 trees per ha, with an average tree height of 5 m. Between the trees was bare soil and the canopy was relatively open. Fetch in the main wind directions (W and N) was 200 to 300 m. The experiment took place from July 27 to August 6, 2002. The tower in the olive canopy supported 7 levels with sonic measurements (6 Campbell CSAT3 and 1 Gill HS), which were mounted at z/h = 0.13, 0.33, 0.72, 0.91, 1.19, 1.6, and 2.43. At the top level an open path gas analyser (Li7500) measured H_2O and CO_2 concentration fluctuations.

The second canopy, a cork oak plantation, is located 35 km SE of Lisbon, PT (38°38'N, 8°51'W; 30 m a.s.l.) on level terrain. The age of the trees was 100 years and they were planted in rows with 10 m distance. The tree density was 76 trees per ha in 2001 with some reduction in early 2003 and the average canopy height was 10 m. The understorey was patchy and varied between dry grass and shrubs (*Cystus crispus*), the latter reached in average up to 0.4 m. Fetch conditions in the main wind direction (NW) were very good, with some variation in tree density further upwind. Measurements were carried out from July 1 to July 13, 2003. The tower in the cork oak canopy supported 9 levels with sonic measurements (8 Campbell CSAT3 and 1 Gill HS), which were mounted at z/h = 0.09, 0.18, 0.43, 0.77, 0.96, 1.17, 1.4, 1.68 and 2.07. At five levels (z/h = 0.18, 0.77, 1.17, 1.4 and 2.07) open path gas analysers (Li7500) additionally measured the H_2O and the CO_2 concentration fluctuations.

The weather during the first campaign was mixed between fine and partly cloudy. Light rain occurred at the beginning around July 26 and a heavy rain event (≈ 25 mm) on July 31. The courses of the energy balance components are displayed in Fig. 1. The sum of net radiation (R_n) and the soil heat flux (G) are plotted together as available energy and reached up to 600 Wm^{-2}. Turbulent heat fluxes are derived from eddy covariance measurements at tower top. The first three days the Bowen ratio (ratio of sensible to latent heat flux H/LE) was

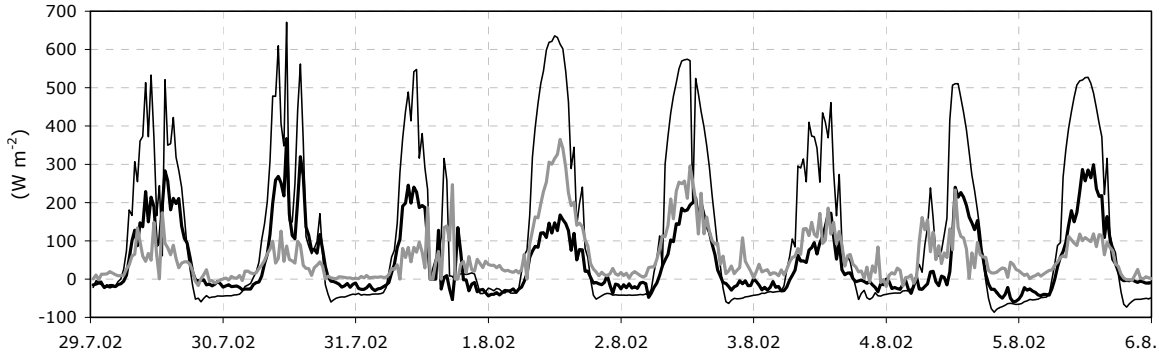

Figure 1: Olive trees. 30 min averages of available energy (R_n+G, thin black line), sensible (H, thick black line) and latent (LE, grey line) heat flux. Measurements are from tower top (z/h = 2.43).

around 2. The heavy rain on July 31 supplied enough water to dramatically reduce it down to 0.34, and a subsequent drying up period was observed with a Bowen ratio of 1.6 at the end. Most of latent heat flux during this period can be attributed to evaporation from bare soil.

The daily values of the energy balance are summarized in Tab. 1 for periods where R_n>0 or R_n<0. Energy flux densities are also expressed as water equivalent. Potential LE (calculated from available energy) varied during daytime between 4 and 7 mm. In canopy LE was around 40 % of above canopy LE and reached up to 70 % the day after the heavy rain event. The closure gap during daytime varied around 25 %. During night-time it ranged between 96 and 76 %. In absolute units the nocturnal closure gap was always less than half of the one during daytime.

Table 1: Diurnal averages (Wm^{-2}) and totals (mm) of components of the energy balance for periods when $R_n > 0$ or $R_n < 0$ (in italic). Number below date indicates frequency of 30 min values for periods with negative R_n. Subscripts *ac* and *ic* denote above and in-canopy LE. Square brackets indicate energy flux densities converted to water flux. *Clos1* is $[R_n+G]-([H]+E_{ac})$ in mm and *Clos2* is $[R_n+G]/([H]+E_{ac})$ in %.

Date/*n*	R_n	G	H	LE_{ac}	LE_{ic}	$[R_n+G]$	$[H]$	E_{ac}	E_{ic}	*Clos1*	*Clos2*
			(Wm^{-2})					(mm)			%
29.7.02	315.3	-25.2	141.3	80.0	38.5	5.36	2.61	1.48	0.71	1.27	76.3
23	*-47.8*	*16.9*	*-13.0*	*4.0*	*9.9*	*-0.52*	*-0.22*	*0.07*	*0.17*	*-0.37*	*29.0*
30.7.02	291.0	-19.3	141.1	60.0	27.7	4.81	2.50	1.06	0.49	1.25	74.0
24	*-56.8*	*19.2*	*-16.3*	*7.1*	*6.4*	*-0.66*	*-0.29*	*0.13*	*0.11*	*-0.50*	*24.3*
31.7.02	247.0	-13.1	111.7	92.3	34.1	3.97	1.90	1.56	0.58	0.51	87.2
25	*-44.0*	*18.2*	*-23.3*	*22.2*	*2.2*	*-0.47*	*-0.43*	*0.41*	*0.04*	*-0.45*	*4.5*
1.8.02	396.8	-20.4	76.1	212.7	149.9	6.96	1.41	3.93	2.77	1.62	76.7
23	*-57.0*	*16.5*	*-25.5*	*21.4*	*13.7*	*-0.68*	*-0.43*	*0.36*	*0.23*	*-0.61*	*10.2*
2.8.02	398.6	-27.8	106.2	169.5	96.5	6.59	1.89	3.01	1.71	1.69	74.4
23	*-62.5*	*17.6*	*-18.9*	*15.5*	*13.8*	*-0.79*	*-0.33*	*0.27*	*0.24*	*-0.73*	*7.6*
3.8.02	271.5	-24.1	58.6	110.8	57.9	4.40	1.04	1.97	1.03	1.39	68.5
24	*-55.5*	*18.5*	*-17.2*	*15.7*	*10.0*	*-0.65*	*-0.30*	*0.28*	*0.18*	*-0.63*	*4.0*
4.8.02	256.5	-26.5	71.9	91.5	49.3	4.28	1.34	1.70	0.92	1.24	71.0
23	*-66.3*	*18.0*	*-32.5*	*16.2*	*14.6*	*-0.82*	*-0.55*	*0.28*	*0.25*	*-0.55*	*33.7*
5.8.02	365.3	-29.5	150.2	93.9	35.7	5.98	2.68	1.67	0.63	1.63	72.7
24	*-71.1*	*18.3*	*-21.3*	*9.4*	*7.0*	*-0.93*	*-0.38*	*0.17*	*0.12*	*-0.72*	*22.6*

The meteorological conditions during the second experiment in the cork oaks showed only little day to day variation, clear sky conditions dominated. This uniformity allows to consider average diurnal courses. Figure 2 (left) shows, that available energy was mainly partitioned into sensible heat flux. The average daytime Bowen ratio was 2.9 ± 0.7. From Fig. 2 (right) one can see, that in-canopy LE is small and contributes in average only 18 % to above canopy LE. The closure of the energy balance is good (Fig. 3) and ranges during daytime between 90

and 100 % (Tab. 2). This reflects possibly the homogeneous surface conditions and also the well mixed conditions due to relatively high wind speed contribute to the good closure. The latter holds also for the nocturnal situation, where the average closure with 60 % is high.

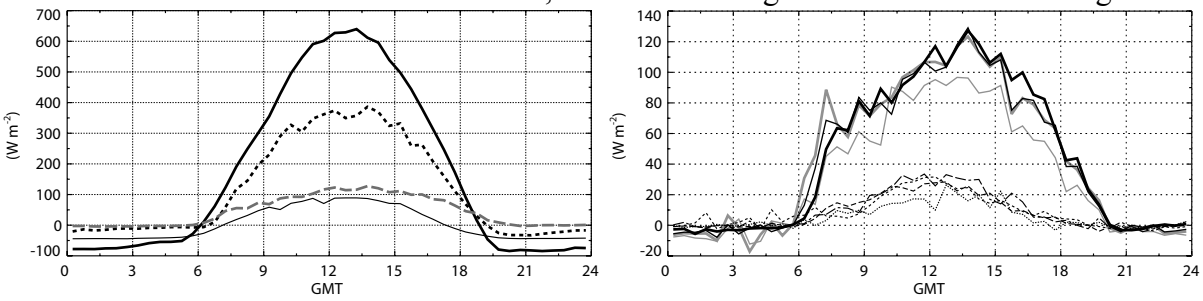

Figure 2: Cork oaks. Left: average diurnal courses of energy balance components. R_n = thick black, H = dotted, LE = dashed, $-G$ = thin black line. Right: average diurnal courses of LE at different levels. Thick black, thin black, thick grey, thin grey are from z/h = 2.07, 1.4, 1.17, 0.77 respectively. Thin dashed or dotted lines are from 4 points inside the canopy (z/h=0.18). Averaging period is July 2 to July 12, 2003.

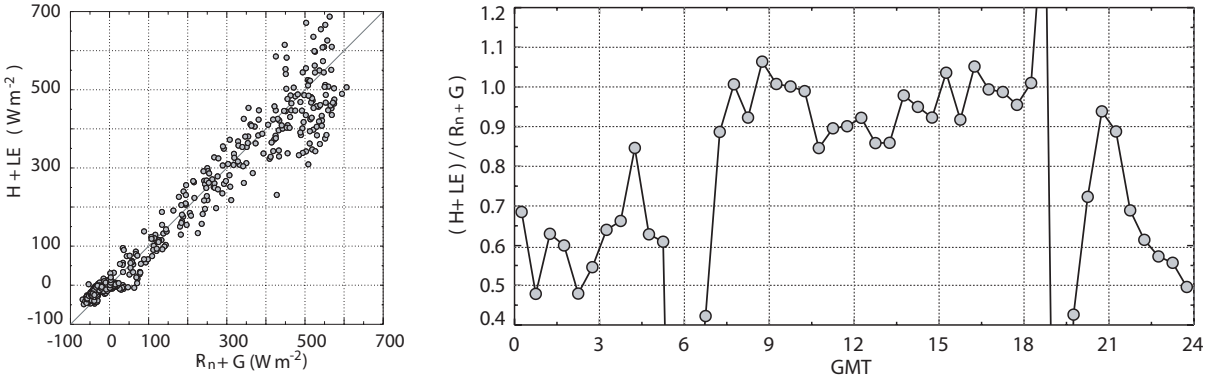

Figure 3: Cork oaks. Left: Sum 30 min values of turbulent heat fluxes versus available energy. Right: average diurnal course of closure ratio. Averaging period is from July 2 to July 12, 2003.

Table 2: Same as Tab. 1 but for cork oaks.

Date/*n*	R_n	G	H	LE_{ac}	LE_{ic}	$[R_n+G]$	$[H]$	E_{ac}	E_{ic}	*Clos1*	*Clos2*
			(Wm^{-2})					(mm)			%
2.7.03	380.4	-43.2	224.1	72.6	14.2	6.45	4.29	1.39	0.27	0.78	88.0
22	*-68.8*	*42.5*	*-20.8*	*0.9*	*-0.2*	*-0.42*	*-0.33*	*0.01*	*-0.00*	*-0.10*	*75.7*
3.7.03	407.5	-47.7	271.5	74.8	14.5	6.89	5.20	1.43	0.28	0.26	96.3
22	*-80.3*	*46.1*	*-24.2*	*-0.6*	*0.6*	*-0.55*	*-0.39*	*-0.01*	*0.01*	*-0.15*	*72.5*
5.7.03	405.8	-41.8	283.6	78.1	13.0	6.96	5.43	1.49	0.25	0.04	99.4
22	*-81.0*	*44.7*	*-24.9*	*-3.9*	*-1.8*	*-0.58*	*-0.40*	*-0.06*	*-0.03*	*-0.12*	*79.4*
6.7.03	416.0	-50.8	254.3	75.6	17.6	6.73	4.69	1.39	0.32	0.65	90.3
23	*-73.4*	*43.2*	*-16.0*	*-2.8*	*-0.4*	*-0.51*	*-0.27*	*-0.05*	*-0.01*	*-0.19*	*62.2*
7.7.03	397.3	-52.0	220.9	90.4	18.4	6.63	4.24	1.74	0.35	0.65	90.2
22	*-65.5*	*44.4*	*-12.5*	*2.3*	*-1.4*	*-0.34*	*-0.20*	*0.04*	*-0.02*	*-0.18*	*48.0*
8.7.03	393.6	-47.6	227.9	96.3	16.9	6.64	4.38	1.85	0.32	0.42	93.7
22	*-75.4*	*44.6*	*-13.8*	*-1.5*	*-0.4*	*-0.50*	*-0.22*	*-0.02*	*-0.01*	*-0.25*	*49.6*
9.7.03	395.0	-48.6	226.6	96.8	14.4	6.66	4.36	1.86	0.28	0.44	93.4
22	*-83.8*	*45.6*	*-19.9*	*-0.8*	*1.1*	*-0.61*	*-0.32*	*-0.01*	*0.02*	*-0.28*	*54.0*
10.7.03	409.6	-55.5	222.5	91.4	15.7	6.55	4.11	1.69	0.29	0.74	88.7
23	*-77.6*	*41.1*	*-20.8*	*1.5*	*7.7*	*-0.61*	*-0.35*	*0.03*	*0.13*	*-0.29*	*53.0*
11.7.03	366.5	-40.1	249.8	74.4	13.9	6.26	4.79	1.43	0.27	0.04	99.3
22	*-67.3*	*40.0*	*-11.5*	*-1.1*	*-1.3*	*-0.44*	*-0.19*	*-0.02*	*-0.02*	*-0.24*	*46.2*
12.7.03	213.3	-19.4	136.3	60.6	10.2	3.71	2.61	1.16	0.19	-0.06	101.6
22	*-33.4*	*28.5*	*-3.6*	*2.6*	*0.3*	*-0.08*	*-0.06*	*0.04*	*0.01*	*-0.06*	*19.4*

3b

MICROMETEROLOGICAL MEASUREMENT OF ET: B. THE ROLE OF THE CANOPY IN MODIFYING THE PARTITIONING OF FLUXES

Andrea PITACCO[1], Valentina ZAMBETTI[1], Roland VOGT[2]

[1] *Department of Environmental Agronomy and Crop Science, University of Padova, Viale dell'Università 16, I-35020 Legnaro, Italy, +39.049.827.2848 andrea.pitacco@unipd.it*

[2] *Institute of Meteorology, Climatology and Remote Sensing, University of Basel, Klingelbergstrasse 27, CH-4056 Basel, Switzerland*

Keywords: evapotranspiration, discontinuous canopies, energy budget, surface resistance, modelling

---

ABSTRACT

Developments in micrometeorological instrumentation and techniques (in particular, sonic anemometry, fast IR gas analysis, and eddy covariance) made possible the collection of very detailed pictures of the Soil-Vegetation-Atmosphere energy and mass exchanges (Vogt *et al.*, these proceedings). These are effectively promoting the advancement of a thorough understanding of the dynamics of canopy environment, where plant physiology, architectural properties of vegetation and a range of physical processes play together a very complex game.

These datasets are being used to implement and run sophisticated models to interpret and predict canopy behaviour, either in relation to the hot topic of carbon exchange, or to the more classical water and energy budgets. However, quite often these efforts turn out to be of little practical use because of the many environmental variables and vegetation parameters these models require to be run. Thus, simpler, yet less detailed models can still have a role in applications where a satisfactory balance between accuracy of predictions, data availability and explanatory capacity is to be sought. In this respect, Penman-Monteith (PM) combination equation is surely the best known and most widely used model to analyze and predict evapotranspiration fluxes for a range of vegetation types, either natural or managed.

In order to deal with discontinuous vegetation, the original PM "big-leaf" framework has been extended to multiple-source systems (Shuttleworth and Wallace, 1981, SW). Actually, a separate estimation of the components of the surface energy balance is crucial to the understanding of the interactions between hydrological cycle and vegetation processes at local and regional scales. This can be especially challenging in arid and semi-arid natural vegetation due to the large spatial and temporal variability of surface characteristics such as moisture, temperature, albedo, vegetation type and cover.

The key assumption behind the original SW approach is that that water vapour and heat enter or leave the atmosphere only via the canopy: understorey and overstorey fluxes merge in the canopy space, where local conditions of temperature and vapour pressure are determined by both. This feature, regarded as soil-canopy "coupling", can be important where –for instance– tree canopy leaf physiology may react to vapour pressure deficit, as influenced by soil fluxes too. On the other hand, this assumption may not always be appropriate in arid and semi-arid regions where the vegetation is often interspaced by large patches of bare soil. Under such condition, heat and mass exchanges between a part of soil surface and the

atmosphere may take place with little interaction with the adjacent canopy, and "mosaic" type of multiple-source models may perform better.

In the framework of the WATERUSE project, the SW double-sorce model has been parameterized for a cork-oak plantation, using eddy covariance measurements of sensible and latent heat fluxes, net radiation and soil heat flux. The dataset that has been collected is a unique database to study soil and canopy fluxes separately and the roughness (that enhanced in-canopy mixing) and the density of the stand justified the use of a coupled, double-sorce model.

Parameterization of soil-canopy and leaf boundary layer resistances followed the empirical functions proposed by Choudhury and Monteith (1988), while aerodynamic resistance has been calculated from friction velocity according to standard formulation and corrected for stability. Weather conditions during the Intensive Observation Period #2 (1-14 July, 2003) have been so regular that the inverse parameterization yielded very stable values for surface resistances during daytime. In particular, soil resistance was around 5000 s m^{-1}, and canopy resistance around 600 s m^{-1}, both quite steady because of the extremely dry conditions encountered in the upper soil layers and the water stress experience by trees.

Simulations of turbulent fluxes using SW coupled model and performed using measured values of net radiation and friction velocity and constant values of surface resistances closely resembled measured eddy fluxes, both for the soil and the canopy source components. These results may help in understanding how fluxes are partitioned between over- and understorey in the medium and long term, especially in connection with ancillary measurements of transpiration like sap-flow gauges.

REFERENCES

Choudhury, B. J. and Monteith, J. L.,1988. A four-layer model for the heat budget of homogeneous land surfaces. Quarterly Journal of the Royal Meteorological Society, 114:373-398.

Shuttleworth, W. J. and Wallace, J. S., 1985. Evaporation from sparse crops - an energy combination theory. Quarterly Journal of the Royal Meteorological Society, 111:839-855.

4

WATER STRESS INDICATORS
USE OF SAP FLOW MEASUREMENTS FOR STRESS DIAGNOSIS

Mª Isabel F. R. FERREIRA[1], Teresa A. PAÇO[2] Nadezhda NADEZHDINA[3]

[1] *Full Professor, Instituto Superior de Agronomia - UTL, Tapada da Ajuda, 1349-017, Lisboa, Portugal, +351.21.3653476*
isabelferreira@isa.utl.pt

[2] *Post-doc research fellow, Instituto Superior de Agronomia - UTL, Tapada da Ajuda, 1349-017, Lisboa, Portugal, +351. 21.3653335,*
tapaco@isa.utl.pt

[3] *Researcher, Institute of Forest Ecology, Mendel University of Agriculture and Forestry, Zemedelska 3,61300 Brno,Czech Republic, +42. 0545134181, nadezdan@mendelu.cz*

Keywords: Water stress, Indicators, Sap flow, Heat field deformation

---

ABSTRACT

Irrigation scheduling can be achieved through a continuously up-dated soil water balance using ET estimates but also by following the evolution of some indicators of plant or soil water status. After the initial approaches using soil measurements, attention has been given in the last decades to the measurements on plants, like stomatal conductance and leaf water potential. Stomatal conductance (g_s) is a variable with an interpretative value and also, while indicator of water stress, with a practical interest in irrigation scheduling. Notwithstanding, its direct measure with porometers is not advisable as a common practice, mainly due to the time required to obtain a representative value. Another reason is that g_s is changing with rapid environmental changes and it is difficult to establish and use a critical value. The alternatives that have been, so far, explored respect to the use of other water-stress related variables, considered as a cause or/and a consequence of stomatal closure. The most commonly used variable is predawn leaf water potential as it can be used in plants with different strategies, the so-called isohydric and non isohydric plants.

One of the consequences of stomatal closure is the change in transpirational cooling of leaves resulting in greater leaf temperatures or greater thermal gradients above the canopy. These variables can be used directly or through other more indirect approaches (for instance, the *Jackson* index). Even for low crops, the measurements require large plots, because of the instability of the observed values in advection conditions. These difficulties became more pronounced on woody stands, owing to the higher turbulence in the canopies and consequent instability of leaf temperature.

Among the factors that determine the stomatal behaviour, the soil water potential (ψ_s) or soil water content (θ_s) have the advantage of its independence on diurnal atmospheric variations. Yet, the relationship between r_S and those variables is of interest, only if they reflect the average conditions in the roots zone. These conditions are difficult to achieve, in practice, with large root systems. The use of a few sensors in a representative point has been often the solution, but it is difficult to extrapolate the location of the representative point to other soils, irrigation and root systems.

Many attempts have also been made using the variations of stem diameter to schedule irrigation, especially in orchards, where traditional methods are difficult to apply. It has the advantage of an easy continuous record and relatively easy automatic data processing.

Relative transpiration (ratio between the transpiration of a stressed group of plants and the transpiration of non-stressed plants), also possible to automate, has been previously used in orchards with interesting results. Daily relative transpiration can be seen as an approximate integrated value - in time and space - of stomatal behaviour response to water stress. Combined with other water stress indicators and their critical thresholds, relative transpiration can provide a useful tool in irrigation scheduling. Some results concerning the practical use of these indicators are refereed, to support the perspectives presented.

An alternative water stress indicator, also based on sap flow measurements, is presented – sap flow index (SFI). For this indicator, the sap flow method used is the heat field deformation method. The SFI is the symmetrical temperature difference, measured around a linear heater in the axial direction of the trunk. It presents two maxima during the daily cycle, one in the morning and another one in the evening, and its values are interesting in two moments of the day: predawn (SFI_p) and midday (SFI_d). The ratio SFI_p/ SFI_d gives the best information about internal plant water status and it increased with plant water deficit. This indicator can be determined with simple and cheap sensors and it is easy to automate. During long-term studies on *Quercus suber* (Rio Frio, Portugal) it has been observed that SFI measured at root surface is a more sensitive indicator than measured at the tree trunk. The ratio of the negative area of SFI ratio (when hydraulic lift in roots is recorded under drought) to the positive one during daily cycle (between two middays, for example) reflects the development of stress conditions in soil independently from evaporative demands. This area ratio could be used as a signal for automatic irrigation scheduling.

5

SURFACE TEMPERATURE MEASUREMENT AND ESTIMATION OF EVAPORATION

Hamlyn G. JONES, Nicole ARCHER

Plant Research Group, University of Dundee at SCRI, Invergowrie, Dundee DD2 5DA, Scotland, UK
h.g.jones@dundee.ac.uk,
narche@scri.sari.ac.uk

ABSTRACT

Measurements of vegetation or land surface temperatures as obtained from land-based, airborne or satellite thermal infra-red sensors provides a key input for the estimation of evaporation rates from vegetation. There are many ways in which this remotely-sensed temperature can be used for calculation of evaporation (E) from vegetation: the main approaches have been summarised by Jones, Archer and Rotenberg (2003) and will be outlined in this talk. The majority of methods available are based on formulations of the canopy energy balance, with the differences between approaches largely being related to where empirical approximations are incorporated into the calculations.

In addition to reviewing the main general methods available for remote estimation of ET, this paper also introduces the special problems involved in the application to heterogeneous surfaces such as Portuguese montado woodland. Some new algorithms for estimation of evapo-transpiration from such heterogeneous surfaces are introduced. The application of some of these methods to data obtained from ground-level thermal imaging and from airborne and satellite thermal data will be described in the following paper by Archer.

Basic theory underlying estimation of ET from surface temperature

Evaporation from *montado* can be separated into two main components: evaporation from the trees which have deep roots and continued water availability throughout the summer, and evaporation from the ground vegetation and soil. The evaporation from the soil can be assumed to be negligible after several weeks without rain, while much of the annual ground vegetation such as grasses dies in summer, leaving only the scattered Cistus and other shrubs still transpiring. The majority of methods available for estimation of E are based on formulations of the canopy energy balance, which can be written: $\lambda E = Rn - G - H$. Where E is the evaporation rate, λ is the latent heat of vaporisation, Rn is the net radiation absorbed, G is the soil heat flux (often assumed to be negligible over 24 h periods) and H is the sensible heat loss to the air. The most usual formulation for meteorological estimates of E is the Penman-Monteith combination equation (see e.g. Jones, 1992).

Single leaves:

The temperature difference between a dry surface and an evaporating surface can be shown to be proportional to E; the difficulty is to estimate the constant of proportionality in any situation. One approach (e.g. Jones 1999) requires only knowledge of the boundary layer conductance according to

$$\lambda E = \rho c_p (g_{HR})(T_{dry} - T_{leaf})$$

where g_{HR} is the effectively the boundary layer conductance for the leaf. An alternative formulation relates λE to the net radiation and to air temperature (T_a) as well as wet and dry leaf temperatures

$$\lambda E = R_{ni} (T_{dry} - T_{leaf})/(T_{dry} - T_a)$$

where R_{ni} is the net isothermal radiation.

Canopy level methods:

The leaf-level methods may be extrapolated up to canopy scale, but there are often difficulties this scaling-up and other approaches have been suggested. A wide range of empirical and more theoretically-based methods have been proposed, with semi-empirical methods being most widely used. Although remotely sensed canopy temperatures may be substituted into the full Penman-Monteith equation, much other information (e.g. on windspeed, vapour pressure deficit and canopy conductance) is also required. Particularly widely applicable approaches involve the use of reference surfaces on the ground (e.g. non-transpiring areas of soil or potentially transpiring water bodies). Particularly promising are methods which also incorporate remote measurement of 'vegetation indices' such as NDVI (see Jones et al. 2003).

The various methods available and their relative merits will be reviewed in detail.

REFERENCES

Jones HG 1992. *Plants and microclimate*. CUP, Cambridge.

Jones HG, Archer NA and Rotenberg E. (2003) Thermal radiation, canopy temperature and evaporation from forest canopies. In *Forests at the Land-Atmosphere Interface* (eds. M. Mencuccini, J. Grace, J. Moncrieff and K. McNaughton), CAB International, Wallingford. pp. 123-144.

6

SOIL WATER MEASUREMENTS – THE MOST USUAL METHODS: GRAVIMETRIC, NEUTRONIC, CAPACITIVE AND TIME DOMAIN REFLECTOMETRY (TDR)

Carlos A. PACHECO[1],

[1] *Instituto Superior de Agronomia - UTL, Tapada da Ajuda, 1349-017, Lisboa, +351.21.3653476 capacheco@isa.utl.pt*

Keywords: soil, water, gravimetric, neutronic, capacitive, TDR

ABSTRACT

In this short communication we give some practical examples about soil water measurements with gravimetric, neutronic, capacitive and time domain reflectometry (TDR) methods.

Some of the advantages are referred and it is emphasized that we must use the complementary methods to study the soil field water content.

The evapotranspiration (ETr) is estimated by these methods and some examples are given on methodologies.

7

GPR FOR SOIL MAPPING/ASSESSMENT AND ROOTS IMAGING

Susanne Lorra, Andreas F. Kathage [1]

[1] *GeoHiRes International Ltd., Borken, Germany*

Keywords: Ground Penetrating Radar, Soil Texture, Roots Zone, 3D-Mapping

ABSTRACT

In the European Union funded project WATERUSE the GPR (Ground Penetrating Radar) method has been investigated and improved in order to supply relevant information for scientists who are working on sap flow measurements as well as on the theoretical modelling of the soil.

This work was focussed on the 3-dimensional mapping of roots zones as well as on the 2- and 3-dimensional mapping of the soil texture in semiarid regions.

Based on several field tests the data acquisition methods were selected and developed. Suitable frequencies were identified as well as matched field equipment configurations and survey layouts were selected. This work was carried out hand in hand with the development of new data processing and interpretation software. Main components of the software development were the 3-dimensional processing-, visualisation- and interactive interpretation tools. These tools are suitable for the interpretation of complex structures like roots, which could not be tracked reliably with the software tools that were available at the beginning of this project.

It was shown during different common field experiments in semiarid regions that the employed GPR method provides valuable information for the teams working on sap flow as well as on soil models. The GPR-method has become a useful tool for soil and root mapping providing that high electrical conductivity values of soils do not prevent the propagation of the electromagnetic waves in the materials for investigation.

The non-destructive determination of the relevant soil and root parameters leads to a considerably better modelling and prediction of the water transportation in the soil – plant continuum. For this kind of investigations the non-destructive methods offer a much better cost-/performance ratio than invasive methods do.

8

HIGH RESOLUTION HYDROGEOPHYSICAL TECHNIQUES

Said A. al HAGREY, Ulrike WERBAN, Rolf MEISSNER, Wolfgang RABBEL and Ali ISMAEIL

Department of Geophysics, Institute of Geosciences, Kiel University, sattia@geophysik.uni-kiel.de

ABSTRACT

A better understanding of the static and dynamic water problem in the heterogeneous vadose soil zone demands developing new 3D mapping and monitoring techniques. Our full scale "GeoModel"erected at the Campus of Kiel University offers a new approach for developing new integrative hydrogeophysical techniques of high resolution and is an ideal link between laboratory (small scale) and field studies (natural large scale). It is used for carrying out fully controlled (infiltration) experiments on simulated soil models of predefined boundary conditions. Moreover, we summarize physical-empirical relationships of water content versus electric resistivity and radar velocity and present a new tomographic radar algorithm for velocity inversion.

Some examples from the laboratory, from the GeoModel and from the field are presented.

(full paper in last section)

9

MODELLING AND SIMULATION OF ROOT WATER UPTAKING AND EVAPOTRANSPIRATION FOR IRRIGATED *Olea Europea*

Guido D'URSO[1], Marianna PANICO[2], Elena DE MARCO[2]

[1] *Assoc.Professor, PhD,Dip. Ingegneria Agraria ed Agronomia delTerritorio, Università di Napoli Federico II, Via Università 100, 80055 Portici, Italy; fax: +30 081 2539412 durso@unina.it*

[2] *PhD student, Dip. Ingegneria Agraria ed Agronomia delTerritorio, Università di Napoli Federico II, Via Università 100, 80055 Portici*

Keywords: Evapotranspiration, Soil hydraulic characteristics, Richards equation

---

ABSTRACT

During the last decades, a much better knowledge of water flow in the soil-crop-atmosphere system has been achieved. This progress has led to the development of mathematical models for the numerical simulation of water flow. If carefully calibrated and validated, these models allow for a much better estimation of water balance terms than reservoir models and they can be used in the practical solution of problems related to the precision management of water resources. In these models, the soil reservoir is a dynamic continuum, where the water flow in the soil-plant-atmosphere system is described by means of the well-known Richards' equation. The behaviour of this system is mainly determined by the soil hydraulic properties, the canopy and root characteristics and the atmospheric conditions. Depending on the availability of input data, the simulation can be made considering simple one-dimensional geometry or complex three-dimensional root and canopy systems. In both cases the root water uptaking can be modeled assuming a macroscopic approach or a single-root approach (Santini, 1992). In the first case, a sink term expressed as a function of soil water potential is often used for his straightforward application. Based on this approach, a family of simulation models have been defined, among which the SWAP algorithm, developed at Wageningen Agricultural University (Feddes et al., 1988; Dam et al., 1997). When unsaturated conditions prevail in a large portion of the soil profile, such as in irrigated areas, water flow can be assumed as mainly vertical, thus neglecting the horizontal components of soil water flux.

This approach has been validated for several agricultural crops under different meterorological conditions and results have been proved to be of great accuracy for irrigation scheduling and water management. However, in the case of a canopy with complex aerial and root systems with incomplete soil cover, Richards'equation modelling approach may appear too crude for achieving a satisfactory description of the hydrological processes involved. In spite of these evident limitations and strong assumptions, this approach has been applied in a number of studies concerning spruce stands (Bouten, 1995; Oltchev et al., 1996), pear trees (Zhang et al., 2003) and olive trees (Dorij, 2003).

In this presentation we show the results of a simulation study based on the experimental data-set acquired in an olive stand in Southern Italy during the summer 2001, within the activities of U.E. Wateruse research project. We applied the models SWAP and Hydrus to estimate the actual evapotranspiration at stand level assuming a one-dimensional modelling scheme. The aim of the simulation study was mainly to assess the level of accuracy of this approach in presence of a limited input data set, with special concern to canopy characteristics and root distribution.

Simulations were performed at both stand level and single tree and the results – in terms of hourly evapotranspiration fluxes- were compared to eddy-correlation tower measurements and sap-flow data, respectively. The comparison confirmed that the proposed approach, even with limited data set, may provide useful indications on the evolution of evapotranspiration fluxes and, possibly, to the presence of water stress conditions.

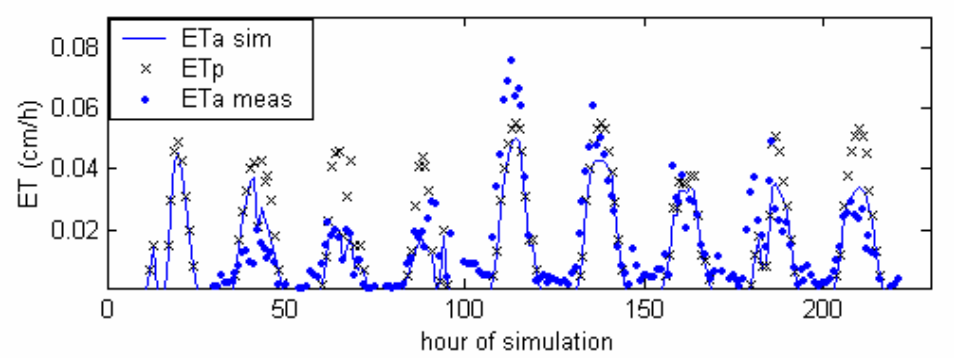

Figure 1 - comparison between measured (dots) and simulated (cross) evapotranspiration fluxes for the Olive stands in Canosa (Italy). Input LAI at stand level was 0.837; reference Eto was calculated with radiative method (Makkink) and Kc value was set to 0.6.
Actual ET measurements and input climatic data are courtesy of Prof. Andrea Pitacco, University of Padova; LAI measurements were provided by Prof. Jan Cermak, University of Brno.

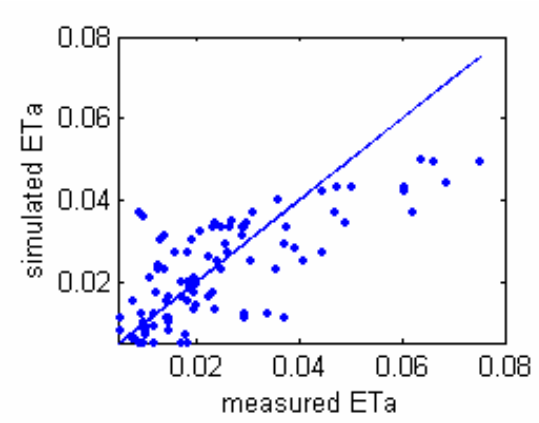

Figure 2 - Correlation between measured and simulated actual evapotranspiration values.
RMSE resulted 0.00912; R^2=0.55.

10

REFERENCE EVAPOTRANSPIRATION AND CROP COEFFICIENTS: HOW GOOD IS THIS APPROACH FOR WOODY STANDS? USE OF STRESS COEFFICIENTS

Mª Isabel F. R. FERREIRA[1], Teresa A. PAÇO[2]

[1] *Full Professor, Instituto Superior de Agronomia - UTL, Tapada da Ajuda, 1349-017, Lisboa, Portugal, +351.21.3653476*
isabelferreira@isa.utl.pt

[2] *Post-doc research fellow, Instituto Superior de Agronomia - UTL, Tapada da Ajuda, 1349-017, Lisboa, Portugal, +351. 21.3653335,*
tapaco@isa.utl.pt

Keywords: Crop coefficient, Stress coefficient, Reference evapotranspiration, Woody stands, Tree

---

ABSTRACT

The answers to the classical questions: when to irrigate and how much water to apply require an evaluation of the water fluxes between plants and the atmosphere (evapotranspiration, ET). The ET measuring methods require the use of expensive equipment and know-how, not currently available, at the farm level. Furthermore, they provide real-time information and not the time-series for statistical analysis usually necessary for the dimensioning of water delivery systems. The ET measurements are used in research, for a better understanding of the physical and physiological process involved and for the evaluation of ET models. The spatial characteristics of woody species, namely when they correspond to non-uniform canopies, have implications on the choice of the techniques for ET measurements but also on the choice of the models.

The estimation of the maximal ET of a crop (ETm) has been approached through an empirical equation using a so-called crop coefficient (Kc), relating the ETm of that crop to a reference ET (ETo). ETo is the ETm of a well irrigated reference crop (usually grass in Europe), measured or estimated (Penman-Monteith equation with grass parameters). Many equations for the estimation of ETo have been developed and used, empirical or more physically based, according to the meteorological data they suppose to be available. In spite of the fact that Kc was often obtained by methods that do not allow a detailed temporal analysis of ET (soil measurements, drainage lysimeters), this approach (ETm=ETo.Kc) has provided good approximations for many applications, mainly in low irrigated crops. However, on woody crops the results seem less satisfactory.

When the crops do not completely cover the soil, as in many irrigated orchards, crop coefficients are not easily extrapolated because they are dependent upon cultural practices (distance between lines, soil cover, irrigation practices, density of foliage and spatial distribution of leaves). Using different independent techniques, values of Kc much lower than those suggested, in currently used manuals, were measured in different row crops, in Portugal (Ferreira et al., 1997; Paço, 2003; Silva *et al*., 2004).

Second, even being able to obtain a good estimation of the maximal ET for the crop in consideration (ETm), the actual ET (ETa) is often below ETm. This can happen because of water restrictions or for quality purposes. But even in well irrigated crops (not daily irrigated), there is experimental evidence that ET (for instance, in sandy soils) is progressively decreasing between irrigations, being average ETa considerably less than ETm.

The impact of stomatal closure on the reduction of transpiration in woody crops is much higher then in low uniform crops, being this aspect quite important in distinguishing the behaviour of canopies with different omega factors, in relation to water transfer to the atmosphere (Ferreira, 1996).

Considering the limitation on stomatal closure records, that aspect could be considered with the introduction of a stress coefficient (Ks = ETa/ETm, being ETa=ETo.Kc.Ks), dependent of the intensity of water stress. A relationship can be used to implicit or explicitly include the increasing stomatal closure, i.e., Ks can be a function of the canopy resistance (r_c) or any other water stress related variable, more accessible.

Some results are shown on Ks functions for two peach orchards in central Portugal, with same canopy geometry, climate and soil type (Ferreira and Valancogne, 1997; Paço, 2003). The comparative analysis reveals the importance of the irrigation system in promoting the development of different roots size and geometry and, thus, different answers to stress. The results also showed the dependence of those trees on quite deep hardly identifiable roots, when severe water stress was applied.

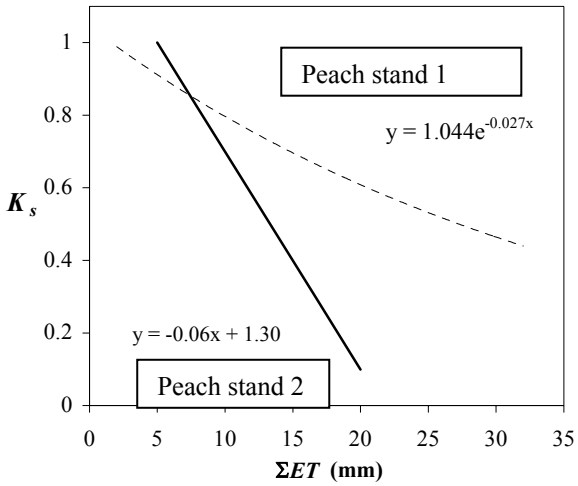

Figure 1 – Comparison of Ks determined for two peach orchards, showing a poorer adaptation to water stress in peach stand 2 connected to degree of root development induced by the irrigation system.

REFERENCES

Ferreira, M.I. (1996) Evapotranspiração e relações hídricas em cobertos arbóreos: revisão e perspectivas. In: (Gomes da Silva, R.; Edt.) *Anais do I Congresso Brasileiro de Biometeorologia,* (Sept. 1995, Jaboticabal, S. Paulo), UNESP, pp 69-100.

Ferreira, M.I. & Valancogne, C. (1997). Experimental study of a stress coefficient: application on a simple model for irrigation scheduling and daily evapotranspiration estimation. *In:* (Farkas,I., Ed.) *Proc. 2nd Intern. Symp. on Mathemathical Modelling and Simulation in Agricultural and Bio-Industries*, (Maio 1997, Budapeste, Hungria).

Ferreira, M.I.; Valancogne, C.; Michaelsen; J. Pacheco, C. A.; Ameglio, T.; Daudet, F-A.(1997) Evapotranspiration, water stress indicators and soil water balance in a *Prunus persica* orchard, in central Portugal. *Acta Horticulturae* 449 (2):379-384.

Paço, M. T. G. A. (2003). *Modelação da evapotranspiração em cobertos descontínuos - Programação da rega em pomar de pessegueiro*. Tese de doutoramento, Universidade Técnica de Lisboa, Instituto Superior de Agronomia, Lisboa, 227 p..

Silva, R. M.; Ferreira, M.I.; Paço, T.A.; Veloso, A.; Oliveira, M. (2004). Determinação das necessidades de rega em kiwi na região do Entre Douro e Minho. 7º Congresso da Água: *Água – Qualidade de Toda a Vida*, Lisboa, 8-12 Março.

11a

MAIN BIOMETRIC PARAMETERS AND LEAF AREA DISTRIBUTION IN AN OLD OLIVE TREES AND ORCHARD IN SOUTHERN ITALY

J. ČERMÁK[1], J. GAŠPÁREK[1], F. De LORENZI[2], H.G. JONES[3]

[1] *Institute of Forest Ecology, Mendel University of Agriculture and Forestry, CZ 61300 Brno, Zemědělská 3, Czech Republic. (corresp. cermak@mendelu.cz).*

[2] *Institute for Mediterraean Agro-Forestry (ISAFOM-CNE), Via Potacca 85, 80056 Ercolano (NA) Italy.*

[3] *School of Life Sciences, University of Dundee at SCRI, Scottish Crop Research Institute, Invergowrie, Dundee DD2 5DA, United Kingdom.*

Keywords: main stem and crown parameters, vertical leaf distribution, radial leaf distribution, LAI, olive

---

Presented study was focused on the description of stand biometry and leaf distribution estimated using geometrical models and image analysis as described in the previous contribution. The study was performed in an 80 year old olive (*Olea europea* L., cv Coratina) grove in southern Italy. Stand density was characterized by stocking density of 132 trees ha^{-1} and mean spacing of 8.71 m. Mean social (territorial) area (proportional to spacing and

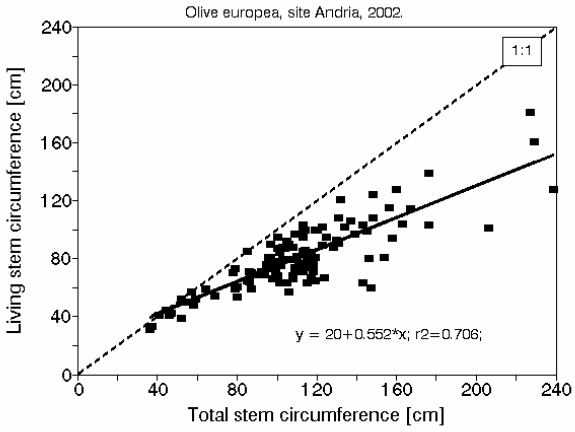

tree stem size) was about 76 m^2 per tree. Total stem circumference for the main tree reached 110 cm and living stem circumference (after subtraction of missing or dead parts of stems) for the main tree reached 81 cm. Relationship of total and living circumferences in trees of different size is shown in **Figure 1.** Projected area of tree crowns reached mean of 17.7 m^2 (23% of the social) and mean tree height of 4.9m. Mean leaf area was about 5 cm^2 and was distributed in a log-norm manner in the

wide range of 2 to 12 cm^2, which characterize old fully developed leave as well as young leaves (**Figure 2**). When considering whole tree crowns, mean leaf density was about 2.6 m^2m^{-3}. Maximum leaf area occurred in canopy layers between 1.5 to 3 m above ground, tailing with a steeper slope to the crown base and less steep slope to the tree-top. It ranged

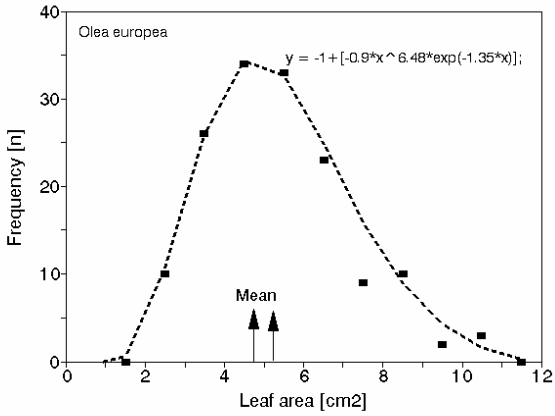

approximately between 4 to 13 m^2 per 0.5 m^{-1} canopy layers in trees of different size. Foliated volume of olive crowns (reaching mean of 33.2 m^3) contained in average 127 thousand leaves of the total area of 63.6 m^2. Tree crowns represented about 9% of the potential phyllosphere (when taking into account stand area and mean tree height).

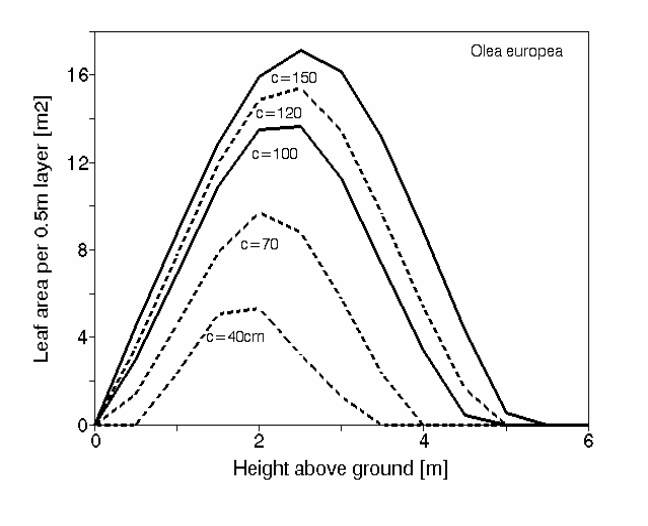

Vertical distribution of leaf area (in 0.5m deep layers) is demonstrated in individual olive trees (examples of trees with different stem circumference, c at 1m, ranging from 40 to 150 cm) - **Figure 3**.

Radial pattern of leaf distribution derived from image analysis indicated peak LAI_{rad} values at about 60 to 70% of crown radius in trees of different size. This should be considered when evaluating remote sensing images. Leaf density under apparent „disks“ is regularly and substantially different.

Corresponding leaf area index on the stand level (LAI_{grove}=0.96), was rather low (e.g. when comparing to closed canopy forests) due to low stocking density of the entire olive grow (**Figure 4**). However when taking into account only the projected crown areas (and avoiding free space between trees), the mean LAI reached about 3.5 ranging between 1 and 7, with very high variation between individual trees.

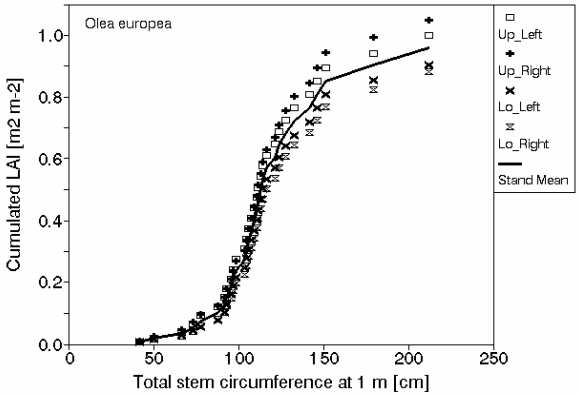

Main biometric parameters of individual whole olive trees and entire orchard and their leaf distribution represent an important structural background for evaluating different physiological processes including water relations and production.

11b

LEAF AREA DISTRIBUTION MEASUREMENTS IN SOLITARY GROWING OLD TREES

J. ČERMÁK[1], J. GAŠPÁREK[1], F. De LORENZI[2], H.G. JONES[3]

[1] *Institute of Forest Ecology, Mendel University of Agriculture and Forestry, CZ 61300 Brno, Zemědělská 3, Czech Republic. (corresp. cermak@mendelu.cz).*

[2] *Institute for Mediterraean Agro-Forestry (ISAFOM-CNE), Via Potacca 85, 80056 Ercolano (NA) Italy.*

[3] *School of Life Sciences, University of Dundee at SCRI, Scottish Crop Research Institute, Invergowrie, Dundee DD2 5DA, United Kingdom.*

Keywords: geometric model, side photo-image, image analysis

ABSTRACT

Irrespectively of long-term growing of olive trees in Mediterranean countries, little is known about leaf distribution in old solitary growing trees in the orchards. Leaf area distribution was estimated using a combination of two approaches: a simple composite geometrical canopy-layer model and ground-based side images evaluated by the image analysis software. This distribution was evaluated separately in a vertical direction, which is particularly important for physiological studies and in a radial direction, which is important for interpretation of remotely sensing images.

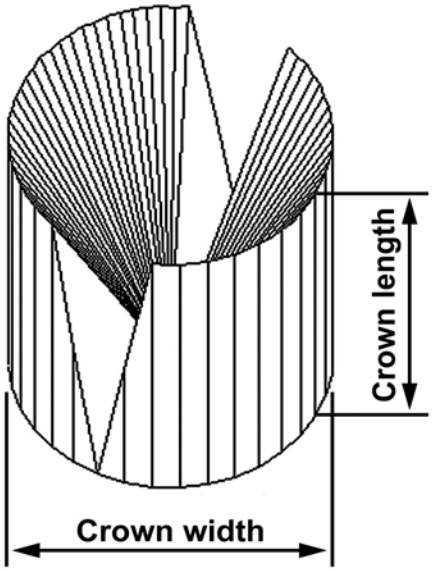

The geometric canopy-layer model, took into account the total volume occupied by crowns, an empty space within this volume (due to regularly severed branches in mid crown by pruning) and an actual volume actually occupied by foliage. (a) The crown volume was calculated as a cylinder volume (V_{cyl}), taking into account crown projected area and a crown length calculated as the difference between heights of crown top and crown base. (b) A volume of an overturned cone (V_{con}), represented the unbranched area at the center of the tree canopy and it was subtracted from the cylinder volume. (c) In addition a volume of the core (V_{cor}) amounting ¼ of the calculated volume was also subtracted (this simulated the regularly removed branches from the crown in the direction of the watering pipeline, which passed through the crowns). Scheme of the geometrical model of an olive crown composed of the cylinder volume, from which is subtracted volume of overturned cone (opened by regular pruning) and volume of the core (opened for watering pipeline) is shown in **Figure 1**.

Leaf area density was measured on a series of about 700 shoots growing on small and large branches. Leaves were counted on each numbered shoot and their area was estimated on a series of sub-samples. There were about 54000 leaves on sampled branches with the overall mean leaf density of 2.56 +-0.31 m^2 m^{-3}, i.e. +- 12%. The vertical distribution of leaf area was

calculated for layers of the canopy 0.5 m deep using a double Gaussian curve, where **y** = leaf area per 0.5 m deep canopy layer and **x** = height, whose parameters have clear physical meaning (**a,d** = amplitude; **b,e**= width ; **c,f** = position, **g**= shift) and can be easily estimated.

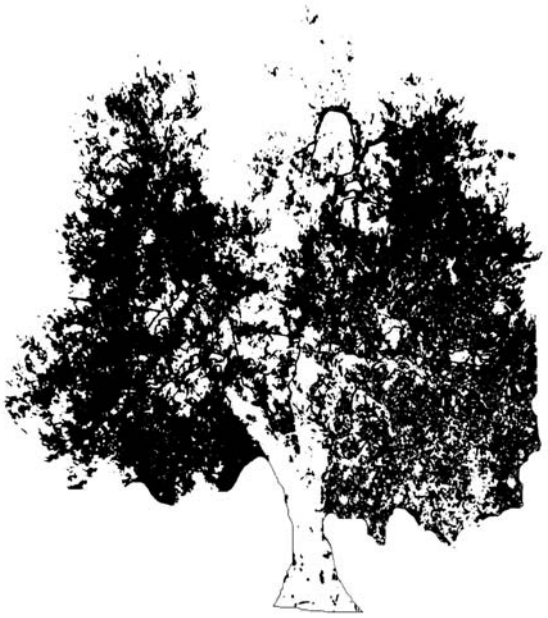

When applying the image-analysis method, entire crowns of 26 trees were photographed, selected crowns whose images did not overlap with other crowns behind them were digitized and the images were analyzed in terms of foliage density using an image-analyzer. The branches where leaf density was analyzed were used for calibration of entire crown images. Images of whole tree crowns and separately of measured branches were prepared by deleting some interfering parts of images and adjusting contrast and brightness, if necessary. Then the images were converted to a binary form and we counted numbers of black and white pixels by the special software (Image Tool, version 3.0, The University of Texas Health Science Center in San Antonio) - Olive tree branch image against free sky and when converted to a binary form is shown in **Figure 2**. Full black objects (branches) and large white areas of the image were hand marked; their area in pixels was counted and subtracted. In this way the final ratio of black and white pixels was estimated and the black area was expressed as image density in percentage of its total area. This was expressed the same way as in the model in 0.5 m layers and used to estimate the general pattern of vertical leaf distribution.

Radial leaf distribution was derived approximately from the same images as used for the vertical distribution, taking account of true crown geometry: tangential view visible on images was converted to a radial according to the scheme shown in **Figure 3**. In addition, radial leaf distribution was also assessed indirectly from measurements of the throughfall across crown and rainwater holding capacity of foliage.

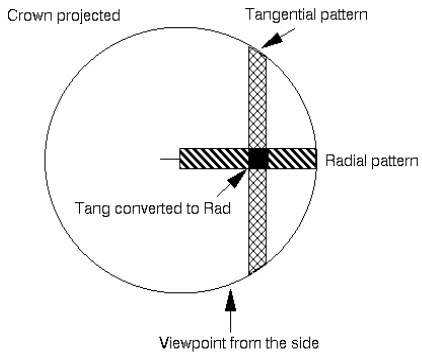

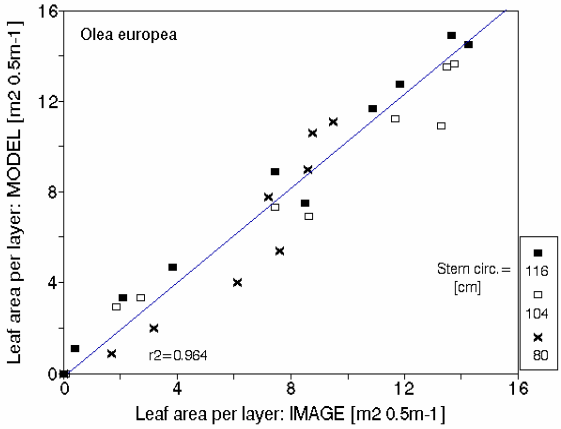

Results of both methods were very similar as demonstrated in three trees of different size on **Figure 4**.

The above methods allow characterizing leaf distribution in canopy layers in vertical (axial) and radial directions quantitatively in a rather fast way and provide a background for many following applications in the orchards and/or sparse plantations.

12

GENERAL OVERVIEW ON WATER MANAGEMENT

Carlos Manuel Martins PAIS

IDRHa - DSRNAH/DHAQA

cpais@ihera.min-agricultura.pt

ABSTRACT

Water is maybe the main natural resource, due to the indispensability to life existence. Additionally to this "vital" component, there is a myriad of economical, social, territorial and political values, over which are defined some of the main contemporary concepts, as "development" and "sustainability".

Globally, water is not a scarce recourse. But the water availability is highly variable, and some even limited, accordingly spatial and time variables.

Human activity, or in a more consistent way, civilisation, added a new concept to the naturalness of the water resource, based on the satisfaction of the water demand, in compliance with quality standards. The increase on the water demand, under the pressure of degradation factors to its quality status, shown that water is no more a usable good, as it is a economical one, for which planning and management plays a vital role.

During the last two decades, concerns on water resources management drive to the establishment of a legal framework at European level, somehow dispersed, in order to deal with single problems, which has been transposed to member states. The lack of a integrated approach drives to the need for the establishment of a "Water Framework Directive", putted in force by the 2000/60/CE Directive, with the purpose of establish a framework for the protection of inland waters, transitional waters, coastal waters and groundwater.

As important point, it must be noted that this Directive was outlined as a water quality instrument, but with definitive repercussions both on water qualitative and quantitative issues, as also it becomes the main water management instrument to comply with in the future, at European level.

The Portuguese mainland features are clearly Mediterranean. Irrigated agriculture plays the major role on water use, demanding for something like 87% of the total national water demand (6550 x 10^6 m^3/year). This figure, under the frame of the economical good which

water represent nowadays, highlighted the importance of increasing of water use efficiency in agriculture.

By other hand, under the described climate conditions, estimation of woody crops water requirements turns to be a major concern, viewed both as irrigated crops as also as natural stands to be adequately managed, under a ecological point of view.

So, not only good legal instruments are needed for enhance water management, but also easy to use tools must be available for water managers and for end users. The WATERUSE project deliverables will be a contribute to enhance the ability of water planners and users to better understand the water relations between soil, woody crops and the atmosphere, aiming to promote the increase of water use efficiency.

The Institute for Rural Development, and Hydraulics (IDRHa), partner of the project, is the main official institution dealing with water use in agriculture, acting as a regulator, water manager, and also on promoting of the building and maintenance of the main public irrigation schemes. Some figures on the main tasks as also the projects in development are shown.

13a

COMBINATION OF TRANSPIRATION AND EVAPOPTRANSPIRATION TECHNIQUES

INTRODUCTION

Mª Isabel F. R. FERREIRA

Full Professor, Instituto Superior de Agronomia - UTL, Tapada da Ajuda, 1349-017, Lisboa, Portugal, +351.21.3653476
isabelferreira@isa.utl.pt

In many regions with mediterranean climate (e.g., Southern Europe) water scarcity has resulted in dominant stands of woody plants that can withstand water deficits. Agroforestry systems, most of the vineyards and many orchards (some olive, carob, almond trees) are not irrigated. Other orchards are irrigated and appropriate water management is crucial to maintain system sustainability. However, because of a lack of appropriate sensors and models to study the systems, there is a lack of knowledge on evapotranspiration (ET) of such stands.

The classical approaches to measure ET include micrometeorological methods making use of flux-gradient relationships or eddy covariance (EC) data, and hydrological methods applied in different space scales, which generally require measurements on changes of water content in the root zone. The flux gradient and EC methods require expensive equipment and the height, anisotropy and/or roughness of the canopies are a limitation. For all micrometeorological methods there is a requirement of relatively large, uniform areas. Thus, in areas with heterogeneity, as it is the case of small fields of woody crops, there are limitations concerning the measurement of ET.

For larger time scales, the use of hydrological methods can be an alternative if it is possible to characterize the root zone. In many cases, this is almost impossible because some of the active roots are too deep and too difficult to locate with sufficient accuracy. Even in irrigated orchards sparse, deep roots played an important role in water uptake, namely during periods of moderate stress (Ferreira et al., 1997); to identify their position and correspondent volume of exploited soil, became a limiting factor for the estimation of ET based on soil water measurements.

Concerning ET modelling, the currently available approaches were developed for uniform low cover crops and are not applicable without modification for vegetation with complex architecture of roots and shoots. Yet, even the single-layer agrometeorological method of Penman-Monteith (Monteith, 1965) requires data on the canopy resistance of the vegetation, controlled by stomatal conductance (g_s). In the case of ET not limited by water supply, an indirect approach by means of reference evapotranspiration (ETo) and the crop coefficient (Kc) is often used. Unfortunately, the adequacy of the currently available crop coefficients to orchards of variable geometry is often questionable (see, for instance, Paço et al., in this volume).

For sparse or discontinuous canopies and for crops experiencing water stress, stomatal control has more impact on ET then for irrigated and/or low crops (Jarvis & McNaughton, 1986) and thus g_s variability in space and time has to be taken into account to determine the ET of orchard crops. Either the study of the stress effects on ET or the calibration of Kc's require good quality ET data.

The availability of sap-flow sensors (see e.g Cohen, *et al.*,1985; Sakuratani, 1981; Valancogne e Nasr, 1993, Granier, 1985,1987) has opened up opportunities for the estimation of transpiration (T), which is typically the main component of ET, especially in arid environments. These techniques can be extended to understand the environmental control of transpiration and to investigate the responses of T to different treatments (e.g. irrigation, fertiliser, pruning, etc). They also allow the estimation of water uptake from different root zones. Data measured on the whole tree level are scaled up to stands and often compared with data obtained by other techniques. However, none of the sap flow methods seem to be able to provide good absolute values in all circumstances.

The challenge is how to obtain long term, inexpensive and reliable data on T or ET of woody crops, even in small areas where micrometeorological methods cannot be applied. This paper shows how to possibly overcome this difficulty. The strategy used is to combine eddy covariance (EC) and a currently available, low-cost sap flow (SF) method to obtain a relationship that can be extended in space or time.

The following three contributions serve as case studies on the use of a combination of EC and SF methods to quantify ET of small areas and/or to obtain long term T estimations.

13b

COMBINATION OF TRANSPIRATION & EVAPOTRANSPIRATION TECHNIQUES – PART B - APPLICATION ON IRRIGATED PEACH ORCHARD

Teresa A. do PAÇO[1], Mª Isabel F. R. FERREIRA[2], Nuno CONCEIÇÃO[3]

[1]*Post-doc research fellow, Instituto Superior de Agronomia - UTL, Tapada da Ajuda, 1349-017, Lisboa, Portugal, +351. 21.3653335,* tapaco@isa.utl.pt

[2]*Full Professor, Instituto Superior de Agronomia - UTL, Tapada da Ajuda, 1349-017, Lisboa, Portugal, +351.21.3653476* isabelferreira@isa.utl.pt

[3]*Agricultural Engineer, Instituto Superior de Agronomia - UTL, Tapada da Ajuda, 1349-017, Lisboa, Portugal, +351.21.3653335* ***nuconceicao@yahoo.br***

Keywords: Evapotranspiration, Peach, Sap flow, Irrigation, Crop coefficient

---

ABSTRACT

The overestimate of irrigation requirements leads to water waste, with increased production costs and undesirable consequences to environment and to natural resources management. The improvement of water productivity in agriculture could be achieved by enhancing efficiency and precision in irrigation scheduling. Approaching water requirement estimates to real water needs can provide this and, for some woody crops, there is still a margin for improvement. This adequateness of irrigation volumes to irrigation requirements is tightly connected to the knowledge of crop evapotranspiration (ET). For woody discontinuous crops, ET measurement presents more difficulties than for short and homogeneous crops and a fewer methods are available. Given the lack of information on ET, estimates can show some deviations. The direct measurement of ET can play a role in the improvement of estimate methods, which are useful in regional applications and at farm level, if the difficulties with the methods can be overcame, for example, using a combination of them. This paper deals with the application of combined techniques to quantify water use in peach.

The present case study results from experimental work carried out in a peach orchard (*Prunus persica* (L.) Batsch), in central Portugal (lat. 38º 42' N, long. 8º 48'), during the summers of 1998 and 1999.

ET was directly measured by the eddy covariance micrometeorological method for short periods during the irrigation season, while tree transpiration (T) has been obtained for long-term periods using the sap flow heat dissipation method of *Granier* (Granier, 1985). The *Granier* method provided an underestimated transpiration of about a 1/5 of transpiration, obtained from ET_{ec} (ET measured by eddy covariance method) by subtracting soil evaporation (E_s). Nevertheless, there was a clear correlation between both sets of results, indicating that sap flow measurements, even if underestimating, were sensitive enough to follow the trends in T.

ET_{ec} was then used as a reference to quantify ET for several months, departing from sap flow automated measurements and microlysimeter soil evaporation (E_s) measurements. The equations relating ($ET_{ec} - E_s$) and T were $ET_{ec} - E_s = 1/(-2.19 + 3.77e^{-T_G})$ (r^2 = 0.89) and $ET_{ec} - E_s = 0.75/(-1.69 + 3.38e^{-(T_G + 0.08)})$ (r^2 = 0.95) for 1998 and 1999, respectively (differences were probably due to reduced sampling). This approach allowed the use of the continuous

records of sap flow to estimate ET, for the whole season, with a low cost and good reliability (Figure 1). Mean evapotranspiration was about 2 mm/day, mean measured soil evaporation was close to 0.3 mm/day and mean measured crop coefficient (K_c) was close to 0.5, for the considered periods. The K_c was lower than the K_c advised for this crop in the FAO (*Food and Agriculture Organization*) *Irrigation and Drainage Paper 56* (Allen *et al*., 1998), either tabled (0.9) or calculated using a basal crop coefficient (0.7). This discrepancy means that the crop coefficients given directly from *FAO 56* may need to be confirmed for local conditions, as it has been observed also in other irrigated orchards in Portugal (peach and kiwifruit).

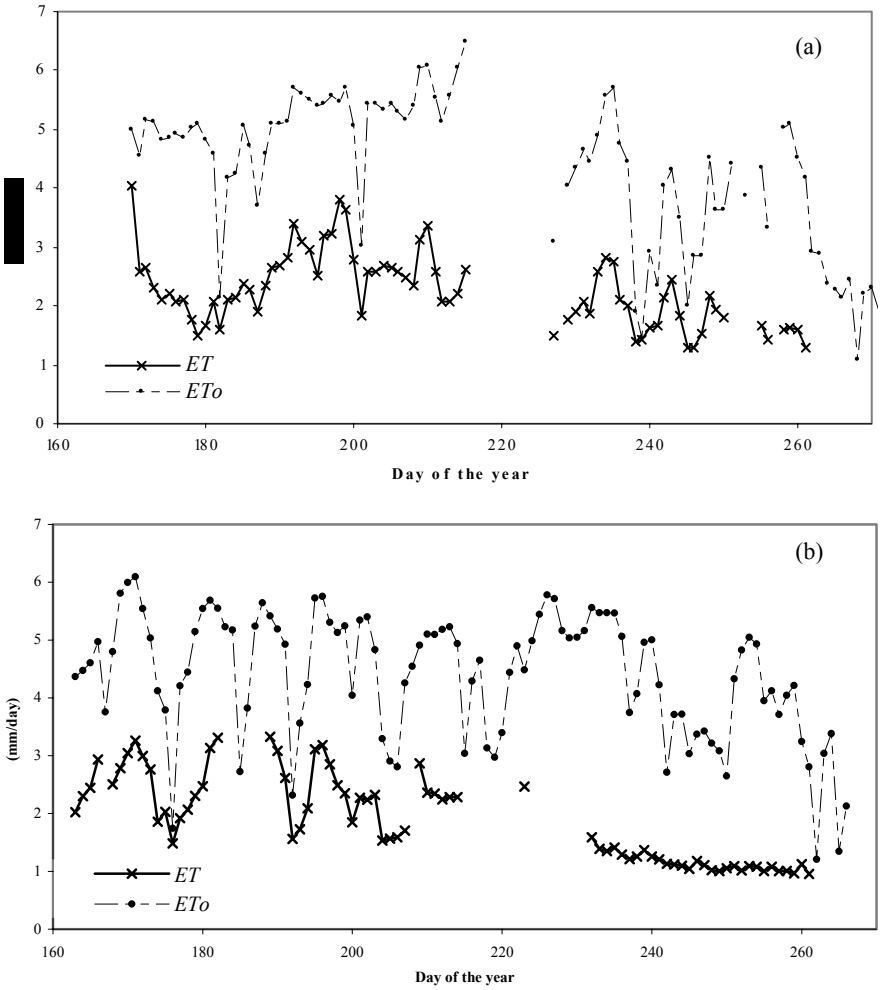

Figure 1 - Evapotranspiration (ET) estimates obtained from transpiration (sap flow measurements) and soil evaporation, using ET measured by the eddy covariance technique as a reference; ET_o - reference evapotranspiration; (a) 1998, (b) 1999.

REFERENCES

Allen, R.G., Pereira, L.S., Raes, D. & Smith, M. (1998). *Crop Evapotranspiration Guidelines for Computing Crop Water Requirements*. FAO Irrigation and Drainage Paper 56. Rome, Italy, 300 p.

Granier, A. (1985). Une nouvelle méthode pour la mesure du flux de sève brute dans le tronc des arbres. *Annales des Sciences Forestières*, 42, 193-200.

13 c

COMBINATION OF TRANSPIRATION & ET TECHNIQUES – APPLICATION ON VINE

José SILVESTRE[1], Mª Isabel F. R. FERREIRA[2]

[1] *Research assistant, INIAP. Estação Vitivinícola Nacional. Quinta da Almoínha, 2565-191 Dois Portos, Portugal, inia.evn.viti@oninet.pt,*

[2]*Full Professor, Instituto Superior de Agronomia - UTL, Tapada da Ajuda, 1349-017, Lisboa, +351.21.3653476 isabelferreira@isa.utl.pt,*

Keywords: Evapotranspiration, Transpiration, Sap flow, *Vitis vinifera* L., Granier method

---

ABSTRACT

Sap flow methods are very useful and well spread techniques applied in water use studies, in particular for woody crops where experimental and modelling limitations are more important then for low crops. However, some limitations appear when the objective is to obtain absolute transpiration (T) values, being gravimetric calibrations difficult to implement in woody plants. Furthermore, the experimental conditions are usually different from field conditions and due to the reduced leaf area of pot plants, flow rates are relatively low when compared with field conditions. Since none of the existing sap flow methods seems to be able to be used as reference, one alternative is to compare sap flow with evapotranspiration (ET) values (obtained with micrometeorological methods). This solution is valid for periods with reduced soil evaporation. Otherwise, an estimate of soil evaporation is also needed. This paper deals with the application of combined techniques to quantify water use in vine.

A comparison between sap flow obtained with the *Granier* method (Granier, 1985) and ET obtained with the eddy covariance method (EC) was made for periods of dry soil surface. Two experiments were made with different types of soils and vine varieties. Measurements were performed in a vineyard cv. "Trincadeira" in a deep clay sandy loam soil during 1996 and 1997 and in a vineyard cv. "Syrah" in a sandy soil during 2001 and 2002. No limitations of fetch occurred in both sites and the accuracy of eddy covariance data was evaluated by footprint analysis, spectral analysis and energy balance closure.

Sap flow was followed in four vines in 1996 and 1997 (cv. "Trincadeira") and at least nine vines in 2001 and 2002 (cv. "Syrah"). Sap flow results showed great heterogeneity between individuals. Considering the low sampling, up-scaling was adjusted based on estimates of the individual leaf area and the average leaf area for the stand. The results suggest that this method is quite suitable to qualitatively follow vineyard transpiration.

For periods with reduced soil evaporation, the comparison between sap-flow (SF) and EC values showed a strong underestimation of sap flow rates, both for daily and hourly values, being more important at high flow rates. This underestimation was also confirmed by gravimetric calibrations and by comparison with sap flow rates measured with a stem heat balance method. The equation correspondent to the relationship between SF (total daily values from *Granier* method, Gr) and T measured by EC method during periods of dry soil surface (Es=0) for cv. "Trincadeira" (1996, 1997) and "Syrah" (2001, 2002) is T=1.1* Gr^1.5

($r^2 = 0.84$), for T within the limits shown in figure 1 (T roughly between 1 and 3 mm.day^{-1}, Silvestre, 2003).

This combination of SF and EC methods was made in two different situations and in two years each, so, the relationship found was used to extend T estimates based in *Granier* sap flow measurements for longer periods and also to estimate T in small areas where the EC measurements where not possible (Ferreira and Silvestre, 2004).

The relationship between the SF and EC was used to estimate T in three vineyards differing in relation to soil type, grape cultivar and local climate. At Santarém (cv. Trincadeira, in a deep clay sandy loam soil), T ranged between 4 mm day^{-1} and 0.5 mm day^{-1}, for the period between floraison and maturity. At Setúbal (cv. Syrah, in a sandy soil), T ranged between 2 mm day^{-1} and 0.5 mm day^{-1}, for the same period. In a third vineyard (Alenquer, cv. Castelão, loamy soil), T was measured along a vegetative cycle at 3 locations with different slopes and same aspect (3%, 10% and 17%). Maximum values for T were 3 mm day^{-1} (at floraison), with some variations between slopes.

REFERENCES

Granier, A. 1985. Une nouvelle méthode pour la mesure du flux de sève brute dans le tronc des arbres. *Annales des Sciences Forestières*, 42, 193-200.

Ferreira, M.I, and Silvestre, J. Medição da transpiração em cobertos descontínuos. Vinha em diferentes declives na região Oeste. In: *APRH* (eds.), *Actas do 7º Congresso da Agua*.

Silvestre, J. 2003. *Evapotranspiração e funcionamento hídrico em Vitis vinifera L.* Dissertação de Doutoramento, Instituto Superior de Agronomia, Universidade Técnica de Lisboa, Lisboa 222 pp.

FIGURES

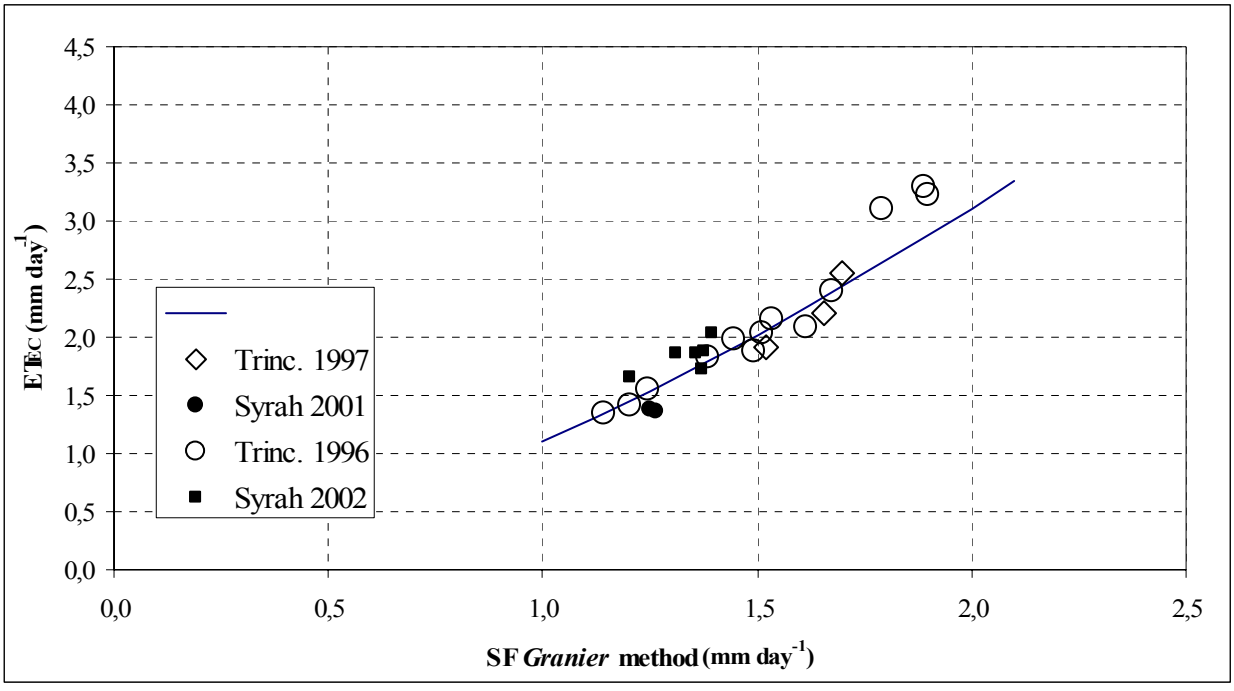

Figure 1 - Relation between evapotranspiration (eddy covariance method) and sap flow (*Granier* method) for periods of negligible soil evaporation.

13 d

COMBINATION OF TRANSPIRATION & ET TECHNIQUES - APPLICATION ON KIWI

Rodolfo M. SILVA[1], Mª. Isabel. FERREIRA[2], Mª. Teresa. PAÇO[1], Anabela VELOSO[3]
Manuel OLIVEIRA[4]

[1] *Ph.D. student, Instituto Superior de Agronomia - UTL, Tapada da Ajuda, 1349-017, Lisboa, +351. 213653335, rodolfo@isa.utl.pt*
[2] *Full Professor, Instituto Superior de Agronomia - UTL, Tapada da Ajuda, 1349-017, Lisboa, +351.21.3653476 isabelferreira@isa.utl.pt*
[3] *Técnica superior de 1ª classe, Divisão de Vitivinicultura e Fruticultura – DRAEDM, Quinta de Sergude, Sendim, 4610-764 Felgueiras, +351.255.312455*
[4] *Técnico superior de 2ª classe, Divisão de Vitivinicultura e Fruticultura – DRAEDM, Quinta de Sergude, Sendim, 4610-764 Felgueiras, +351.255.312455 dvf@draedm.min-agricultura.pt*

Keywords: Evapotranspiration, *Actinidia deliciosa*, Eddy covariance, Sap flow, Crop coefficient

---

ABSTRACT

The kiwi vine (*Actinidia deliciosa* A. Chev.) assumed a growing importance in the *Entre Douro e Minho* (EDM) region in the last years. Being a recent crop in Portugal and in Europe, there is a lack of instrumentation to support water management decisions, with its known implications in water deficit or in nutrient percolation, and in energetic overusing.

It is known that irrigation is essential for these crops under Mediterranean climatic conditions, but it is frequently excessive.

With the aim of determining the water requirements of this crop, evapotranspiration (ET) has been measured in a kiwi vine – Var. 'Hayward', with a plantation distance of 5 x 5 meters (T – bar training system) and irrigated with micro sprinklers. The experimental site was near Guimarães (41º 31' N, 8º 27' W). The results shown are from the year 2003.

ET was measured with the eddy covariance technique, transpiration (T) was measured by sap flow and the understorey water losses were measured by microlysimeters. Sap flow measurements started at the beginning of the vegetative cycle, using the ET and Es measurements to adjust T estimates, upscaling the sap flow measurements to the stand level.

The understorey evaporation (soil + grass) was 15 to 20 % of total ET. These low values (obtained when the wetted soil was 25%) reflect the low vapour pressure deficit at the ground level.

ET ranged from 3 to 4 mm/day, in the middle of the vegetative cycle (August) and the crop coefficient (Kc) for this period was 0.7 to 0.8, lower than the 1.05 value, given by FAO (Allen *et al*., 1998) for this crop.

REFERENCES

Allen, R.G., Pereira, L.S., Raes, D. & Smith, M. (1998). *Crop Evapotranspiration Guidelines for Computing Crop Water Requirements*. FAO Irrigation and Drainage Paper 56. Rome, Italy, 300 p.

15a

SEASONAL TRENDS OF TRANSPIRATION FROM OPEN *QUERCUS ILEX* STANDS (*MONTADOS*): A COMPARISON BETWEEN TWO SITES IN SOUTHERN PORTUGAL

Teresa S. DAVID[1], Jorge S. DAVID[2], Manuel O. HENRIQUES[2], M. Isabel FERREIRA[2], Shabtai COHEN[3], João S. PEREIRA[2]

[1] *Estação Florestal Nacional, INIAP, Quinta do Marquês, Av. República, 2780-159 Oeiras, Portugal*
teresa.david@com.pt , +351.21.4463737

[2] *Instituto Superior de Agronomia, UTL, Tapada da Ajuda, 1349-017 Lisboa, Portugal*
soaresdavid@isa.utl.pt , +315.21.3653493
isabelferreira@isa.utl.pt , +315.21.3653476
jspereira@isa.utl.pt , +315.21.3653483

[3] *Institute of Soil, Water and Environmental Sciences, A.R.O., P.O.Box 6, Bet Dagan, 50250 Israel*
vwshep@agri.gov.il , +972.3.9683701

Keywords: Transpiration, Sap flow, Leaf water potential, Hydraulic conductance, *Quercus ilex*, *Montados*

ABSTRACT

Mediterranean evergreen oak woodlands of southern Portugal are adapted to a strong seasonality in climatic conditions, particularly to irregular annual water availability and long and dry summers. Nevertheless, increase in tree mortality has been observed and may be ascribed to enhanced climatic drought, due to global warming, pathogens and deleterious management practices. Therefore, strategies for the conservation and management of *montados* should be improved, aiming at long lasting sustainability.

This study reports on a long-term study of tree water use carried out in (b) open holm oak stands, located near Évora (32º 38'N; 8º 00'W). Holm oak is the dominant tree species in the drier eastern inland areas of southern Portugal. The study aims at a better understanding of holm oak strategies to cope with summer climatic constraints. Measurements of sap flow, leaf water potential, environmental variables, estimation of whole-plant hydraulic conductance and water table level monitoring were conducted in the experimental plots, 3 km apart from each other. Tree density is low, about 20 to 45 trees/ha. The understory consists of a mixture of shrubs and grasses, dominated by *Cistus* spp. In site 1, measurements took place from 1996 to 1998. The soil is a shallow (30 cm deep) *Distric cambisol* overlying a fractured gneiss rock, with a permanent water table at around 13 m depth. In site 2, the experiment was performed from 1998 to 2003. The soil of site 2 is around 1 m deep, established on a granitic bedrock. In this site the water table level fluctuates between 1.5-2 m depth in winter and 5 m in summer. Stand tree age varies between sites: in site 1, trees are around 90 years old and, in site 2, around 65 years old. During the experimental period, rainfall was higher than average. In site 1, holm oak trees remained well watered throughout the year and there was no evidence of water stress during the summer drought. Sap flow rates peaked in summer and predawn leaf water potential was high throughout, with no significant seasonal variations. In site 2, trees suffered from water stress in late summer: sap flow was greatly reduced in late summer and predawn leaf water potential decreased to –1.7 MPa. In both sites, daily minimum leaf water potential was similar, around –3/–3.2 MPa. Therefore, the summer sap flow driving force (predawn leaf water potential minus minimum leaf water potential) was

higher in site 1 than in site 2. Whole-tree hydraulic conductance was of a similar magnitude in both sites, without evident variations during the summer drought. The seasonal trend of daily tree transpiration, observed in site 1, followed closely the patterns of solar radiation and vapour pressure deficit, and was not related to the seasonal distribution of rainfall. In site 2, the seasonal variation of daily tree transpiration was strongly influenced by rainfall seasonality: sap flow peaked in spring, decreased as summer drought progressed and recovered after the onset of autumn rainfall. The relationship between daily tree transpiration and vapour pressure deficit showed a typical asymptotic shape, with well-defined plateaus for maximum daily tree transpiration. In site 1, this relationship was unique over the entire experimental period whereas, in site 2, a marked seasonal variation was notorious: an absolute maximum plateau occurred in spring, followed by a minimum in summer and an intermediate plateau in autumn, after precipitation. All evidence suggests that, in site 1, the trees have a continued access to the ground water reservoir at 13 m depth, avoiding summer drought conditions. In this site, tree transpiration was mainly driven by the evaporative potential of the atmosphere (solar radiation and vapour pressure deficit). In site 2, root access to groundwater seems to be partially disrupted in summer, as evidenciated by the decrease in both predawn leaf water potential and tree transpiration. In this plot, the seasonal trend of transpiration seems to be more determined by the topsoil moisture and rainfall distribution in time, than in site 1.

Results suggest that root access to groundwater in summer was less efficient in site 2 in spite of the shallower water table level. Tree age and the magnitude of bedrock fracture may explain the differences in seasonal water use patterns between sites. It is well known that evergreen trees, which must survive a hot and dry season, frequently rely on the direct access of roots to permanent water tables. Our results from site 1 suggest that this may also be the case of holm oak trees in southern Iberian Peninsula. However, the comparison between sites shows that tree access to groundwater sources may be highly variable, depending on local hydrogeological conditions. Since a correct inference of summer tree transpiration will depend on the belowground conditions of *montados*, further research is needed to identify with more precision the sources of water uptake by oak trees in southern Portugal, at a regional scale.

15b

SEASONAL CHANGES IN WATER USE OF EVERGREEN OAK WOODLANDS

PART B – EVAPOTRANSPIRATION AND TRANSPIRATION FROM A *QUERCUS SUBER* STAND (*MONTADO*) IN THE REGION OF LISBON

Mª Isabel F. R. FERREIRA[1], Rodolfo Miranda SILVA[1]

[1] *Full Professor and Ph D student, Instituto Superior de Agronomia - UTL, Tapada da Ajuda, 1349-017, Lisboa, Portugal, +351.21.3653476/3335, isabelferreira@isa.utl.pt, rodolfo@isa.utl.pt*

Keywords: Evapotranspiration, Transpiration, Eddy covariance, Sap flow, Cork oak, *Montado, Granier* method

ABSTRACT

Evapotranspiration (ET) estimates from heterogeneous crops are scarce. Often, in such stands, the quantification of the water balance components is limited by the difficult accessibility to roots that, in ecosystems with Mediterranean climate, have an important role during stress periods. It is partially because of the deepness of part of their root systems that many trees and shrubs are able to withstand the extremes of wet and dry seasons during the year, characteristics of such climate. Cork oak (*Quercus suber*) is the dominant tree species in the southwest of Portugal and Europe, where it occupies about 30% of the total world area for this species. These ecosystems (*montado,* dominated by *Quercus suber* and *Quercus rotundifolia*) are endangered and this can be partly related with changes in the local water cycle. The interdisciplinary study made in the frame of the WATERUSE project aims at a better understanding of the cork oak strategies to cope with dry summer conditions. This contribution describes the results on the water use of a cork oak stand, during one cycle of soil dehydration.

The field plot (38°38' N 8°51' W, 30 m) is located between Lisbon and Setúbal and the estuaries of Tagus (*Tejo*) and Sado rivers. The trees are 80-100 years old, the plantation distance 10 x 11, the density 76 and 66 trees/ha (2001 in 2003, respectively), the average height, 10 to 12 m, the understorey being dominated by several *Cistus*. The climate is Mediterranean with Atlantic influence (precipitation 750 mm/year, maximum in Winter, around zero in July). Average temperature is 16.1°C, average minimum (January) 5.3°C and average maximum (August) 28.9°C. The soil is sandy derived from moderately deep sandstone, with some gravel, compact, very low carbon content and available water.

The components of energy balance, including ET, were recorded using the eddy-covariance method (EC). Transpiration (T) was recorded in 18 points (10 trees), in the area of influence of EC measurements, using the so-called *Granier* method. ETo was calculated from data from a nearby station.

The closure error for the energy balance equation ranged between 10% and 15% along the season, so the results were considered of good quality. Four periods (A to D: May, June, July and September) were identified in the analysis of the relationship between ET, T and reference ET (ETo) with ET/ETo of 0.78, 0.37, 0.24 and 0.21 respectively, T/ETo of 0.20, 0.18, 0.13 and 0.13 respectively and T/ET of 0.25, 0.49, 0.51 and 0.61 respectively. ET was close to ETo at the beginning of May and close to T at the end of September. During July, T was apparently decoupled from changes in atmospheric conditions, while after rain (occurred until late April, with a short event in late August), the response was very clear. The descriptive analysis presented here will be followed by an interpretative analysis about the role of roots (contribution C, in this session) in relation to water status.

15c

SEASONAL CHANGES IN WATER USE OF EVERGREEN OAK WOODLANDS

PART C - SAP FLOW IN ROOTS AND STEM OF *QUERCUS SUBER* TREE

Nadezhda NADEZHDINA[1], Maria Isabel FERREIRA[2], Rodolfo SILVA[2], Carlos Arruda PACHECO[2]

[1] *Institute of Forest Ecology, Mendel University of Agriculture and Forestry, Zemedelska 3, 61300 Brno, Czech Republic*

[2] *Instituto Superior de Agronomia, T. University of Lisbon, Tapada da Ajuda, 1349 017 Lisboa, Portugal*

ABSTRACT

It is well known that water can move passively from wet to dry soil zones via roots according to gradients of water potential, in order to ensure appropriate management of water by plant. Different types of hydraulic redistribution were reported: vertical upward transfer of water from deep to more dry shallow soil layers; downward transport or inverse hydraulic lift, horizontal redistribution of water via relatively superficial lateral roots. Which mechanisms are relevant for non irrigated stands in Mediterranean climate?

The aim of this study was to analyse the mutual interaction between soil, atmosphere and plants in a *Quercus suber* stand trying to understand the water uptake strategy of this species during the period of summer drought. Sap flow techniques, as the best tools for examining hydraulic redistribution in root systems, have been used from late Winter to early Autumn 2003 (Rio Frio, near Lisbon), in order to access the seasonal variation of tree water uptake. The heat field deformation, HFD, method was applied for sap flow measurements in five small shallow roots (diameter of 3-4 cm), 1 to 2 m distant from the tree trunk. Sap flow was also measured in four azimuths and different xylem depths at the stem base, using multi-point HFD sensors.

The pattern of sap flow differed among the five lateral roots measured. Two of them demonstrated reverse flow during night, followed by positive flow during daytime. Reverse flow is a typical primary component of hydraulic lifting from the lower to the upper soil layers through roots. Lifted water may provide moisture that facilitates favourable biogeochemical conditions for enhancing mineral nutrient availability and microbial processes. Reverse flow started to occur in one root from the middle of June, when mean water potential in upper horizons (15-85 cm) dropped below 120 hPa (Figure 1). Then, this negative flow gradually increased in July and practically did not change till rain occurred at the end of August. Reverse flow in the second root started from the middle of August and was observed also until rain. Reverse flow was stable from the evening until the following morning, what is consistent with limiting level of water availability in soil. Rainfall modified the pattern of flow by eliminating reverse flow in the superficial roots and by significantly increasing their uptake for transpiration (Figure 1). Reaction of these two roots to rain events was clearly higher then for the three other superficial roots. These later continued to absorb water during all period without reverse flow recorded. The highest flow in those three roots was recorded during drought period. Contrary, when soil was wet (March-April and the beginning of September) flow was higher in the two roots that demonstrated evidence of

hydraulic lift during dry period. The best relationship was found between sap flow in one of the root (with hydraulic lift observed) and the outer stem xylem layer (5 m below cambium) from the corresponding tree side. The flow in this stem xylem layer progressively decreased with drought developing in soil, suggesting correspondence of this layer with the most superficial soil horizons.

The best relationship, between flow in one of the roots (where no hydraulic lift was observed) and the flow in the correspondent azimuth of stem xylem, was found for the deeper depth (25 mm below cambium). Correlation between flow in that root and flow in all other stem xylem layers measured was significantly higher than those described above, with the root using lifted water.

This study provides evidence that *Quercus suber* trees have root systems in which deep roots access groundwater to supply tree, when shallow soil layers are dried out. In case of *Quercus suber,* access to groundwater could be expected through numerous sinkers connected to superficial roots. During the dry period, using these sinkers as conduits, water moves in the lateral roots in direction of prevailing gradients in water potential, either to crown for transpiration or, in the opposite direction, in order to prolong or enhance fine-root activity by keeping them hydrated. The importance of the sinkers in water supply decreased during rainy periods. Stem outer xylem seems to be mostly responsible for water movement from surface soil horizons, whereas water moves from deeper roots through all sapwood (but probably more through deeper stem xylem).

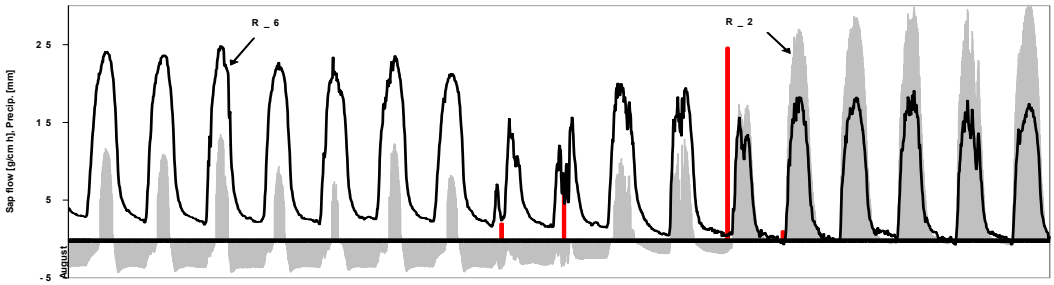

Figure 1 - Sap flow dynamics in roots 2 and 6 in seven last days of dry period, broken by rain events (shown as red bars in August 26, 27 and 31) and following period with wet soil.

16a

HYDROGEOPHYSICS OF SOILS AND TREES

Said A. al HAGREY, Ulrike WERBAN, Rolf MEISSNER, Wolfgang RABBEL and Ali ISMAEIL

Department of Geophysics, Institute of Geosciences, Kiel University

ABSTRACT

Static and dynamic behaviour of water in soils and trunks can be assessed by applying various geophysical techniques. Geoelectric measurements show a firm relationship between resistivity and water content for nearly all soil types (with exception of clayey soils); they observe irrigation and water uptake in the roots of trees and plants and can map various root zones. Even the water content and its distribution and movement (sap-flow) in trunks can be observed by modifying electric techniques using multiple ring electrodes and refined inversion methods. Radar measurements show an inverse relationship between the radar velocity and the water content; hence they also can monitor efficiently water content, irrigation processes and water uptake in roots and even observe inhomogeneites of roots and rocks in the subsurface and perform a tomography.

(full paper in last section)

17

18

USE OF GROUND, AIRBORNE AND SATELLITE REMOTE SENSING FOR ESTIMATING EVAPORATION

Nicole ARCHER and Hamlyn JONES

Plant Research Group, University of Dundee at SCRI, Invergowrie, Dundee DD2 5DA, Scotland, UK

narche@scri.sari.ac.uk

h.g.jones@dundee.ac.uk

ABSTRACT

Remote sensing of canopy temperatures provides probably the most important tool for the remote estimation of evapo-transpiration (E) rates. As shown in a review by Jones *et al*. (2004), there are many algorithms using different variables to estimate E. The choice of algorithm using remotely sensed data to estimate E depends mainly on three factors: 1) The frequency (hourly, daily or less frequent intervals) and scale (leaf, canopy or a whole region) of observations; 2) The type of canopy (homogeneous as for many crops, or heterogeneous; 3) The available variables to input to the energy balance, especially the ground-based meteorological data.

In our study we use surface temperature and image classification techniques (based on hypoerspectral imagery) to identify the different surface components (e.g. different types of vegetation, soil and water) as the main inputs for estimation of E. We therefore must ensure that surface estimates derived from thermal wavelengthes are precise, the classification method is effective in identifiying the surface components of interest and that our methods of extraction of temperature from different surface components are correct.

Following from the theoretical approaches presented by Professor Hamlyn Jones, this presentation will describe the procedure for estimating and extracting surface temperature of different types of surfaces at different scales and using different algorithms to estimate E.

ABSTRACTS – POSTERS

Page

P1

WATER USE EFFICIENCY AND WATER SOURCE CHANGES IN A DUNE COMMUNITY AFFECTED BY LOWERING GROUND WATER TABLE LEVELS

Graça OLIVEIRA[1], MJ. PINTO[2], Pedro CARVALHO[1], Paulo GASPAR[3], Rodrigo MAIA[1], Marco LAUTERI[4], Amélia MARTINS-LOUÇÃO[1], Cristina MÁGUAS[1]

[1] *FCUL, Stable Isotope Lab. (CEBV/ICAT), Campo Grande, 1749-016, Lisboa, Portugal*
[2.] *Museu e Jardim Botânico, R. da Escola Politecnica, Lisboa, Portugal*
[3.] *Transgás S.A, Portugal*
[4.] *CNR Istituto di Biologia Agroambientale e Forestale, Via Marconi 2, 05010 PORANO (TR), Italy*
email: cristina.maguas@icat.fc.ul.pt

ABSTRACT

Water availability is a key determinant of plant community structure, biodiversity and functioning. Sand dune habitats are particularly sensitive to stress and disturbance, and plants present various adaptations for acquiring and conserving soil moisture. Rainfall and groundwater are their primary water sources, but the water vapour condensation driven by amplitudes is also an important source for shallow-rooted species, which may thus colonize dry dune slacks, together with deep-rooted species. Biodiversity significantly influences ecosystem function, and at the scale of functional groups or species it may affect water distribution and movement. Some deep-rooted plants are able to alter the water table depth locally. Phenomena such as descent water of groundwater levels may affect species differently and thus change their competitiveness and overall effect on soil and stream hydrology. Stable isotope analysis of water in the plant and in the environment provide good insights on plant water use. Using the natural D/H and $^{18}O/^{16}O$ ratios, water sources can be identified by matching the isotopic signature of plant xylem water with that of the water sources. Moreover the regulation of Water Use Efficiency (WUE) is particularly important in these systems where plants are periodically exposed to severe water stress during summer time. An important technique to measure WUE is carbon isotope discrimination ($\Delta^{13}C$) in leaf material, which represents an integrative measure over the lifetime of a leaf. However, under conditions of limited resources, interpretation of $\Delta^{13}C$ may not be straightforward. During seasonal changes in environmental conditions regulation may occur through a coherent change in stomatal restriction of CO_2 diffusion and down-regulation of photosynthetic capacity, which may result in unchanged WUE.

In this work we have studied the impact of a continuous and significant extraction of groundwater in plant coast dunes communities at Osso da Baleia (160 km north of Lisbon), located in the Meso-mediterranean climate region. This extraction started in October 2001 and has the final objective the installation of natural gas reservoirs. The possible impact of such extraction and the consequent effects of increase of water table depth on dune flora is poorly known, but some studies indicate that it may destroy the plant communities. The studied communities are mainly constituted by primary dune systems (e.g. *Corema album*) and pine forest (*Pinus pinaster*) mixed with *Acacia longifolia* and *Myrica faya*, and associated understory species. A protected species (*Salix arenaria*) find here its southern distribution limit at the dune slacks. In order to assess possible effects during this lowering of the groundwater levels, seasonal measurements were performed according to the position of wells and piezometers along 1 km distance, in a total of 11 sampling points. Measurements of pre-

dawn water potential, WUE through leaf organic material $\Delta^{13}C$ of young and old leaves, $\delta^{18}O$ and δD of xylem water were determined in all 5 species. $\delta^{18}O$ and δD of precipitation and groundwater were also analysed. The results indicated that: i) water table is isotopically heterogeneous; ii) plant water sources changes due to increase depth of the water table are also heterogeneous iii) WUE is dependent upon leaf age, seasonality and site location.

P2

COMPETITION ABILITY and RESOURCE DYNAMICS in PORTUGUESE COASTAL DUNE ECOSYSTEMS: INVASIVE vs NATIVE PLANT SPECIES

PEREIRA* A. J.[1], M. J. PINTO[3], H. MARCHANTE[2], E. MARCHANTE[2], J. FERREIRA[1], C. SCHRECK[2], H. FREITAS[2], M. A. MARTINS-LOUÇÃO[1], O. CORREIA[1], C. MÁGUAS[1]

[1] *Centro de Ecologia e Biologia Vegetal, University of Lisbon, Portugal*
[2] *Instituto do Mar, University of Coimbra, Portugal*
[3] *Museu Laboratório e Jardim Botânico, University of Lisbon, Portugal*

ABSTRACT

Sand dunes are habitats of great nature conservation interest, with a very characteristic and rich flora. Species like *Acacia* sp. (alien plant), have been introduced, in the past, with the objective to stabilize sand dunes. However, some of these species became dominant, reducing native species density and biodiversity, causing serious ecological problems. It is our aim, to present the aspects related to the vegetation patterns, focusing on the interactions of invasive and native species. In particularly we want to determine the competitiveness of both invasive and native species in relation to water and demographic aspects, witch are crucial for the interpretation of community dynamics and plant competition abilities. The chosen areas are located at the South and Center of Portugal with a Mesomediterranean climate, but with different annual precipitation values. In each study area, a gradient was defined, according to the "invasive specie position" i) control - well preserved sand dune; ii) disturbed sand dune with introduced plant specie, *Acacia longifolia* iii) edge zone, a contact area between native species and the invasive plant. In order to obtain an integrative view of the competitive patterns, several methods concerning remote sensing, numerical vegetation analysis, stable isotopes ($\delta^{13}C$, $\delta^{18}O$) and water relations studies have been performed. The obtained results underlie the hypothesis of a strong correlation between water availability and invasive patterns (regional scale), as well as a microclimate influence of the "invasive stand" upon the water and light competition abilities.

P3

ANALYSIS OF SAPFLOW OF *Pinus pinaster* Ait. TREES AT SAN ROSSORE REGIONAL PARK DURING THE PERIOD 2001-2003: PRELIMINARY RESULTS

M. TEOBALDELLI*, G. MATTEUCCI, I. GODED, G. M. SEUFERT

Climate Change Unit, Institute for Environment and Sustainability – IES, Joint Research Centre, I-21020 Ispra (VA), Italy
** Corresponding author: maurizio.teobaldelli@jrc.it*

Keywords: Pinus pinaster, sap flow, canopy fluxes, eddy covariance

---

ABSTRACT

The interactions between environmental conditions, particularly precipitation, vapour pressure deficits (VPD), water table level, tree water use and stand-level evapotranspiration were studied during the period 1st of January 1999 to 1st of May 2004 in one of the two Joint Research Centre Experimental sites.

The studied site is located along the northern coastline of Tuscany in the San Rossore Regional Park (43º13'40.3''N; 10º17'04''E), close to the city of Pisa and is formed by a 40 years old *Pinus pinaster* Ait. forest, with sporadic presence of *Pinus pinea* L. and *Quercus ilex* L. trees. The stand has a density of 567 trees ha^{-1}, 18 m height, mean DBH of 29 cm and Leaf Area Index of 4.2 m^2 m^{-2} and is growing on sandy soil. The site is characterised by a typically Mediterranean climate, with mean annual temperature of 14.2 ºC and total precipitation of 920 mm, with maximum in autumn and spring.

The site is part of the CarboEurope network and is equipped with a tower to measure all relevant micrometeorological variables along the canopy profile and stand-level carbon and evapotranspiration fluxes with the eddy covariance technique. Tree level sap flow was also measured on several *Pinus pinaster* Ait. trees using the thermal dissipation technique developed by Granier (1985).

The poster will present preliminary results for the period between the 1st of January 2001 - 31st of December 2003.

Tree level transpiration resulted different in the three study years due to different climatic conditions: 2001 being a typical Mediterranean year, 2002 a year with a wet summer, while 2003 was characterized by a long-term drought and warm period ("heat wave").

Transpiration appeared to be driven mainly by recent rainfall, VPD and light. In 2003, continuous water table measurements were started and also this parameter appeared to explain different transpiration in varying season.

Although this is a preliminary report, an overall good agreement was found between tree-level sapflow measurement and eddy covariance derived evapotranspiration fluxes.

P4

TDR-MEASUREMENT FOR THE STUDY OF THE SEASONAL VARIATIONS OF SOIL MOISTURE ON *Quercus ilex* DEHESAS

Elena CUBERA[1], Gerardo MORENO, Alejandro SOLLA

Departamento de Biología y Producción de los Vegetales. Universidad de Extremadura.
Ingeniería Técnica Forestal. Av. Virgen del Puerto 2, 10600-Plasencia, Spain
[1]*For correspondence: ecubera@unex.es*

Keywords: Soil water content, scattered trees, root distribution, leaf water potential

---

ABSTRACT

Most evergreen oak forests growing in the flat areas of the southwestern Iberian Peninsula have been gradually transformed into a unique kind of pastoral woodland, the Spanish dehesas and Portuguese montados, by means of an agroforestry use. Eagleson and Segarra (1985) have emphasised that, where a marked seasonality in water availability occurs, a mixed formation of grasses and woody plants is the only stable state of equilibrium. A positive effect of trees on soil bulk density, water-holding capacity and water content has been shown by Joffre and Rambal (1988) in dehesas.

We have investigated how holm-oak trees use the soil water in four dehesas of CW Spain (39º 41' N, 6º13' W) by measuring the soil moisture at different distances from the tree trunk (maximum 30 m), from the soil surface until a maximum depth of 2 m, in intervals of 20 cm. Soil moisture was measured monthly by TDR technique, between May 2002 and October 2003. Additionally, tree and herbs root systems have been studied by mean of 2 m-depth soil cores (Obrador et al., 2003) and the water stress experienced by trees have been characterized by mean of leaf water potential (Montero et al., 2004).

We did not found any significant difference in soil moisture with regards to distance to the tree (Fig 1), which differ from those reported by Joffre and Rambal (1988). Soil water depletion beyond the tree canopy projection continued even when herbaceous plants dried up (mid-may) (Fig 1), indicating that trees could use water from open areas, a clear benefits from tree spacing on soil water consumption. Results have also shown a high dependence of holm-oak on deep water reserves throughout late spring and summer, which contributes to avoiding competition for water between trees and herbaceous vegetation (Fig 2).

In conclusion, we have not found a positive redistribution of soil water near the trees, however we have found an very extended tree rooting system in dehesas (both in depth and distance; Fig. 3), which allows them to use efficiently the soil water of a huge volume of soils and to maintain a near-optimum water status along the summer (Fig 4).

REFERENCES

Eagleson, P. S. and Segarra, R. I. (1985): Water limited equilibrium of savanna vegetation systems. Water Resources Research 21:1483-1493.

Joffre, R. and Rambal, S. (1988): Soil water improvement by trees in the rangelands of southern Spain. Oecology Plantarum 9: 405-422.

Montero, M.J., Obrador, J.J., Cubera, E. and Moreno, G. (2004): Importance of soil management on tree water status in dehesas of Central Western Spain. Advances in Geoecology , 37 (in press).

Obrador J.J., Bordet, M., García, E. and Moreno, G. (2003): Root distribution in intercropped dehesas of Central-Western Spain. International Symposium on Sustainability of Dehesas, Montados and other agrosilvopastoral systems. European Soil Science Society. Cáceres, Spain.

Sala A. (1999): Modelling Canopy Gas Exchange during Summer Drought. In: Rodá F., Retana J., Gracia C.A., and Bellot J. (eds). Ecological Studies vol 137. Ecology of Mediterranean Evergreen Oak Forests. Springer Berlin, pp. 149-159.

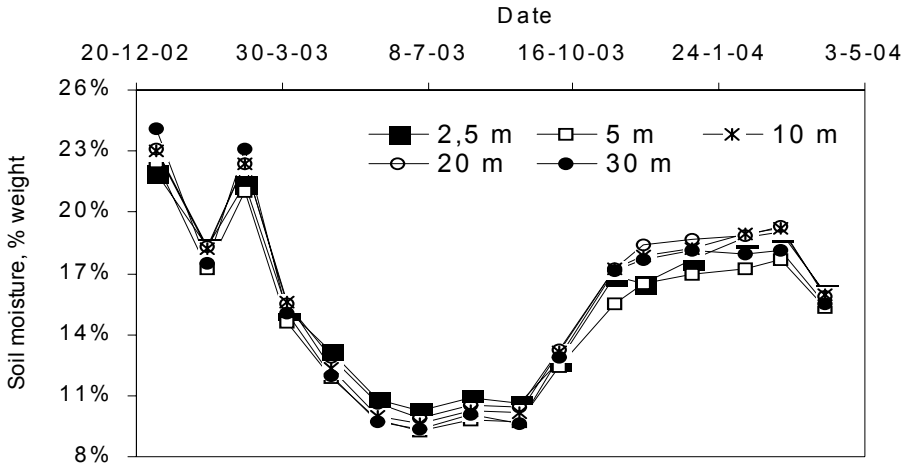

Figure 1.- Seasonal variation of soil moisture (average form dat of 1 m depth) at different distance of holm-oaks in dehesas.

Figure 2.- Monthly variation in soil moisture profile from soil surface till 2 m. Most of the water was depleted between May and June.

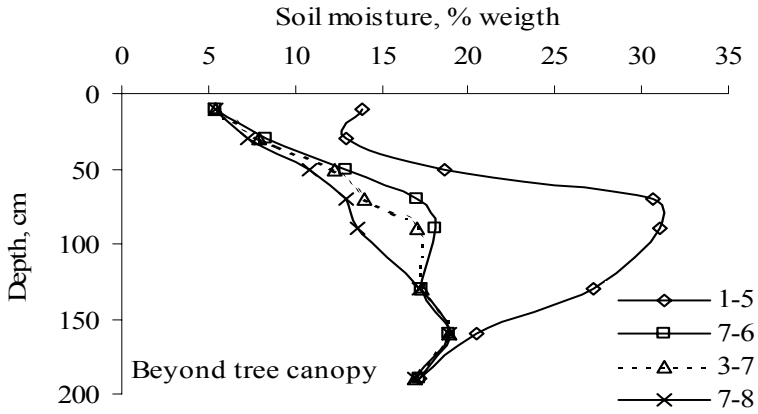

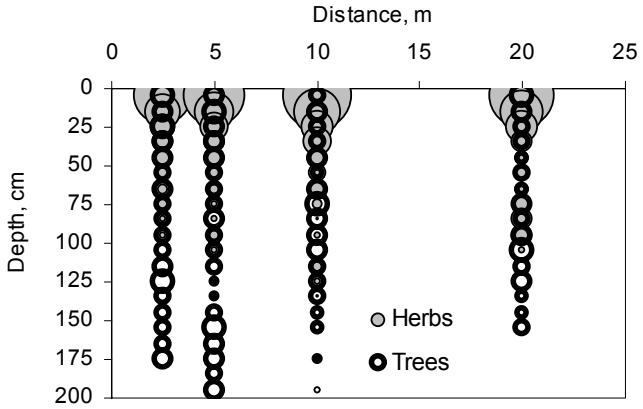

Figure 3.- Profiles of Root Lenght Density (RLD, Km m^{-3}) of herbs and trees in dehesas at different distances of the trees (holm-oak).

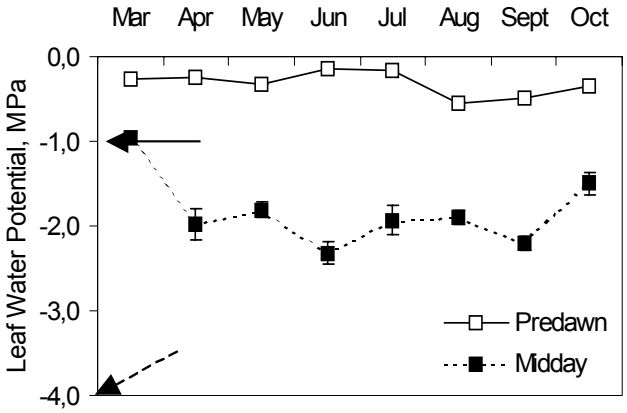

Figure 4.- Monthly variation in leaf water potential of holm-oaks in dehesas. Arrows indicate the thresholds of significant water deficit (Sala, 1999).

Acknowledgement
This study was supported by E.U. (SAFE project), Spanish Government (MICASA project, MCyT) and Junta de Extremadura (CASA project and E. Cubera was awarded a grant).

P5

SOIL WATER CONTENT DETERMINES RECOVERING OF *Quercus ilex* TREES INFECTED WITH *Phytophthora cinnamomi*

Lorena GARCÍA, Elena CUBERA, Gerardo MORENO, Alejandro SOLLA[1]

Departamento de Biología y Producción de los Vegetales. Universidad de Extremadura.
Ingeniería Técnica Forestal. Av. Virgen del Puerto 2, 10600-Plasencia, Spain
[1] *For correspondence: asolla@unex.es*

Keywords: Forest Pathology, Chemotherapy, Disease control, Oak decline

---

ABSTRACT

Oak decline is one of the most serious problems that presently affect the Mediterranean oak forests. Among the possible pathogens involved, *Phytophthora cinnamomi* has been proposed as a major factor since it causes root rot with successive defoliation and oak mortality. Trunk injections of potassium phosphonate (PP) have shown promising results on *Quercus ilex*, although some trees above a certain level of wilting do not recover. The objective of this work was to study the influence of soil water content on the recovering of such treated trees.

On April 2002, ten *Q. ilex* trees located at Dehesa de Santa Amalia (Cáceres, Spain), and showing pronounced symptoms of oak decline were selected. Five trees were PP treated on both spring and autumn 2002 and 2003, and five trees were left as untreated controls. Time Domain Reflectometry probes were installed at 50 and 80 cm depth, and soil moisture content was measured monthly during 2003. Tree condition was registered on a scale in which 0= healthy tree; 1= few decline symptoms; 2= moderate symptoms; 3= pronounced symptoms; and 4= very advanced decline.

Q. ilex trees having pronounced symptoms of decline (rating =3) did not recover significantly if treated with PP. On April 2004, treated and control trees reached ratings of 1.9 ± 0.4 (average ± SE) and 2,3 ± 0.4, respectively, both values not significantly different (P>0.10).

Figure 1A shows the differentiation made between unrecovered and recoverd trees, both for the control and the treated trees. Soil moisture on unrecovered control trees was significantly lower than soil moisture on recovered control trees from March to May (Figure 1B). Soil moisture on unrecovered treated trees was significantly lower than soil moisture on recovered treated trees on January, March-June and July-September. Differences indicate that oak decline recovering could be determined by the soil water content. The effect of root damage caused by *P. cinnamomi*, which reduces water absorption, seems to be critical for the tree health if water availability is low, especially during the summer.

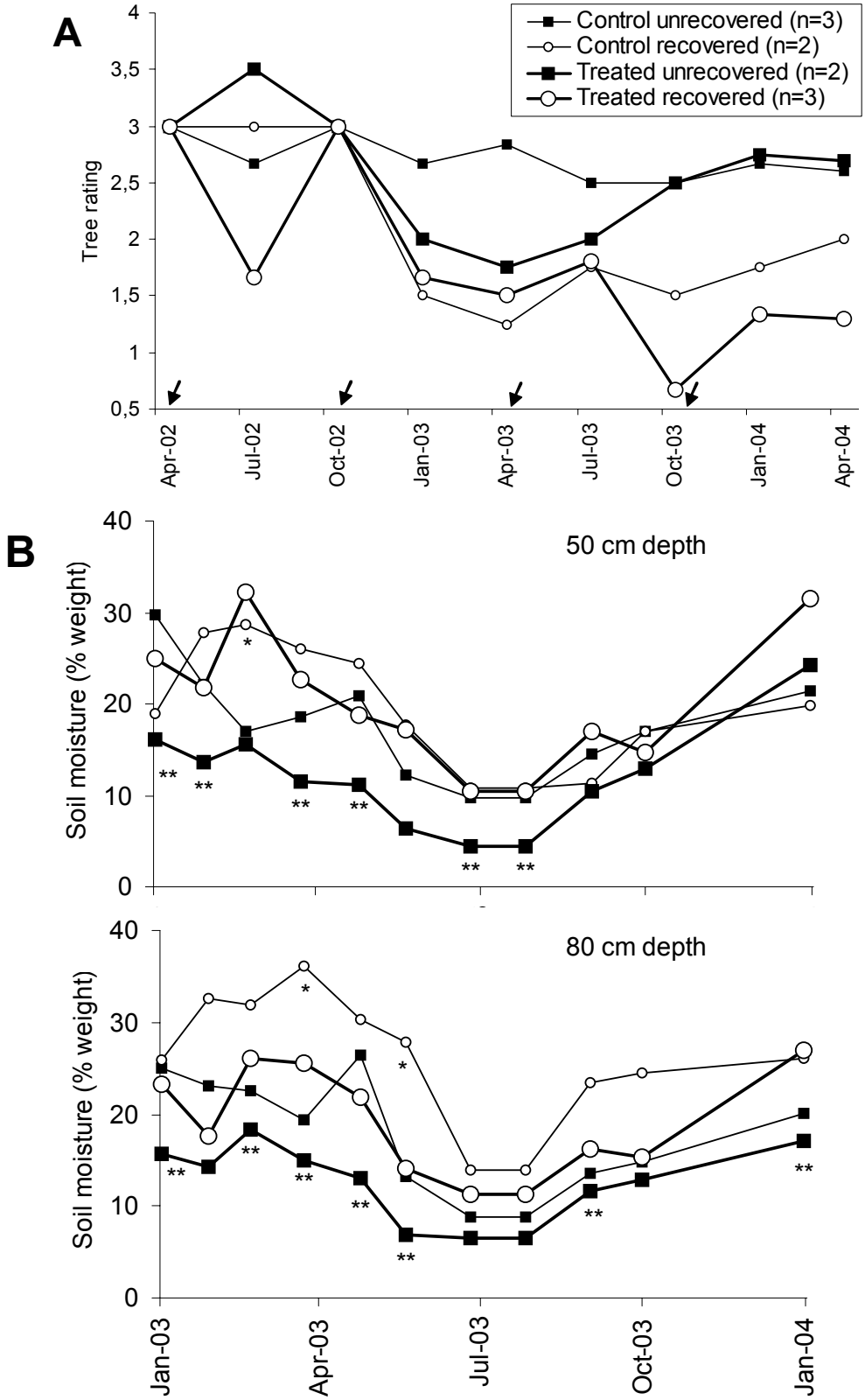

Figure 1 - Average values of tree condition (**A**) and soil moisture (**B**). Arrows indicate treatment dates. Asterisks denote significant differences in soil moisture within control (*) and treated (**) trees ($P < 0.10$; LSD).

P6

ARE CORK OAK AND HOLM AOK USING THE SAME WATER SOURCES IN THE MONTADO? INDICATIONS FROM DEUTERIUM NATURAL ABUNDANCE.

Cathy KURZ-BESSON [1], Rolf SIEGWOLF [2], Cécile BARBAROUX [1], Teresa Soares DAVID [3], Jorge Soares DAVID [1], João Santos PEREIRA [1], Manuela CHAVES [1]

[1.] *Instituto Superior de Agronomia, Tapada da Ajuda, 1349-017 Lisboa, Portugal,* cbesson@isa.utl.pt

[2.] *Laboratory of Atmospheric Chemistry, Paul Scherrer Institute, CH-5232 Villigen-PSI, Switzerland,* rolf.siegwolf@psi.ch

[3] *Estação Florestal Nacional, 2780-159 Oeiras, Portugal,* teresa.david@efn.com.pt

Keywords: *Quercus suber*, *Quercus rotundifolia*, δD, water source, hydraulic lift

---

ABSTRACT

In the future climate water deficits may increase, as arid and semi-arid climate will probably expand throughout southern Portugal, due to global warming. A dramatic increase in the number of dry months is expected to occur and the ecophysiological limits for water stress tolerance may be overdue, leading to large-scale tree mortality. In order to improve our understanding on plant adaptation to summer drought and specific differences in water use, we studied the most important ligneous plants (*Quercus suber* and *Q. rotundifolia*) of an evergreen oak woodland ecosystem (Montado).

The aim of the study was to identify the depth of root water uptake in *Q. suber* and *Q. rotundifolia*, located in a Montado agroforestry system near Evora (38º32'N, 8º00'W) within a Mediterranean mesothermic humid climate. To characterize seasonal changes in water sources for both species, soil samples were collected in May and October 2001, and June and August 2002 at 0.2m intervals till 1m depth. Samples of twigs, precipitation and ground water (GW) were collected monthly in 2001, 2002, and 2003. Water was extracted from samples by cryodistillation and analysed by mass spectrometry to determine the hydrogen/deuterium ratio (δD) relative to VSMOV standard.

There was no significant interspecific difference in xylem δD signature in 2001, 2002 and 2003, except in June 2002 and March 2003. Water uptake patterns were similar for both species, indicating that *Q. suber* and *Q. rotundifolia* were using the same water sources. The significant difference observed in June 2002 suggests that *Q. suber* was using soil moisture at

1m depth whereas *Q. rotundifolia* seemed to withdraw water from deeper soil layers or even from GW.

The results also show that in Spring and in Fall both tree species were using topsoil water, at 0.6m depth. During Summer, xylem water signature for both tree species was more negative (-35 to –38°/oo) than that of GW (-30°/oo), but generally less negative than soil water signature at the estimated maximum root depth (-41 to –45°/oo). It is unlikely that trees were taking water from the top 0.2m soil layer during summer since its soil water content was then only 2% in volume. Thus three hypothesis may explain these results:

1/ Trees are performing hydraulic lift, redistributing water during the night from the GW to the top soil at about 0.6m depth, through the shallower root system. Due to the low water content, water diffuses until morning, leading to a more negative signature in the soil and an intermediate signature in the roots and twigs compared to GW. In this last hypothesis, trees would withdraw water from GW only during the night due to an inversion of water potential after stomata closure, and use soil redistributed water during the day.

2/ Trees are not performing hydraulic lift but have access to GW trough vertical root system. They are using soil water and GW at the same time, leading to an intermediate twig isotopic signature.

3/ Trees are not taking water directly from the GW, but using water from the unsaturated zone immediately above, that should have a more negative signature compared to GW, due to H_2O migration through a diffusion process.

Further investigation through isotopical labelling is needed for more conclusive results on water sources for oak species in the Montado during the summer drought period.

PAPERS

18

USE OF GROUND, AIRBORNE AND SATELLITE REMOTE SENSING FOR ESTIMATING EVAPORATION

Nicole ARCHER and Hamlyn JONES

Plant Research Group, University of Dundee at SCRI, Invergowrie,

Dundee DD2 5DA, Scotland, UK

narche@scri.sari.ac.uk

h.g.jones@dundee.ac.uk

---

1. INTRODUCTION

Remote sensing of canopy temperatures provides probably the most important tool for the remote estimation of evapo-transpiration (E) rates. As shown in a review by Jones *et al*. (2004), there are many algorithms using different variables to estimate E. The choice of algorithm using remotely sensed data to estimate E depends mainly on three factors: 1) The frequency (hourly, daily or less frequent intervals) and scale (leaf, canopy or a whole region) of observations; 2) The type of canopy (homogeneous as for many crops, or heterogeneous; 3) The available variables to input to the energy balance, especially the ground-based meteorological data.

In our study we use surface temperature and image classification techniques (based on hypoerspectral imagery) to identify the different surface components (e.g. different types of vegetation, soil and water) as the main inputs for estimation of E. We therefore must ensure that surface estimates derived from thermal wavelengthes are precise, the classification method is effective in identifiying the surface components of interest and that our methods of extraction of temperature from different surface components are correct.

Following from the theoretical approaches presented by Professor Hamlyn Jones, this presentation will describe the procedure for estimating and extracting surface temperature of different types of surfaces at different scales and using different algorithms to estimate E.

2. MATERIALS AND METHODS

The test site was located on the Mitra Farm of the University of Évora, in the Alentejo Region of Portugal. Measurements were centred on a 25 m meteorological tower erected in an area of low density evergreen oak woodland/pasture consisting primarily of *Quercus rotundifolia* Lam. with some *Quercus suber* L. and an under-storey of mixed grasses and small shrubs including *Cistus* and *Lavendula* spp.. The average tree density for the scene studied was between 35 and 45 trees per hectare with an average cover of 25 %. The area has a typical Mediterranean climate, i.e. hot dry summers and a cool wet winter. Mean annual air temperature has been estimated at 15°C, ranging from 8.6 C in January to 23.1 °C in August (David, et al., 2004). Mean rainfall has been estimated over 1951-1980 to be 665 mm per year and open water evaporation is 1760 mm (INMG, 1991).

Ground measurements were made between 28th June 2001 and 7th July 2001, with overflights of DAIS and ROSIS hyperspectral scanners on 29th June 2001 between 11:17 to

11:56 UTC. Imagery from NOAA-AVHRR 16 and Landsat 5 were acquired on 29th June 2001 13:41 UTC and 28th June 2001 10:48 respectively.

Ground measurements included standard meterorological data from instruments located on the tower (net radiation, solar radiation (Kipp & Zonen CM6b solarimeter), air temperature, atmospheric humidity, wind speed) together with measurements at 2 m (solar radiation, net radiation, air temperature and humidity, windspeed logged at five minute averages). Water temperature was obtained for one reference lake using a fine-wire thermistor floating within 2 cm of the surface. Thermal images were obtained on the ground or from the tower using an Infrared Solutions SnapShot 225 camera (Infrared Solutions, Inc, Plymouth, USA). This camera consists of an uncooled long-wave (8 – 14 μm) Honeywell thermoelectric array detector with 120 × 120 pixels and has 16 bit resolution giving temperatures to better than 0.1 °C. The normalised vegetation index (NDVI) was estimated from the red and near infra-red channels of an Agricultural Digital Camera (Dycam, Woodland Hills, California). Stomatal conductances were measured using either a LiCor 1600 steady-state porometer (Li-Cor Inc., Lincoln, Nebraska) or a ΔT-Devices AP4 automatic porometer (ΔT-Devices, Burwell, Cambs, UK).

The DAIS instrument provided hyperspectral images including thermal data at a resolution of 3.3 m for each pixel, while the ROSIS instrument gave higher resolution (1.2 m) of the visible and near infra-red wavelengths. Reservoirs, bare soil and road areas were included in each image for calibration purposes. All images were atmospherically corrected using the ATCOR4 model. The terrain around the site of interest was relatively flat so no DEM correction was employed. Further analysis was in ENVI (Research Systems Inc., USA) software.

Several different ways of classification in ENVI was checked for accuracy by comparing manually classified pixels, with automated classified pixels. The best classifiers were estimated to be either spectral angle mapping or minimum distance. The ROSIS hyperspectral data at 1.2 m (which included wavelengths between 486 and 874 nm), was used to classify the field area, as this was the highest available resolution for the area. Estimation of the characteristic patch sizes of different classes of land cover was achieved by analysing the frequency distributions of the number of contiguous pixels of each cover type. This determined the size of vegetated component areas within a scene. Images taken by the hand-held camera were also analysed to verify the heterogeneity of surface components within small areas.

Eight different methods were compared for determining the temperatures of the five main component surfaces: tree, shrub, grass, soil and water. The first four use temperature data at the observed resolution, while the remaining four attempt to derive information for smaller areas than the observed individual temperature pixels.

An alternative approach to the estimation of tree and grass temperatures made use of the two or three angles of view possible with the three DAIS flights. The temperatures observed for each flight were corrected for the temporal drift in air temperature recorded at the tower. For the solar zenith angle of 21^o, we have image areas around the meteorological tower at three view angles ($+21^o$, -21^o and 0^o). The total area of common image was ascribed to trees, visible shade and the remaining visible sunlit ground (mostly grass) using the formulae given by Irons *et al*. (1992) which are based on the assumption that the canopy can be represented by a series of spheres resting on the ground. From the mean temperature observed for an area at each of these angles, together with the nadir tree fraction (estimated using the image classification) we estimated the tree temperature and the ground temperature

for the area. These temperatures were used to estimate E using various algorithms. The theory of these algorithms will be explained by Hamlyn Jones in his theoretical presentation.

3. RESULTS

Figure 1 shows the frequency distribution of the linear dimensions of homogeneous vegetation patches averaging results for both the east-west and north-south directions. Bare soil areas tended to have the smallest characteristic size (modal dimension = 2.4 m) followed by trees, shrubs and grass (all with modal dimensions = 8.4 m). Water had a bimodal frequency (modal dimensions were at 10.8 m and 37.2 m), which showed the linear dimensions of two small lakes. Bare soil occurred mainly as tracks in the field site. Both shrubs and grass had additional smaller peaks at 2.4 m which represented patches between trees. Grass areas had the greatest variability of patch size. For all classes the modal size was greater than the pixel size, suggesting that the ROSIS imagery available is of an appropriate scale for this scene.

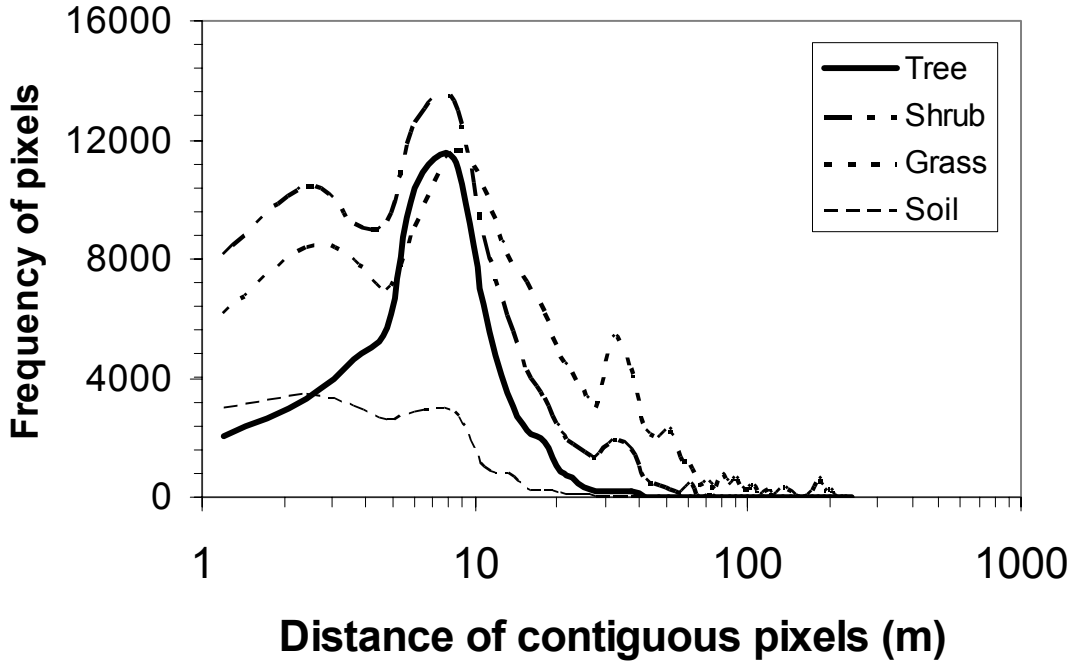

Figure 1 - Frequency of contiguous pixels of ROSIS 1.2 m SAM classification of the main cover types. The highest frequency for tree, shrub and grass occurs at 8.4 m, for soil it is 2.4 m.

For small homogeneous areas viewed from the tower (mostly less than 1 m^2), the mean hand-held temperature estimates were 34.4°C (±0.36) for shaded areas, 49.9 °C (±4.04) for grass and 56.7 °C (±3.46) for soil. The temperature range measured at the airborne level was smaller than at ground level. Within a 3.3 m area on the ground, areas around the tower which were considered to be soil or grass at the DAIS level contained small shrubs, grass, shade and soil, thus lowering the temperature as compared with pure areas. These areas had particularly high temperature ranges ranging from 57.3 °C (pure soil area) to 32.2 °C (shrubs in shade). The average temperatures estimated by DAIS for larger areas which relate to the

hand-held camera images are 33.9 °C (± 0.51) for tree areas, 42.4 °C (±2.68), for shrub areas, 46.8 °C (±1.26) for grass areas and 47.1 °C (±1.48) for soil areas.

Figure 2 a) shows an example of a classified ROSIS image using the spectral angle mapper classifier. As trees, shrubs and grass areas are generally bigger than 1.2 m, these areas were precisely classified using the spectral angle mapper classifier. Figure 4 b) shows the corresponding temperatures derived from the DAIS thermal bands indicating a particularly hot area in the south west corner which was found to be a grazed area.

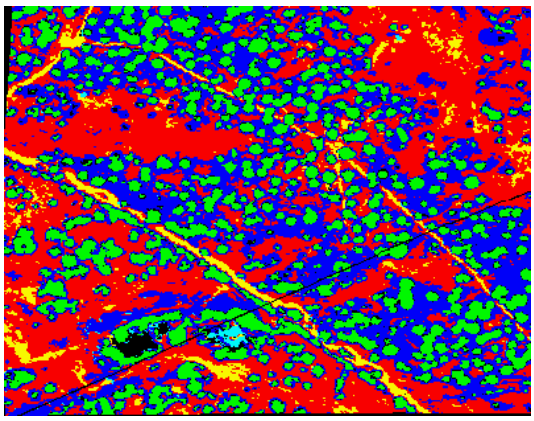

a)

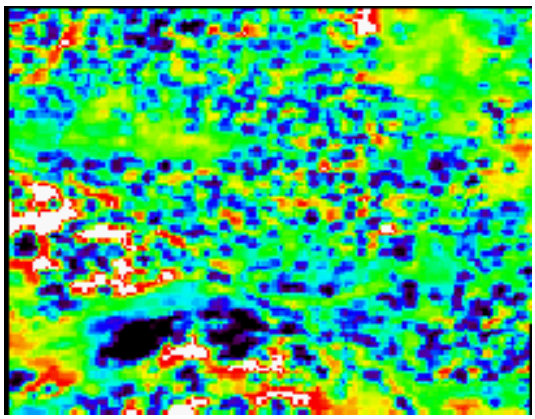

b)

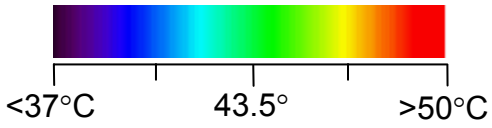

Figure 2 - Use of SAM classifications to extract component temperatures. a) shows the SAM classification of ROSIS (1.2m). For the classifications: Light grey is trees, Black is shrubs, Mid grey is grass, white is soil, Dark black is water. b) shows the temperatures derived from DAIS thermal bands at 3.3 m.

Table 1 shows some examples of estimates of E using different algorithms. The temperatures given in Table 1 were extracted from DAIS 3.3 m pixels representing lakes, well watered trees growing at the margin of the lakes/ponds, trees growing away from water, shrub areas and grassland areas.

	Calibration areas		Test surfaces			
	Lake	Soil	Trees by lake	Trees by tower	Grass	Shrub
Temperature (°C)	30.5	46.1	32.0	37.0	43.4	40.8
Evaporation estimates (W m^{-2})						
1) ATCOR estimate of λE (Richter, 2001)	720	390	721	707	492	541
2) g_{aH} from wet and dry surfaces (Jones, 1992)			691	653	219	326
3) Corrected for Rn (Jones and Archer, 2003)			752	708	221	349
4) CWSI (Inoue *et al*. 1994)			706	378	55	151

Table 1 - Evapotranspiration estimates (λE, W m^{-2}) for different vegetation at the Mitra site. Air temperature and air humidity at 10 m at the time of flights was 30.2 C and 1542 Pa, respectively. g_{aH} is boundary layer conductance, Rn is net radiation, CWSI is crop water stress index. The four different algorithms are: 1) The ATCOR model, 2) Uses boundary layer conductance and wet and dry references, 3) corrects Rn by removing soil heat flux from Rn and 4) uses a vegetation index to estimate absorbed radiation and CWSI.

Overall there was good agreement between the rates of evapotranspiration estimated by the different methods, except for ATCOR, which appeared to significantly overestimate E from the grass/shrub areas, while the CWSI method underestimates E.

4. DISCUSSION AND CONCLUSION

Differences between estimates of component temperatures using ground and airborne sensors are related to differences in the measurement scale. As the pixel area decreases the chance of detecting pure extreme pixels (soil or water, sun or shade) increases, significantly affecting the derived temperature distributions of different surfaces. The use of a hand-held thermal IR camera allows one to obtain temperature information at much higher resolution than does the airborne imagery, and shows the real range of extreme temperatures within a 3.3 m pixel.

The estimation of the surface component scales using SAM classification at 1.2 m resolution gave an indication of whether the pixel sizes used when extracting temperatures were sufficient to classify most surface components adequately, given the fact that there will

always be some mixed pixels. As the 3.3 m pixels are larger than the dominant scale for soil, it is clear that they are too large to separate soil and grass correctly. This caused underestimation of soil temperatures when soil was classified at 3.3 m resolution. The choice of method for extracting temperature depends on whether a surface temperature distribution of each surface component is required or simply the average of an area.

The use of a simple shadow model assuming that the tree canopies could be represented by spheres, combined with temperature estimates from contrasting view angles gave a valuable approach to the automated estimation of the temperatures of specific scene components such as trees and grass/soil areas. The use of reference dry and/or wet pixels for estimation of boundary layer conductance and for estimation of potential evaporation rates appeared to give reasonable estimates of evaporation from the various surfaces, and certainly for the mixed grass-shrub areas seemed likely to be much more reliable than the values derived from ATCOR. The temperature of the dry reference surfaces is a critical requirement for effective use of the algorithms presented above, and it may be that the pixels chosen for this were unrepresentative of either the radiative or aerodynamic properties of the transpiring pixels. The ATCOR algorithms, however, did attempt to estimate the differences in radiative properties of the different surfaces. A further key assumption is that the apparent thermal time constant should be similar for all surfaces (as temperatures were changing significantly over the period of measurements and just prior to them); unfortunately the soil and lake surfaces have different temperature dynamics than do the various types of vegetation. These differences remain to be quantified for the particular area used for this study.

The presentation will also discuss how this procedure for estimating E can be scaled to satellite images and how these values relate to estimated ground values of E.

REFERENCES

Archer, N. A. L., Jones H. G. (Submitted Feb. 2004). Integrating hyperspectral imagery at different scales to estimate component surface temperatures. submitted for Special Issue in *International Journal of remote sensing*.

Irons, J. R., Campbell, G. S., Norman, J. M., Graham, D. W., and Kovalick, W. 1992: Prediction and measurement of soil bidirectional reflectance. *IEEE Trans. Geosci. and Remote Sens*. 30, pp. 249-260.

Inoue, Y., Moran, M. S., Pinter Jr., P. J. 1994. Remote sensing of potential and actual daily transpiration of plant canopies based on spectral reflectance and infrared thermal measurements – Concept with preliminary test. Journal of Agricultural Meteorology. 49 (4), 237-246.

Jones, H. G. & Archer, N. A. L. 2003. Airborne imaging spectrometry (DAIS/ROSIS) for estimation of evaporation from heterogeneous *Montado* vegetation in Portugal. In: *Proceedings of the 3rd European Association of Remote Sensing Laboratories Workshop on Imaging Spectroscopy.* 13 – 16th May 2003. Oberpfaffenhofen, Germany.

Jones, H.G., 1992. Plants and microclimate. Cambridge University Press, Cambridge.

Richter R., 2001: Value adding products derived from the ATCOR models. Paper DLR-1B 564-01/01, DLR, Oberpfaffenhofen, Germany.

7

GPR FOR SOIL MAPPING/ASSESSMENT AND ROOTS IMAGING

Susanne Lorra, Andreas F. Kathage[1]

[1] GeoHiRes International Ltd., Borken, Germany

ABSTRACT

In the European Union funded project WATERUSE the GPR (Ground Penetrating Radar) method has been investigated and improved in order to supply relevant information for scientists who are working on sap flow measurements as well as on the theoretical modelling of the soil.
This work was focussed on the 3-dimensional mapping of roots zones as well as on the 2- and 3-dimensional mapping of the soil texture in semiarid regions.
Based on several field tests the data acquisition methods were selected and developed. Suitable frequencies were identified as well as matched field equipment configurations and survey layouts were selected. This work was carried out hand in hand with the development of new data processing and interpretation software. Main components of the software development were the 3-dimensional processing-, visualisation- and interactive interpretation tools. These tools are suitable for the interpretation of complex structures like roots, which could not be tracked reliably with the software tools that were available at the beginning of this project.
It was shown during different common field experiments in semiarid regions that the employed GPR method provides valuable information for the teams working on sap flow as well as on soil models. The GPR-method has become a useful tool for soil and root mapping providing that high electrical conductivity values of soils do not prevent the propagation of the electromagnetic waves in the materials for investigation.
The non-destructive determination of the relevant soil and root parameters leads to a considerably better modelling and prediction of the water transportation in the soil – plant continuum. For this kind of investigations the non-destructive methods offer a much better cost-/performance ratio than invasive methods do.

Keywords: Ground Penetrating Radar, Soil Texture, Roots Zone, 3D-Mapping

1. INTRODUCTION

The objectives in the EU funded project WATERUSE were the development and test of novel integrated techniques appropriate to describe and quantify water flow through the continuum soil-plant-atmosphere (SPA) suitable for use in heterogeneous stands. The GPR (Ground Penetrating Radar) was identified to be a suitable method for the investigation of the root zones as well as for the investigation of the soil structure in the stands.

2. MATERIALS AND METHODS

The Ground Penetrating Radar method uses a device which consists of a control unit, an antenna and a survey wheel. The control unit sends electric trigger signals to the antenna, which forms an electromagnetic impulse of a certain centre frequency. This impulse is propagating in the ground and can be reflected at interfaces or discontinuities where the electromagnetic impedance of the subsurface material changes. A part of the reflected signals reach the antenna and these received signals are pre-processed and displayed as well as stored at the control unit.

Figure 1 – The Ground Penetrating Radar method. The Picture shows the control unit carried in a harness, the 400 MHz antenna and attached to the antenna is a survey wheel.

Metallic as well as non-metallic discontinuities can cause detectable reflections. Therefore the GPR is suitable for detecting tree roots as well as soil interfaces.
Different tasks had to be performed for this project. Firstly the required hardware configuration had to be tested. Secondly the processing as well as the interpretation of the GPR data had to be established, software tools needed to be developed. Last not least the complete survey system consisting of hardware and software needed to be tested and applied under real field site conditions.
The final proof of usefulness was carried out in the cork oak stand at Rio Frio, Portugal.

3. RESULTS AND DISCUSSION

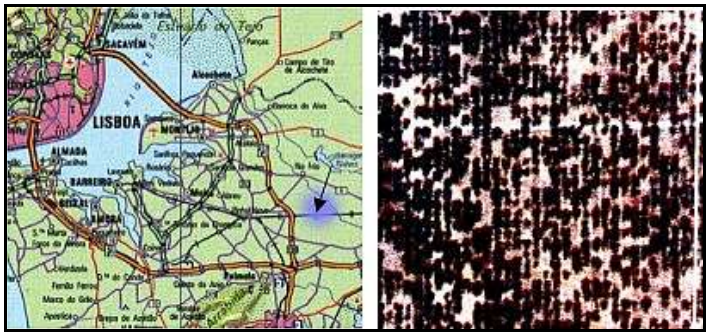

Figure 2 – Location of the comprehensive field tests at Rio Frio (see arrow on map) and aerial photograph of the cork oak stand.

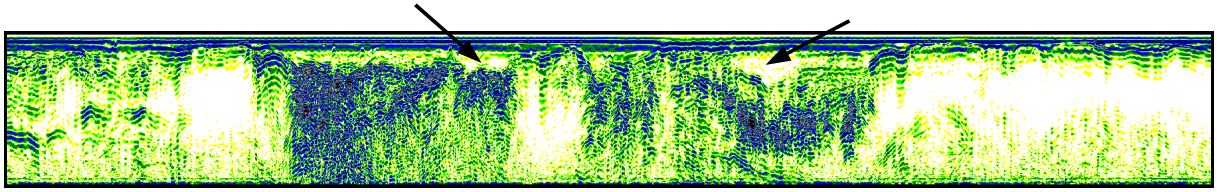

Figure3 – The radargram shows one of the reconnaissance lines, which were surveyed in order to get an overview of the soil structure in the survey area. Horizontal length of this section is about 100 metres. Vertical scale is 100 nanoseconds. The reflection patterns of former water channels (left and right of the centre of the profile, indicated by arrows) and of potentially sandy material are obviously located in the neighbourhood of silty or clayey material (for example the last part of the profile, to the right). These soil differences have impact on the moisture/water distribution in the ground.

At Rio Frio the GPR was used for mapping the soil as well as for imaging the lateral parts of the root zone of cork oaks. Besides 100 metres long reconnaissance lines (see figure 3), which were surveyed in order to get an overview on the soil structures around the stand the GPR was also used on orthogonal survey grids in order to obtain a 3-dimensional image of the soil texture.

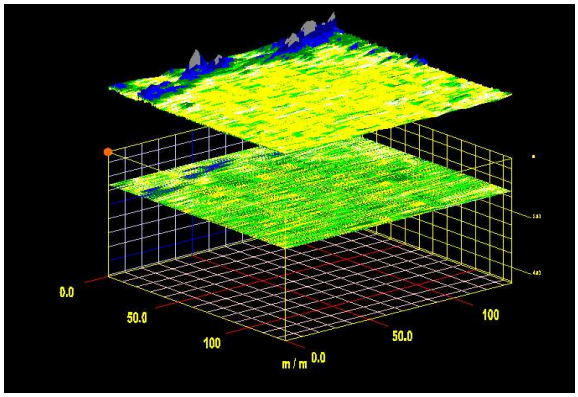

Figure 4 - *The picture above shows a 3-D contour view of GPR data in the survey area at Rio Frio. It was collected between tree coordinates SE-Corner K05, NE-Corner K19,SW-Corner X05, NW-Corner X19. The SW-corner is indicated by a red dot on the upper left edge of the grid. An area of about 135 m by 135 m was covered by this measurement.*

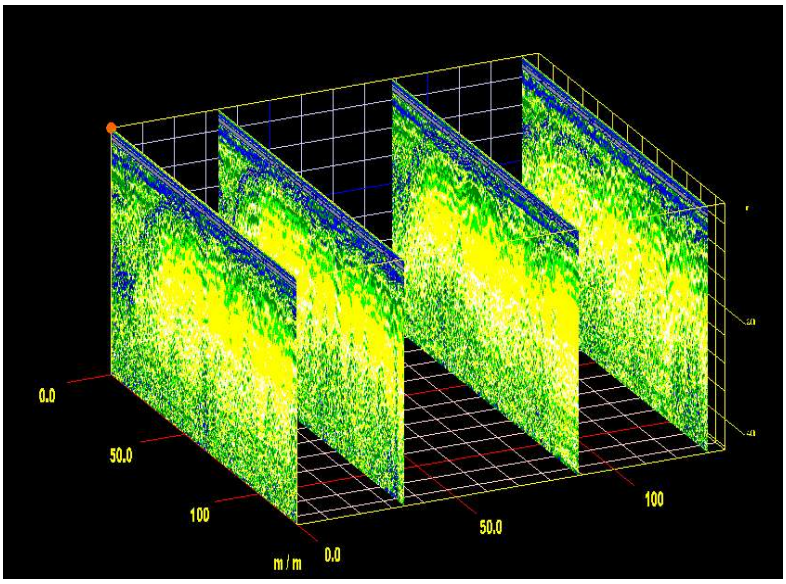

Figure 5 - The picture shows different GPR-profiles collected in the above mentioned 3-D survey area at Rio Frio. The dipping reflections of the clay water barrier are visible at the western part of the area.

The GPR measurements showed that former stream channels occurred in direct neighbourhood with clayey planes. The 3-D image allowed to obtain an understanding for the modelling of the moisture distribution and the water transportation in the stand area.

The ground surface around the cork oak roots was covered by an orthogonal grid of GPR measurements. The antenna frequency was 400 MHz (time range 30 ns).

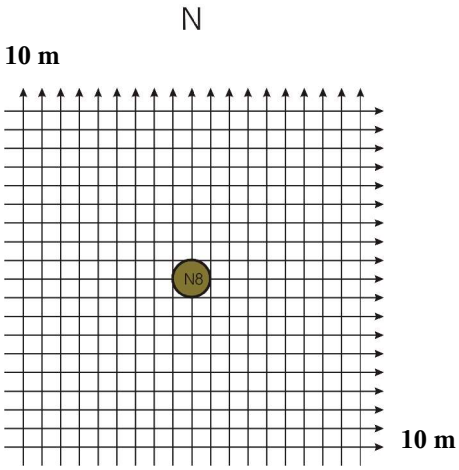

Figure 6 – Orthogonal survey grid for 3-d GPR measurements on tree roots. Profile separation is 0.5m.

Most horizontal roots were detected on top or above the clay layer (see figure 7). This layer behaves as a barrier for water transportation in the soil. Vertical roots are not detectable by GPR surface measurements.

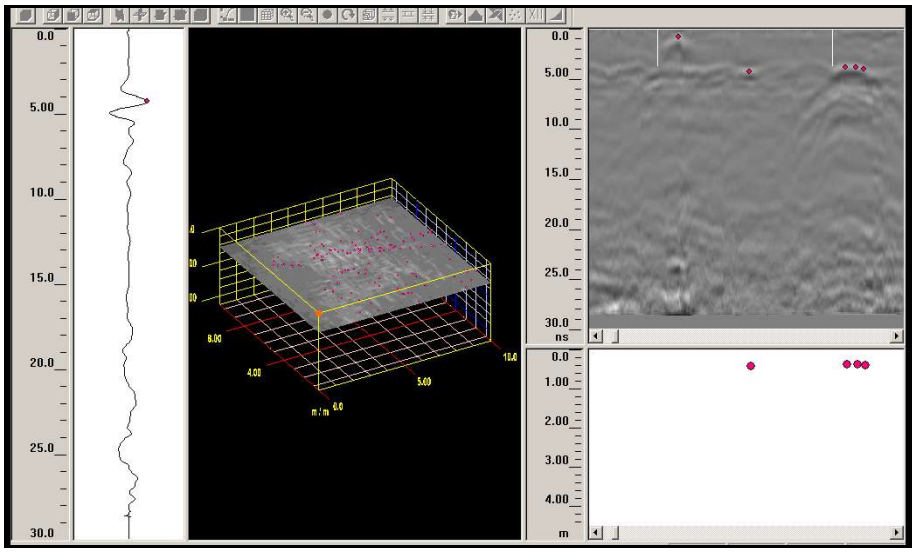

Figure 7 - The interactive 3-D interpretation allows the simultaneous working with 3 D views, radargrams, signal traces and 2-D interpretation views. This combined view allows to track complex objects like roots by correlating between different visualisations. Red dots indicate picked target reflections in this picture.

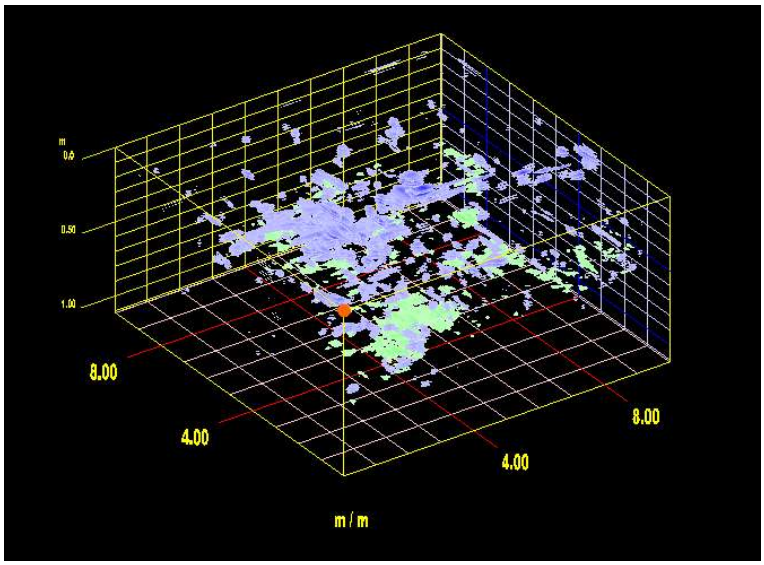

Figure 8 – 3-D visualisation of the tree roots reflections. The blue coloured spots represent GPR reflections from roots, which are situated around a sample oak at Rio Frio.

The 3-D visualisation shows where root concentrations are located in the soil around the oaks. Vertical roots are not detected by this configuration.

4. CONCLUSIONS

It could be proven during common field experiments that the employed GPR method provides information, which is useful and supporting the teams working on sap flow as well as on soil models. The developed methods are working practically and reliably in the field.

5. ACKNOWLEDGEMENTS

The demonstrated results have been funded by the European Union under the project "Evaluation of alternative techniques for determination of water budget components in water-limited, heterogeneous land-use systems - WATERUSE (EVK2-CT2000-00079)"

6. REFERENCES

(1)Kathage, A., 1991, Anwendung geophysikalischer Methoden zur Erkundung ehemaliger Betriebsgelände, gwf Gas Erdgas 132 Nr. 1, pp. 26 – 30.
(2)Kathage, A. and Pohlschmidt, R., 1991, Investigation of the Underground Soil and Pipe Structure for Trenchless Pipe Installation, 3R international, 30 Heft 9, September, pp. 506-510.
(3)Kathage, A.F., 1992, A Challenge: GPR in Advance of Horizontal Drilling, GPR'92, Proceedings of the Fourth International Conference on Ground Penetrating Radar, Rovaniemi, Finland, June 8-13, 1992, pp. 119-124.
(4)Greeuw, G., De Feijter, J.W. and Kathage, A., 1992, Field and Laboratory Tests on Line Scatterers, GPR'92, Proceedings of the Fourth International Conference on Ground Penetrating Radar, Rovaniemi, Finland, June 8-13, 1992.
(5)Guenther, M. and Kathage, A.F., 1994, The Geophysical Investigation of Drilling Obstacles for Microtunneling Projects by Means of GPR, GPR'94, Proceedings of the Fifth International Conference on Ground Penetrating Radar, Kitchener, Ontario, Canada, June 12-16, 1994, Vol. 3, pp. 1151-1165.
(6)Kathage, A.F., 1998, The Development of a Multi-Polarization GPR for Mapping the Geological Conditions and Subsurface Utilities in Advance of Pipelaying, Proceedings of the International Gas Research Conference, Nov. 1998, San Diego, USA.
(7)Kathage, A.F., Formanski, T., 1999, Georadartechnik und ihre Einsatzmöglichkeiten, Proceedings of the GAT'99, DVGW, Erfurt.

8

High resolution hydrogeophysical Techniques

Said A. al Hagrey, Ulrike Werban, Rolf Meissner, Wolfgang Rabbel and Ali Ismaeil
Department of Geophysics, Institute of Geosciences, Kiel University, sattia@geophysik.uni-kiel.de

Abstract

A better understanding of the static and dynamic water problem in the heterogeneous vadose soil zone demands developing new 3D mapping and monitoring techniques. Our full scale "GeoModel" erected at the Campus of Kiel University offers a new approach for developing new integrative hydrogeophysical techniques of high resolution and is an ideal link between laboratory (small scale) and field studies (natural large scale). It is used for carrying out fully controlled (infiltration) experiments on simulated soil models of predefined boundary conditions. Moreover, we summarize physical-empirical relationships of water content versus electric resistivity and radar velocity and present a new tomographic radar algorithm for velocity inversion. Some examples from the laboratory, from our GeoModel and from the field are presented.

Introduction

Soil formations (with the exception of large clay contents) possess a very high specific electrical grain (or matrix) resistivity ρ. Their electric conductivity σ (= 1/ρ) is related mainly to the interstitial (pore) water, which is normally slightly mineralised. The pore water conductivity is proportional directly to the amount of water content, the minerals contained in the water (ion concentration and mobility), the degree of interconnection between the pores (hydraulic conductivity/permeability) and temperature that decreases the viscosity and increases the mobility and conductivity (Keller, Frischknecht, 1966; McNeill, 1980). Usually subsurface temperature effects on resistivity are negligible except in extreme cases of e.g. permafrost regions. The presence of clay minerals decreases the resistivity significantly through effects of ion-exchange processes and the double ionic layer (Schön, 1997).

Soil water content θ is linked to petrophysical parameters of specific formation dc-resistivity ρ and radar velocity v by empirical laws of Archie (1942) and Topp et al., (1980), respectively. Hydrogeophysical techniques, based on these relationships are able to find the (static) amount of water content and even determine its (dynamic) behavior by repeated time-dependent measurements (or time lapses) during infiltration-or growth-experiments. We will first describe these relationships and discuss their applicability in the field.

The electromagnetic wave propagation of radar waves is governed mainly by the dielectric constant and DC conductivity of the medium. In the low-loss medium of earth's materials (σ < 100 mS/m) and for the high radar frequency (f = 10-2000 MHz) the wave velocity v is mainly controlled by the relative dielectric constant ε_r of the medium. For water ε_r (= 83) is very high relative to that of soil sediments (ε_r<7, e.g., Shen et al., 1985). Therefore, the pore water content θ dominates the effect of the radar velocity v. For a wide range of soil samples with varying degrees of water saturation the Topp equation states that

$$\theta = -0.053 + 0.029\varepsilon_r - 5.5x10^{-4}\varepsilon_r^2 + 4.3x10^{-6}\varepsilon_r^3 \qquad \text{and} \qquad \varepsilon_r \approx (c/v)^2$$

where ε_r = relative dielectric constant with respect to that of vacuum and θ = water content, c = v-vacuum (≈ 30 cm/ns, e.g., Hagrey and Müller, 2000).
For a partially saturated, granular sedimentary formation (with negligible clay content and electrical matrix conductivity σ) Archie (1942) suggested from petrophysical measurements an empirical equation to relate the lithology to resistivity of the form (Schön, 1997):

$$\frac{\rho}{\rho_w} = \frac{a}{S^n \Phi^m} = F, \qquad S = \frac{\theta}{\Phi} \qquad \text{and} \qquad \rho = \frac{a\rho_w}{\Phi^{m-n}}\theta^{-n}$$

ρ = bulk resistivity
ρ_w = pore water resistivity
Φ = volume fraction porosity
θ = volumetric water content
a = constant =0.6-1 for loose sand
m = cementation factor, decreases with particle sphericity =1.3-2.2
n = saturation exponent (n= 2 for loose sediment)
S = fractional water saturation
F = formation factor, depends on pore geometry

Principles of DC resistivity technique: For a point source signals of very low-frequency AC with negligible magnetic properties in an infinite homogeneous isotropic medium Maxwell's equation reduces to (e.g., Keller and Frischknecht, 1966):

$$U(r) = \frac{I\rho}{4\pi r}$$

U = potential of a single current point source
r = distance
I = current source strength
ρ = medium resistivity

Given 2 current electrodes C1, C2 over a hemispherical surface, the potential at arbitrary point P1 is (Fig. 1):

$$U_{P1} = \frac{I\rho}{2\pi}\left[\frac{1}{r1} - \frac{1}{r2}\right]$$

r1 = P1-C1 distance
r2 = P1-C2 distance

In DC resistivity survey, a pair of potential electrodes measures the difference by subtracting the potential at P2 from that at P1

$$\Delta U = \frac{I\rho}{2\pi}\left[\frac{1}{r1} - \frac{1}{r2} - \frac{1}{r3} + \frac{1}{r4}\right] = \frac{I\rho}{k} \qquad \text{or} \qquad \rho_a = k\frac{u}{I}$$

where

$$k = \frac{2\pi}{\left(\frac{1}{r1} - \frac{1}{r2} - \frac{1}{r3} + \frac{1}{r4}\right)}$$

r3 = P2-C1 distance
r4= P2-C2 distance
k is the geometric factor which depends on the electrode arrangement

For an inhomogeneous earth, this equation will produce values that vary according to the geometrical arrangement of electrodes on the surface.

Geolelectrical surveys from the ground surface and in boreholes yield a distribution of specific electrical resistivities characterising geological layers and structures in the underground. The sur-

vey is carried out using 4-point electrodes (often stainless steel, sometimes non-polarizing Cu - CuSO4); one pair for injecting current (C1 and C2) in the heterogeneous subsurface material and

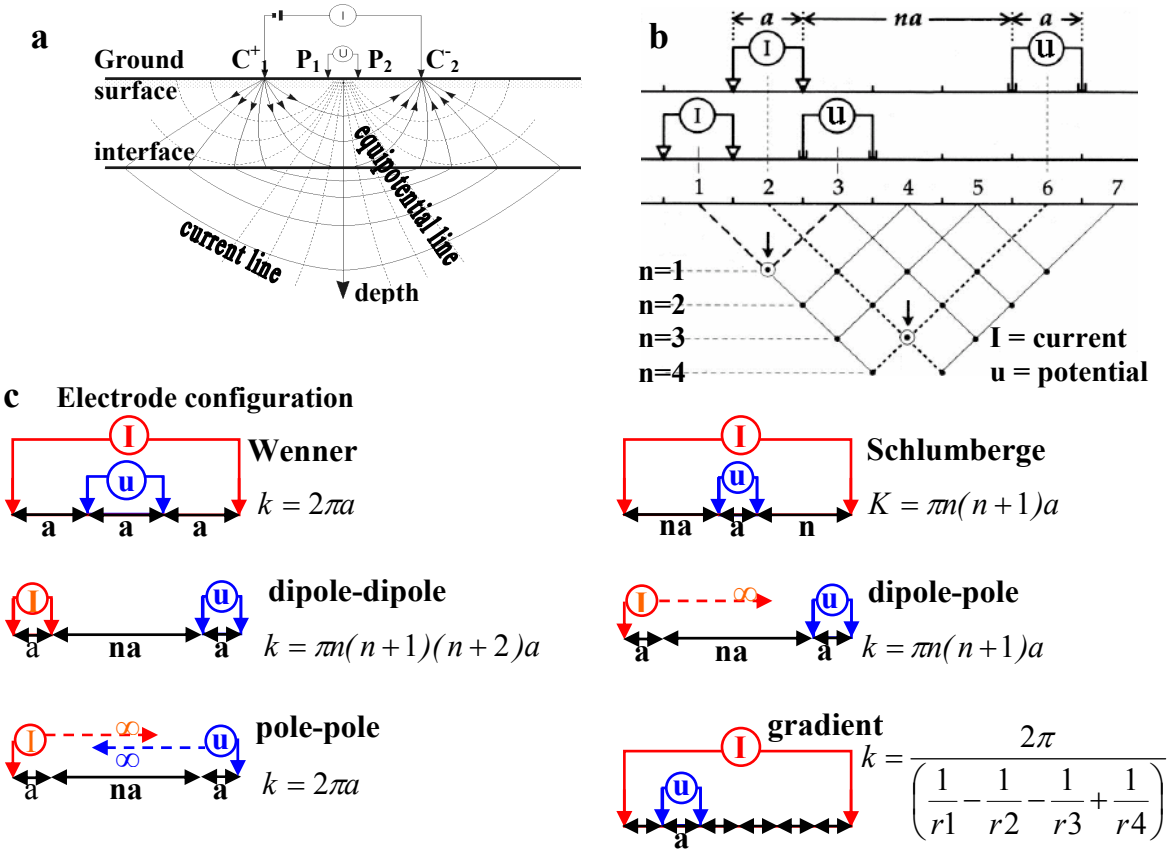

r1, r2, r3, r4 = distances of P1-C1, P1-C2, P2-C1 and P2-C2, respectively

Fig. 1: a) 4-Point electrode configuration of Schlumberger, b) acquisition of resistivity pseudosection using dipole-dipole array, (c) common electrode arrangements of dc survey

another pair for measuring the potential difference (P1 and P2) of the resulting inhomogeneous electric field (Fig. 1). From the current I and voltage u value, an apparent resistivity ρ_a is calculated from $\rho_a = k(u/I)$.

The geoelectric survey is carried out now using modern multi-electrode/multi-channel data acquisition systems along individual profiles (in 2D pseudosection) and along grids of multi-electrodes for continuous vertical sounding and 3D mapping of the study site. Diverse electrode configurations (e.g., Schlumberger, Wenner, dipole-dipole array) are used depending on the goal of the survey, the resolution of results, the depth of penetration, etc (Fig.1). The resulting apparent resistivity (ρ_a) data are inverted into 2D or 3D subsurface models of true resistivity ρ using complex relationships solved by computer programs. The geoelectric method is suitable for hydro-geological mapping and prospecting for water and landfills. High resolution surveys are increasingly applied for environmental studies, geotechniques and engineering, agronomy and forestry.

High resolution "GeoModel" approach

Our approach to develop novel integrated hydro-/biogeophysical 3D techniques of high-resolution includes also accomplishing controlled experiments at our full scale tank analog or GeoModel (3x5x2m) at the University campus (Hagrey et al., 1999, Trinks, et al., 2002, Schmalz, et al., 2002),

Table 1. The GeoModel which is unique in constructing components and functions, simulates vadose soil zones of different structural, textural, lithological and hydrological properties in their natural scale. It is a bridge between scaled laboratory models (typical size of $1m^3$) and field surveys (several km^3) and takes advantages of both. The GeoModel is currently equipped with instruments of dc resistivity, radar, TDR (time domain reflectometry), and tensiometer as well as irrigation, filter, drainage and vacuum suction devices for carrying out highly spatiotemporal resolving experiments (in cm and seconds range). The hardware allows 3D data acquisition and tomography using electrode grids from all sides in numerous arrays, antenna configurations (surface and boreholes) and a distribution of probes for water content and tension. It is used to carry out controlled irrigation (infiltration) experiments of varying scenarios; (e.g., natural rain, ponding and drip irrigation) and to study flow structures (e.g., fingering, macropores) of different duration, intensity and background moisture similar to that applied in agroforestry. The GeoModel is also used to study the water content for soils and plants and water uptake by roots. Before erecting our final GeoModel we performed various tests using a large former model.

Fig. 2: GeoModel at the university campus of Kiel

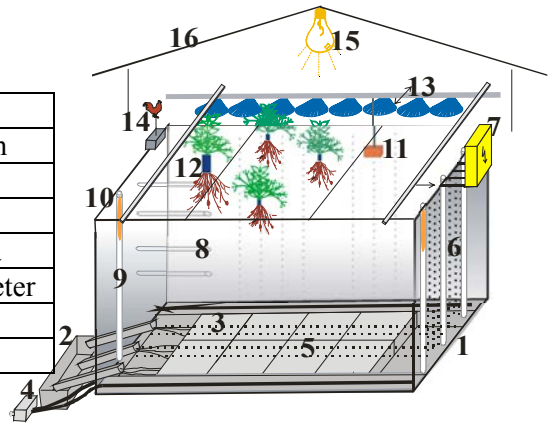

1	filter layer	2	drain water
3	bottom drain	4	vacuum suction system
5	bottom electrode grid	6	side electrode grid
7	switch box, geoelectric	8	TDR/Tensiometer
9	borehole	10	borehole GPR-antenna
11	surface GPR-antenna	12	plant with sap flow-meter
13	irrigation system	14	meteorological station
15	light	16	roof, isolated hall

Table 1: GeoModel at Kiel University, facilities and instruments

Soil model body	5x3x2m³ size, filled now with fine sand
Submodel filter layer	5x3x0.5m³ of pebble (grain size: 4-8, 8-16, 16-32mm)
Drain filter containers	6x2 (each 0.5m²) in the 6m² central area, 3 for boundary zones
Model boundaries	model is bounded by hydraulically isolated, electrically conductive wall; Dirichlet boundary conditions of field continuity
Monitoring chamber	5x3x4m³ room equipped by discharge and vacuum aperture
Vacuum suction system	automatic pump to prevent hydraulic barrier at the sand-gravel (filter)-interface
TDR and Tensiometer	3 vertical profile of sensors at model front, 20 cm interval
Vertical electrode grids	40x16 electrodes at the 4 bounding sides, 12.5cm interval
Bottom, surface grid	each 17x47electrodes, 10cm interval
Switch box	for all electrode/decoder outlets which define electrode array
GPR data acquisition frame	mechanically driven 3D survey, antennas of varying frequency (50 Mhz-1.5Ghz antennae, mono-/bistatic mode), spacing and height.
GPR tomography	16 boreholes set along the vertical bounding sides at 1m interval
Irrigation device, static	automatic recording of irrigation rate and volume with time
Monitoring discharge	automatic recording rate and volume as a function of time
Computer room	equipped by aperture for all sensors used in the measurement
Tree	transplantation of a single tree
Covering Hall	131m2, protecting against weathering, controlled boundary conditions
Subsurface ring drain	for draining soil water from surroundings

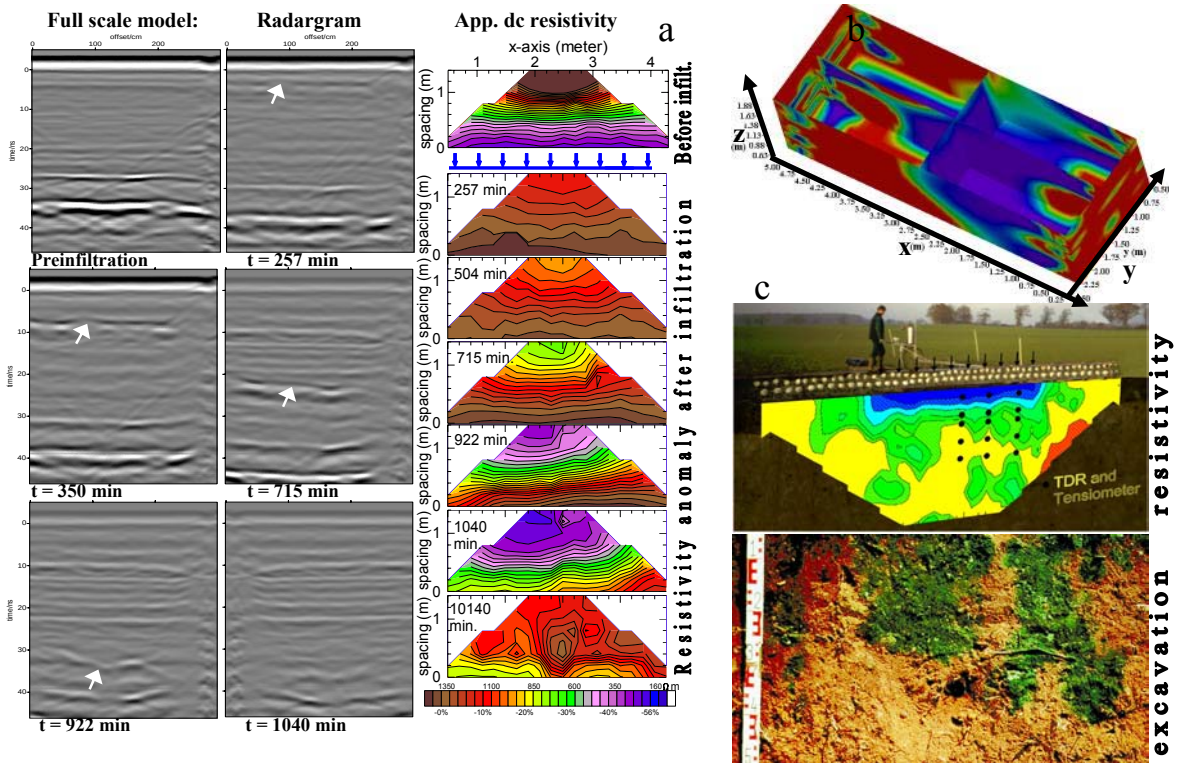

Fig. 3: (a) Infiltration experiment at the GeoModel showing the deepening of water front with time. (b) 3D resistivity soil model that can be calculated into water content, (c) Infiltration experiment using dye tracer at Bokhorst (Germany) showing preferential flow fingering in 2D resistivity model and excavation

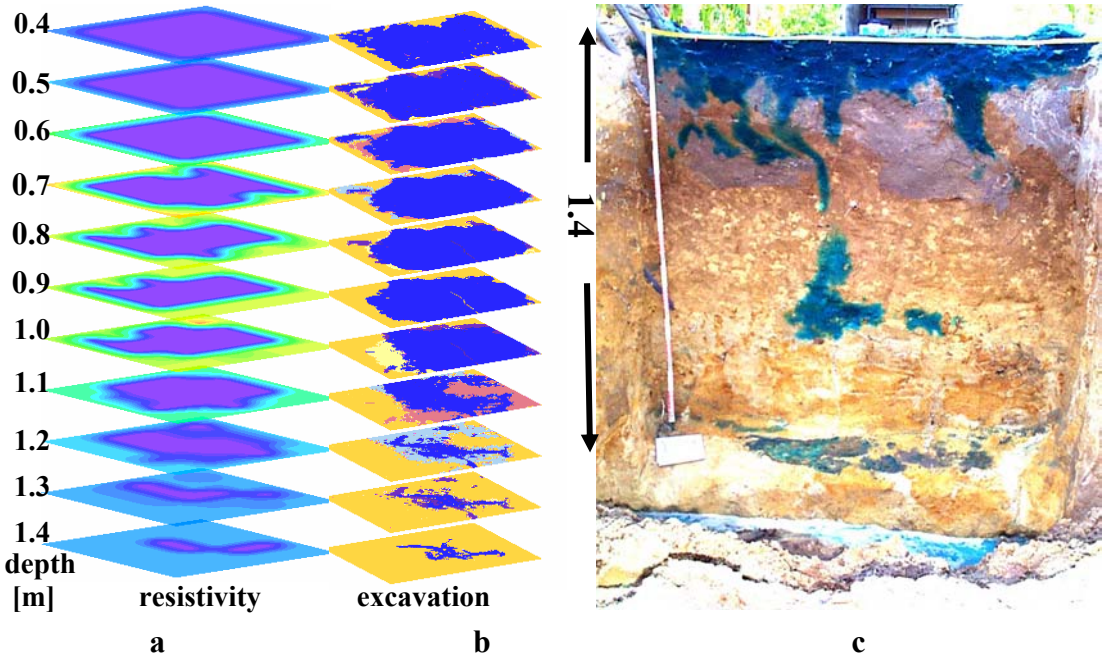

Fig. 4: Results of dye tracer experiment in the vadose soil zone, Atalaia, Portugal showing 3D resistivity model (a), excavated horizontal slices in photos (b) and excavated vertical section with depth (c). The results show capability of the resistivity technique to map the heterogeneous preferential water flow paths.

Preferential flow: In one of the experiment water was uniformly infiltrated with time continuously until its front crossed the soil model and released from the bottom drain. The hydrogeophysical monitoring before, during and after the infiltration shows that the radargrams (along the surface profile) and resistivity pseudosections (of Wenner array along a profile of the lower grid) image clearly the proceeding of the infiltrated water front with increasing elapsed time from infiltration start. The irregularities in the front indicate a heterogeneous (preferential) flow. Radargrams show the apparent deepening of the two fixed boundaries of the model base and some strong reflections from the percolating water front (arrows), an effect of the decrease of the radar velocity due to the increasing water content. Comprehensive software for data acquisition, processing and inversion in the GeoModel is available for its special boundary conditions. A 3D inversion of resistivity measurements carried out using diverse electrode combinations from all grids show a cell resolution down to 0.0625 m of cell length, i.e., within the GeoModel a total sum of 5x3x2 m^3= 30,000,000 cm^3 = 122,880,000 cells.

Two examples of filed infiltration experiments are shown at Bokhorst site (north Germany) of boulder clay soils and at Atalaia peach orchards (Portugal) of sandy soils. Before, during and after infiltration of the dye tracer at both site, hydrogeophysical measurements (using techniques of DC resisticity, radar, TDR and tensiometer) were accomplished. The results show that the applied techniques (here geoelectric) are capable to resolve the heterogeneous preferential flow paths and structures in dm ranges, where a satisfactory similarity between the model and excavation results can ob observed.

Monitoring water uptake in root zone, a hibiscus plant in laboratory

This experiment aims at monitoring water uptake by roots and studying its daily (day and night, hydraulic lift process? which explains water movement from moist to dry layers using the plant root system as conduit (e.g., Caldwell et al., 1998) and seasonal variations. A hibiscus plant was planted in fine sand within a cylindrical plastic pot; its surface covered by plastic foil to minimize the evaporation, i.e., the water uptake by roots is consumed for transpiration. A surface geoelectric profile (of 16 electrodes at interval of 1.5cm) was installed at the sand surface; one peripheral and one central TDR probes and one tensiometer probe was installed in the top 15 cm. The data acquisition of TDR, tensiometer and Dc resistivity pseudosections (Wenner and dipole-dipole configurations) were monitored continuously for some weeks during the spring and autumn seasons.

The observed TDR-water content, the tensiometer water potential and the average resistivity, calculated for all configurations, show similar results with time; they reflect clearly the decrease of the porewater content with time and its abrupt increase directly after every irrigation cycle (Fig. 4). TDR- and tensiometer curves are nearly parallel and are mirror images of the resistivity curve (ρ is inversely proportion to θ and tension). Considering the daily variations, we can observe a general increase in the soil water content during the night time (i.e., when the plant transpiration was suppressed) relative to that during the day time. Topp et al. (1996) related similar observations for maize plant roots to night changes in water content within the roots without necessarily affecting the soil, i.e., it can not be related to the phenomenon of the hydraulic lift. The long term observation shows that the behavior of the plant regarding water uptake is a function of the background moisture content in the root zone. The maximum water uptake occurs at intermediate saturation ($10\% < \theta < 18\%$) which is the optimum range for the growth of this plant. Above and below this range the water uptake decreases. Seasonal variations in the soil water uptake by the roots could be observed; the water uptake in Mai is obviously twice that of November. This can be explained by the fact that the available light (required for photosynthesis) was higher in Mai than in November. Also the effect of the day light on the water uptake is clear; the light sunny days show higher water uptake than the dark rainy days of a minimum water uptake (Fig. 4). The peripheral water content values are much lower than that of the central root zone, they decrease continuously with time and

show nearly no night and day changes. This may imply that the central TDR probe measures the water content both within the wet root branches and the bounding soils, whereas the peripheral TDR reading represent the soil porewater only.

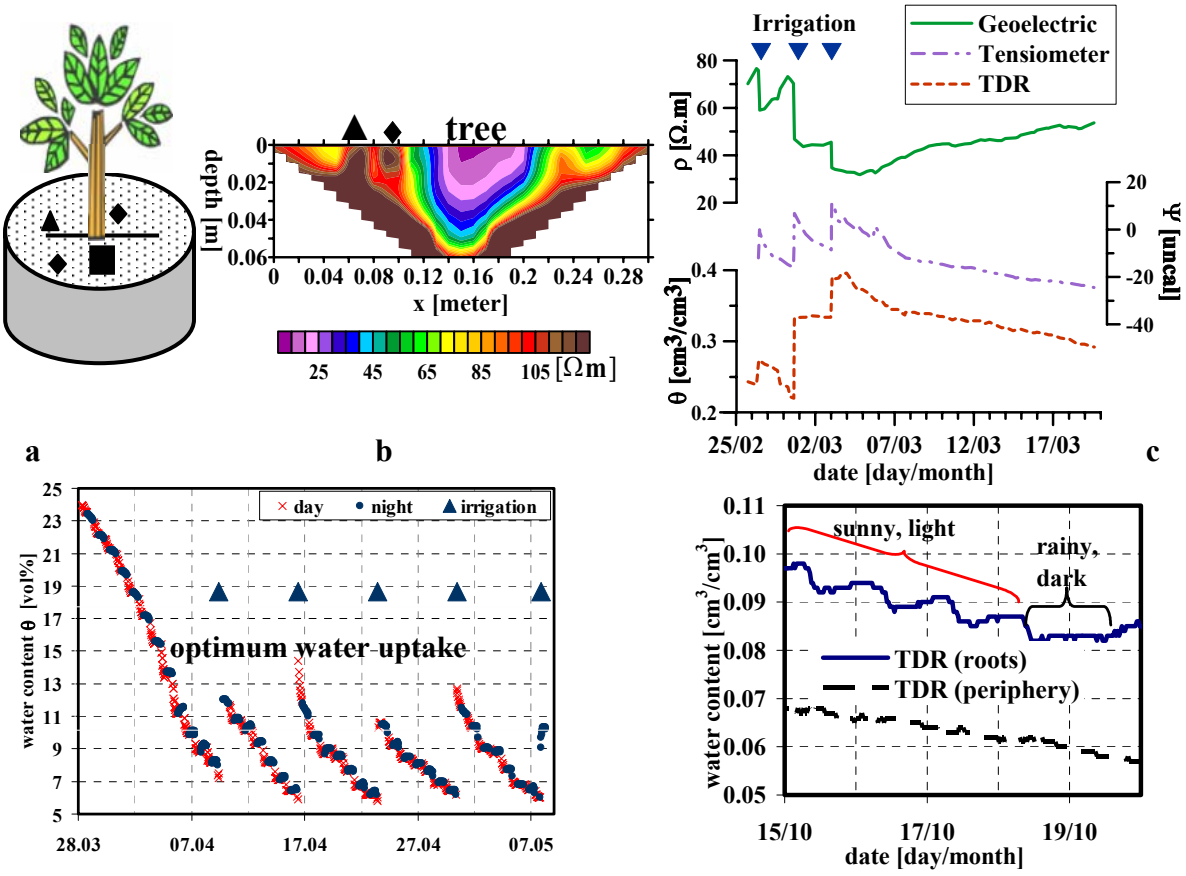

Fig. 4: Monitoring water content in the root zone of a hibiscus plant in a pot (Ø =25 cm) filled with fine sand. (a) Experimental set up of a geoelectric profile (—), radar antenna (■), TDR (♦) and tensiometer (▲). (b) 2D electrical resistivity model from pseudosections of Wenner and dipole-dipole configurations showing negative resistivity anomaly in the root zone. (c) Monitored average resistivity ρ, tensiometer water potential ψ and TDR-water content θ for three weeks. (d) TDR-water content monitored for six weeks and five irrigation cycles. It shows the plant behaviour during day and night times and an optimum root water uptake at soil humidity θ= 9-17%. (e) The soil water content measured θ by TDR-probes set inside the root zone and at the periphery of the pot. Root curves show the effect of day light on the amount of water uptake.

A new GPR tomography technique for mapping soil moisture, lab and field experiments

A new GPR tomography code "SeismoRad" is developed by merging the well known seismic tomography and the finite difference (FD) methods for inverting surface and crosshole data. Tomographic reconstruction technique is based on solving a system of linear equations iteratively. The principle of the method shows a typical ray path *Ri* from the transmitter (Tx) to a receiver (Rx). Multiple locations of Tx and Rx yield a number of such rays crossing the intervening material in different directions. The region between Tx and Rx lines are discretized into j cells, each cell has a constant slowness *p*j. The recorded travel time is expressed as integral over the ray path of the form

$$t_i = \int_{R_i} p(x,y)da$$

Each of these integrals, in discrete form, becomes one equation in the linear tomographic system that is to be inverted for velocity and/or layer shape (from travel times) or for attenuation (from amplitudes). The linear system of equations has the form

$$t_i = \sum_{j=1}^{m} \Delta a_{ij} p_j ,$$

where Δaij = the length of the ray i which penetrates pixel j, m = the total number of pixels intersected by the ray i. We used this principle to develop a new GPR tomography algorithm (SeismoRad computer program) for inverting surface and crosshole data (Hanafy, 2002).

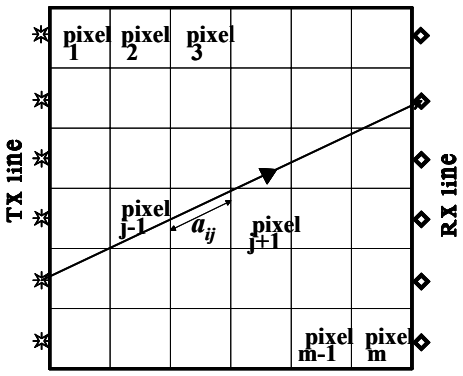

Pixel geometry and ray path from transmitter Tx to receiver Rx. For the ray i the distance traveled in a pixel j is denoted by aij.

Theoretical tests show that our tomographic inversion technique reproduces the original velocity model better than that of published technique (e.g., Peterson, 2000; Jackson and Tweeton, 1996).

In laboratory experiments, tomographic travel time measurements were acquired for four, variously saturated sand objects buried in uniform dry sand. On the resulting velocity tomograms of laboratory experiments we can map the sand objects and characterize the different saturations. We can differentiate between the adjacent anomalous objects and the boundaries of each one. The wet objects display velocity minima that decrease with increasing saturation.

Field application to study the root zone of a poplar tree at the Botanic Garden, Kiel shows that the inverted GPR velocity increase generally with radius away from the tree. The root system below the tree occupies the centre of a low velocity zone (8.14–8.76 cm/ns) due to the relatively higher moisture content within the whole medium of GPR wave propagation. The humidity of the entire root envelope medium includes the total sum of the water content inside all individual root branches and the pore water of the surrounding soil material. An additional low velocity zone (5.25–7.98 cm/ns) located at the south eastern corner of the site may be caused by a higher water content within a friable zone which was excavated previously for investigating soil materials at this site.

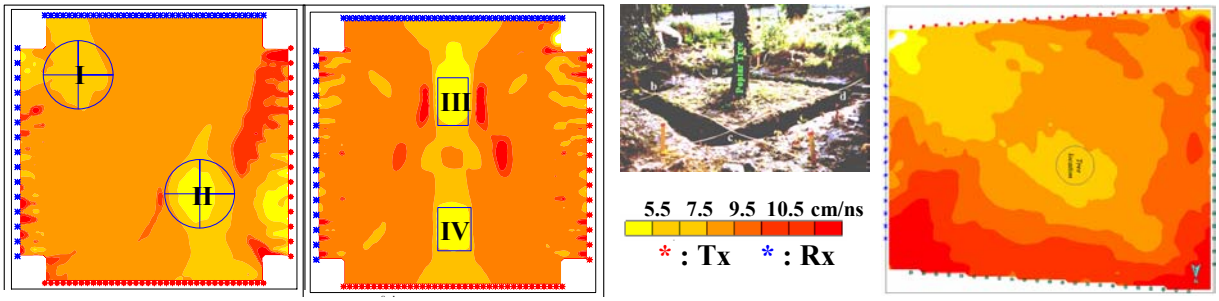

laboratory: sand box (90x90x30 cm^3)				field 260x225 cm^2
cylinder I	cylinder II	prism III	prism IV	tree root
27 %	54 %	80%	100%	estimated water content 0.46 (vol.)
11.5 cm x 7 cm		10 cm x 10 cm x 15 cm		
each of 1994 data points at interval of 2cm				2213 data points at interval of 10 cm

Fig. 5: Laboratory and field results of radar tomography experiments using travel times for signals transmitted between the transmitter (Tx) and receiver (Rx) antennas that set at the corresponding opposing sides. Velocity tomograms which are inverted using the SeismoRad program show a negative velocity anomaly directly above the high saturated objects.

Conclusion:

Our GeoModel which fills the gap between scaled laboratory experiment and field survey of natural scale is necessary to develop new integrative hydrogeophysical 3D techniques of better resolution and of more realistic solution. Refined techniques like 3D modelling of DC resistivity or tomograpic interpretation of radar velocity help in improving the resolution. Examples for mapping of preferential flow paths and monitoring water content are performed in the GeoModel, and in the field. Also small scale laboratory experiments for monitoring wateruptake by roots and high resolution radar tomography technique are presented.

Acknowledgements
Thanks for Dr J. Michaelsen, former participant of the WATERUSE-Project and now at Water supply authority in Hamburg, Prof. J.J. Sauter and U. Werban at the University of Kiel for their help. This work is carried out in the scope of the WATERUSE and GeoModel projects funded by the European Commission and the German Federal Ministry of Research.

References

Archie, G.E., 1942. The electrical resistivity log as an aid in determining some reservoir characteristics. Transactions of the American Institute of Mining Engineers 146, 54-62.
Caldwell, M.M., Dawson, T.E and Richards, J.H., 1998. Hydraulic lift: consequences of water efflux from the roots of plants, Oecologia 113, 151-161.
Hagrey, S. A. al. & Michaelsen, J., 1999. Resistivity and percolation study of preferential flow in vadose zone at Bokhorst, Germany, Geophysics, , 64, 746-753.
Hagrey , S. A. Al. & Müller, C., 2000. GPR-study of pore water content and salinity in sand, Geophysical Prospecting, 48, 63-85.
Hanafy, Sh. M., 2002, GPR/seismic tomography for delineating subsurface structures: Ph.D. thesis, Cairo University.
Keller, G.V.& Frischknecht, F.C., 1966. Electrical methods in geophysical prospecting. Pergamon Press, Inc.
McNeill, J.D., 1980. Electrical conductivity of soils and rocks: Geonics Ltd. Tech. note TN-6.

Schmalz, B., Lennartz B. & Wachsmuth, D., 2002. Analyses of soil water content variations and GPR attribute distributions. J. Hydrology 267:217-226.

Shen L.C., Savre, W.C., Price, J.M. & Athavale, K., 1985. Dielectric properties of reservoir rocks at ultra-high frequencies: Geophysics, 50, 692–704.

Schön J.H., 1997. Physical Properties of Rocks: Fundamentals and Principles of Petrophysics, Handbook of Geophysical Exploration. Elsevier Science Ltd, Amsterdam.

Trinks1, I., Wachmuth, D., Stümpel, H, 2001, Monitoring water flow in the unsaturated zone using georadar, First break, 19:679-684.

Topp, G.C., Watt, M., Hayhoe, H.N., 1996. Point specific measurement and monitoring of soil water content with an emphasis on TDR. Can J Soil Sci 76, 307-316

Topp, G.C., Davis, J.I.& Annan, A.P., 1980. Electromgnetic determination of soil water content. Measurements in coaxial transmission lines: Water Resources Research, 16, 574-582.

16

Hydrogeophysics of soils and trees

Said A. al Hagrey, Ulrike Werban, Rolf Meissner, Wolfgang Rabbel and Ali Ismaeil
Department of Geophysics, Institute of Geosciences, Kiel University

Abstract

Static and dynamic behaviour of water in soils and trunks can be assessed by applying various geophysical techniques. Geoelectric measurements show a firm relationship between resistivity and water content for nearly all soil types (with exception of clayey soils); they observe irrigation and water uptake in the roots of trees and plants and can map various root zones. Even the water content and its distribution and movement (sap-flow) in trunks can be observed by modifying electric techniques using multiple ring electrodes and refined inversion methods. Radar measurements show an inverse relationship between the radar velocity and the water content; hence they also can monitor efficiently water content, irrigation processes and water uptake in roots and even observe inhomogeneites of roots and rocks in the subsurface and perform a tomography.

Introduction

Water is the dominating agent for all biological processes. The global increase of water and land use in terms of quality and quantity calls for sustainable management of water catchments and better understanding of water and solute movement. The aim of our EU-project WATERUSE is to develop integrated techniques to quantify water flow through the soil-plant-atmosphere continuum (SPAC) adequate for use in heterogeneous stands in water stressed areas. We concentrate in this paper on observing and mapping the static and dynamic water or moisture in soils and trunks. Specifically, this work aims at: (1) mapping the hydrogeological situation in the near surface zone, (2) deriving water content from empirical hydro-petrophysical relationships established from in-situ and laboratory data, (3) mapping objects and structures in the heterogeneous vadose zone (e.g., characterising root zones), (4) imaging internal ring structure of trunks, (3) exploring capability of geophysical techniques to monitor processes (e.g., water flow in vadose zone, water uptake by roots, sap flow in trunks). Our measurements are a contribution to identify zones of water surplus or deficiency and from the basis for hydrological modelling.

Soil water content θ is linked to petrophysical parameters of specific formation dc-resistivity ρ and radar (or GPR "ground penetrating radar" velocity v by empirical laws of Archie (1942) and Topp et al., (1980), respectively. Hydrogeophysical techniques, based on these relationships are able to find the (static) amount of water content and even determine its (dynamic) behaviour by repeated time-dependent measurements (or time lapses) during infiltration-or growth-experiments.

Within the WATERUSE project two intensive observation periods (IOP) were accomplished with participation of all partners in summer 2002 to Canosa, southern Italy in an olive farm and in summer 2003 in Rio Frio (Portugal) in an endangered cork oak plantation. Moreover, diverse small experiments devoted to root mapping or trunk imaging and many single experiments in our GeoModel were carried out with partners related to this subject. Also many single experiments are carried out independently during developing and testing of hard and software of new techniques (e.g., diverse experiments in our GeoModel and laboratory, GPR-tomography measurements, trunk imaging tests). The applied techniques and setups for surface and subsurface surveys and trunk imaging in the field are summarised in Table 1.

Table 1: Field setup and arrays of hydrogeophysical surveys.

Experiment/method	array/mode	setup
surface electric	2D pseudosections, 3D grids (rectangular, radial or star), diverse arrays of α, β, γ-Wenner, dipole-dipole etc.	up to 256 electrodes, spacing (a) = 0.02-0.5m
subsurface electric		up to 16 electrodes, a= 0.02-0.15m
electric imaging of trunk	ring array, dip.-dipole	Multi-electrodes (>16), constant angular interval
radar survey	Reflection, CMP mode, profiles and girds (rectangular)	bistatic antenna, 100, 200, 400, 500, 900, 1500 MHz
TDR, Tensiometer	single point data	horizontal and vertical installation

TDR denotes for time domain reflectometry

In a new area a reconnaissance study was usually carried out before beginning of the main study. Techniques of radar profiling, electromagnetic inductions (EMI) and geoelectric pseudosections with coarser resolution are applied for the general subsurface mapping of the field site. Detailed hydro- and biogeophysical investigations of high resolution of the vadose zone and single trees followed by in-situ measurements using geoelectric, TDR and tensiometer techniques that took place at different time intervals (time lapses) in order to monitor different processes related to movements of water and nutrients.

Hydrogeophysical mapping

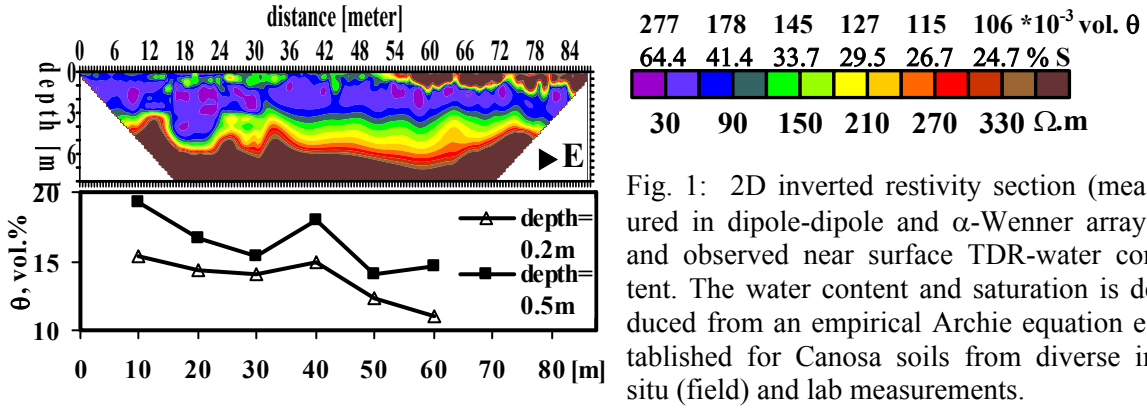

Fig. 1: 2D inverted restivity section (measured in dipole-dipole and α-Wenner arrays) and observed near surface TDR-water content. The water content and saturation is deduced from an empirical Archie equation established for Canosa soils from diverse in-situ (field) and lab measurements.

The olive farm at Canosa (of nearly 100 years old trees) is covered mainly by loamy carbonate soil materials. For general mapping of the subsurface soil layers long profiles were located to cross most of the whole plot of 90*90m^2, at the northern and eastern sides. A 2D-pseudosection resistivity survey was accomplished in the Wenner and dipole-dipole array using a fixed electrode spacing of 0.5m and in all possible dipole-dipole offsets. Within the investigation depth of 8m, the inverted 2D subsurface sections show clearly a succession of three layers overlain by a thin surface cover (Fig. 1). The surface cover displays an increase in thickness (from 0 to 0.8m) and resistivity (from 150 to 500 Ωm). This surface layer approaches its maximum thickness at the NE corner of the plot where the ground surface is elevated gently and the soil material becomes harder. Below the surface cover, the underlying layers show a continuous increase of resistivity with depth. The TDR-measurements at depths 0.2 and 0.5m show a general decrease of water content with distance from W to E. This moisture distribution is inversely proportional to the resistive surface layer distribution, i.e., the humidity is the main factor governing resistivity. The second layer with the lowest resitivity values (20-90 Ωm) may reflect the weathered carbonate sediment with partial water saturation and is considered the main waterfed for the trees. This may be related to the strong affinity of carbonate sediments to absorb and retain the surface rain water. These results are supported by the excavation and radar data. The third base layer is characterised by high resistivity values (>300 Ω.m) and is considered to represent the parent (less weathered) carbonate rocks.

Deriving water content from dc resistivity and GPR-velocity

The soil cover at the olive farm of Canosa consists mainly of loamy carbonates with small clay content. These soil material is considered to have a very high grain (matrix) resistivity; their conductivity is mainly electrolytic through the pore water. We have accomplished diverse controlled infiltration experiments for measuring electrical resistivity as a function of water content in the field (along vertical walls of excavated pits) and in the laboratory on soil samples collected during our field campaigns (Fig. 2). The water content data determined by TDR (time domain reflectometry) probes and the gravimetric technique using cylindrical sampling showed a good agreement, i.e., inaccuracies in TDR readings e.g., due to clay effects, can be neglected.
This best fitting curve linking ρ and θ for the soils has the numerical expression:

$$\rho = 2.05\theta^{-2.09} \qquad \text{or} \qquad \theta = 1.30\rho^{-0.46}$$

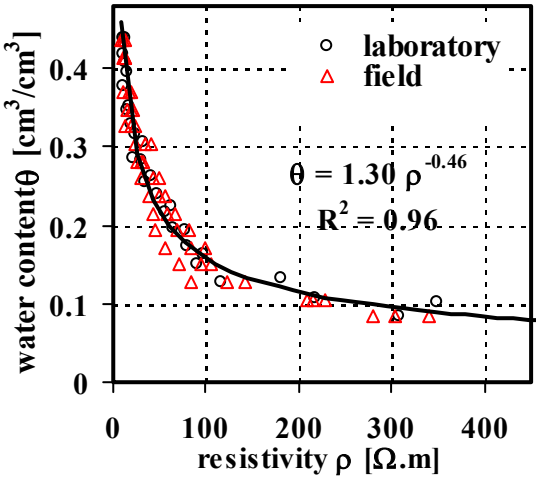

Fig. 2: Bulk resistivity ρ versus water content θ with fitting Archie's regression for Canosa (Italy) soils from in-situ and laboratory data.

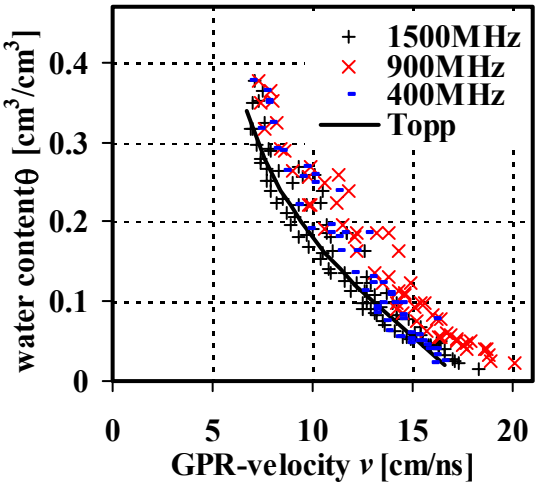

Fig. 3: Water content θ versus GPR-velocity v for diverse soil samples. Note dispersion effects, often neglected; v (900 MHz)-values are higher than those of 400 MHz and 1500 MHz.

From these equations we have deduced the constants m and n of the Archie equation by applying the values of a, ρ_w and Φ that have been determined during the experiment or obtained from literature for similar carbonate soils (Schön 1997). We applied the Archie regression values and deduced the water content θ from the resistivity models obtained at the study site (see the scale legend of Fig. 1). The moisture of this layer may be related to the strong affinity of the carbonate sediment to absorb and retain the surface water and the rain water. Uncertainties in our determinations include effects of temperature and ground water mineralization on ρ_w and the possible departure of the effective porosity value determined in the laboratory from the in-situ porosity which decreases with increasing depth. We minimized these effects in our experiments by using water with similar resistivity in the laboratory like that of ground water. The water we used for saturating the laboratory sample originated from calcareous formations with a relative high Ca-content and accordingly a low resistivity ρ_w of 12.9Ω.m.

GPR-velocity versus water content has been determined in a similar manner in the laboratory for different soil samples (e.g., silty fine sand, middle and coarse sand, loam, calcareous sediments, clayey sand) from various experiment sites, Fig. 3. The measurements were carried out using antennas of 400 MHz, 900 MHz and 1500 MHz. We found that the Topp equation fits generally the

data sets of 400 MHz and 1500 MHz but not to the 900 MHz. Velocity values for the 900 MHz antenna are systematically higher than those for the 400 MHz and1500 MHz antennas. The same result was observed also in sand samples of different grain size where v for f = 900 MHz antenna was systematically higher than those of 500 MHz antenna (e.g., Hagrey and Müller, 2000). This velocity difference is relatively small. In this respect, previous experimental data show an inverse relationship between $\sqrt{\varepsilon_r}$ (ε_r is the dielectric constant relative to that of the vacuum of 1) and the frequency f in the range from 1-3000 MHz (e.g., Wensink, 1993). This yields a direct proportionality between v and f (ε_r inversely proportional to v). In the intermediate frequency range the dispersion effect is often neglected. For media with electric conductivity σ < 100 mS/m, v decreases with f for f > 900 MHz (e.g., Davis and Annan, 1989). A general conclusion regarding velocity dispersion as a possible explanation for the v-difference as shown here should be further investigated for a broader spectral range (f = 10-2000 MHz) with better resolution and using different velocity techniques. The v-θ relationship at different frequencies in the range 400 MHz-1500 MHz manifests the dispersive nature of the GPR velocity.

Mapping root zone

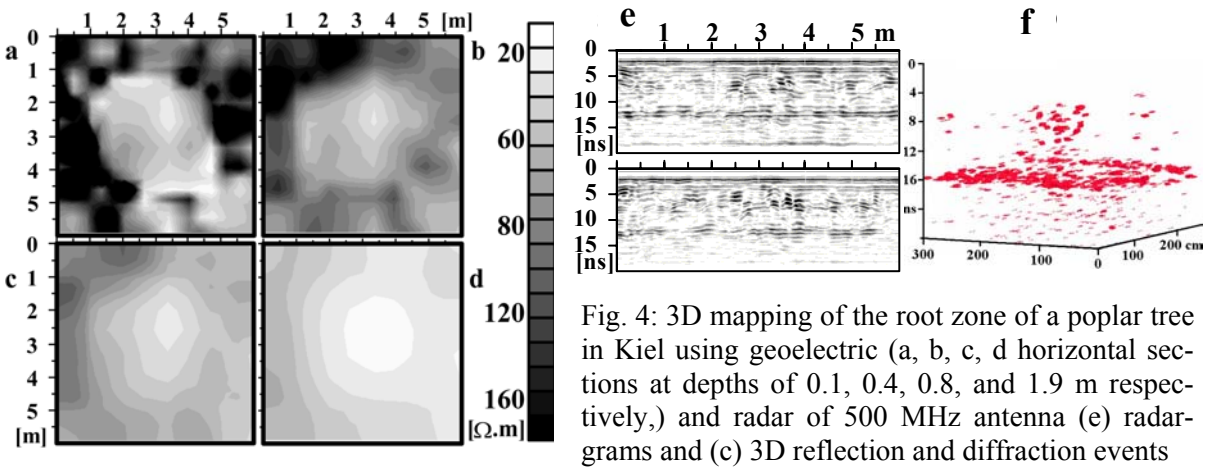

Fig. 4: 3D mapping of the root zone of a poplar tree in Kiel using geoelectric (a, b, c, d horizontal sections at depths of 0.1, 0.4, 0.8, and 1.9 m respectively,) and radar of 500 MHz antenna (e) radargrams and (c) 3D reflection and diffraction events

A root zone consists of a mixture of organic root branches bounded by the soil material. Fine roots absorb water and nutrients (sap) from the surrounding soils, guide them to wooden roots which transport them upwards to the trunk and the leaves. The (di)electric nature of a root zone is generally a consequence of relatively high moisture contents, and only woody, thick and isolated roots show a high electric resistivity. Soft, fine roots are electrically and hydraulically conductive.

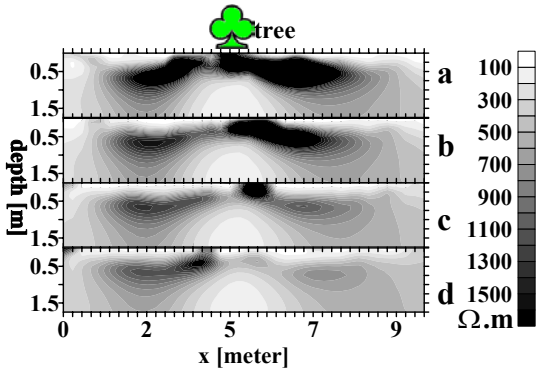

Fig. 5: 3D mapping of the root zone of an oak tree in Borken, Germany (a, b, c, d vertical sections at offsets of 0.5, 0.75, 1 and 1.25 m, respectively, away from tree).

In the botanic garden of Kiel, northern Germany a young poplar tree was studied by geoelectric and radar measurements. The soil consists of silty sand to boulder clay with some buried stones and old organic debris of dead roots and a temporary ground water table at a depth of 1.5 m. Its roots were fine and hydraulically and electrically conductive, decreasing in size away from the tree middle point with depth. The electric survey was carried out by eight collinear star-profiles, each consisting of 32 electrodes with a spacing of 0.2 m. We inverted the data into 3D using the algorithm

of Loke and Barker (1995). The resulting model (Fig. 4a-d) shows low ρ anomalies, decreasing with depth and concentrating exactly below the tree. Certainly the root zone and its water consumption and guiding process is responsible for the concentric low resistivities. A transmission radar survey also reflects the high moisture content of the root zone, giving a minimum of the radar velocity in the center (not shown here, Hanafy and Hagrey, 2002).

For the same poplar tree, the surface radar survey using a bistatic antenna of 500 MHz was also carried out at a square area of 6 m x 6 m symmetrically surrounding the poplar tree at a grid of two perpendicular profiles (of 26x26, 20cm interval). These radar results are shown by two examples of individual radargrams and a 3D reflection and diffraction events isolated by amplitude filter in the middle part of 3 m x 3 m (Fig. 4). These events can be related mainly to the single root branches; some may be caused by stones in the heterogeneous sediments.

In Borken, Germany, a resistivity study was carried out near an isolated old oak tree. 10 parallel geoelectric profiles with an electrode spacing of 25 cm were carried out and inverted into a 3D subsurface model (Fig. 5). Below the tree high resistivities are observed down to about 2 m depth. These values near the surface are caused by dry thick woody roots with some dead cork tissue. These thick roots extend radially away from the trunk axis (more than 4 m), supporting the tree stability. In the depth range 1m-2 m low values of ρ dominate directly below the tree trunk, apparently caused by the increased water content of the smaller and softer roots.

Infiltration processes, Canosa, southern Italy

The area the old olive farm near Canosa, southern Italy was studied along two 2D resistivity sections. The water content generally decreases with depth except for the second layer at 4-5 m depth which shows the lowest resistivity values (20-90 Ωm) and may reflect weathered carbonate sediments with higher water content, being probably the main source for providing the olives with water and nutrients.

The hydrological situation around a single tree (area of 9x4.5m^2) was studied by an electrode grid (at intervals of 0.3 m) around the tree and by a continuous infiltration of water intro a small area 1x1 m, only1.8 m away from the tree. TDR-probes controlled the water content within the upper 0.5 m. While in total 417 l of water was successively infiltrated within 48 hours (terminated by a heavy rain) the resistivity depth sections along the profiles were continuously mapped. As seen for one of the sections (Fig. 6a), the resistivity (resulted from 2D/3D inversion) is strongly modified by the intruding water which can be clearly followed in the difference diagram (Fig. 6b) by the semi-circles of resistivity isolines up to 48 hours. After 98 h the effect of the heavy rain decreases the resistivity strongly everywhere in the near surface zone.

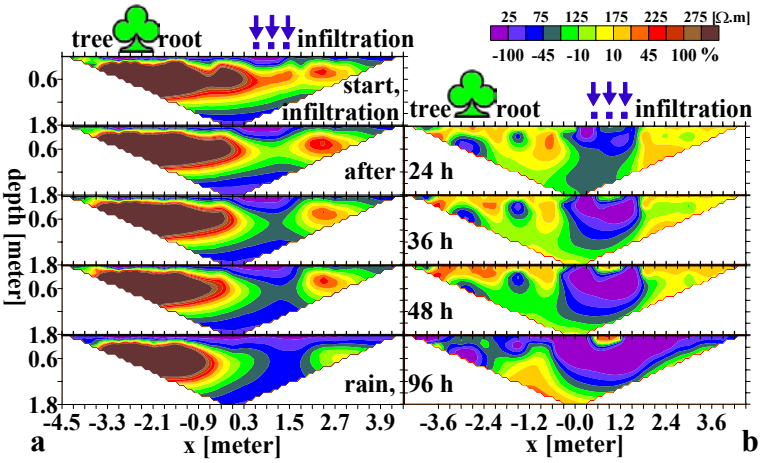

Fig. 6: 2D inverted resistivity section (a) and difference relative to the pre-infiltration model (b) along a profile which crosses the infiltration site. A strong ρ-decrease after 96 h is caused by heavy rains.

Water uptake by roots from spatiotemporal resistivity variations, Rio-Frio, Portugal

Monitoring data sets of apparent resistivity pseudosections along profiles P1 (along nearly levelled ground surface) and P2 (ground surface slopes toward profile end) were inverted using the 2D time-lapse of joint dependent resistivity inversion (Loke 1999, deGroot-Hedin & Constable 1990, Clearout & Muir 1973). The inversion model of the initial data set is used as a reference model to constrain the inversion of the later time-lapse data sets. Resulting subsurface section consists of 3-layers; the middle low resistivity (wet) layer (depth ≈ 1.5-8m, where most roots exist) is the main water fed during summer time for the cork oak trees, Fig. 7. Profile P2 (not shown here) shows that the surface porous sand layer thickens at its upslope side where more shrubs survived for a long time due to the larger pore retention water available at this side. Along both profiles electric and radar give similar results of a surface dry layer underlain by a conductive wet zone. Radargrams show fine lateral variations in the near surface reflector; an apparent deepening (travel time increase) under the upslope side of profile P2.

In Rio Frio, Portugal, an area with and without trees was studied. Monitoring data sets of apparent resistivity pseudosections were inverted using the 2D time-lapse of joint dependent resistivity inversion (Loke 1999), Fig. 7. Here, the differences in resistivity ρ, compared to the first measurement, was plotted in order to observe the water uptake by the roots. Certainly, the roots cause an increase of ρ and dryness in the uppermost 2 m of the sections within 15 days of monitoring, most probably caused by the water consumption and uptake by roots. Tree areas with water uptake by roots show higher dryness than areas without trees.

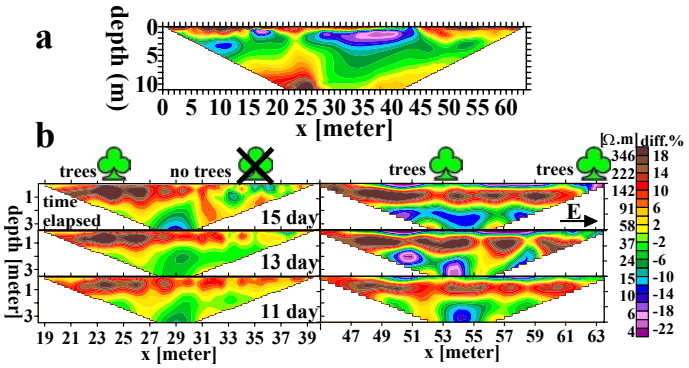

Fig. 7: 2D resistivity model of the subsurface (a) and differences of the time lapses (b) at Rio-Frio showing an increase in dryness by root water uptake in the top 2 m within 15 days of monitoring. No irrigation.

The spatiotemporal humidity variations along P1 are shown by resistivity differences of the time lapses that show an increase in resistivity and dryness in the uppermost 2m within 16 days of monitoring. Tree areas with water uptake by roots are dryer than areas without trees and water uptake.

Electrical imaging of internal structure of trunks

We use a ring array of needle multi-electrodes set at constant angular offset around the trunk circumference for minimising the destructive effect of data acquisition on trees, Fig. 8. Electrodes of gel (NaCl brine hardened by starch), fixed on trunks by air suction or stainless steel (diameter = 1 mm) are set carefully in contact with the outermost living tissues just below the dead cork. Dc resistance measurements on standing trees and trunk discs are conducted using dipole-dipole and/or Wenner configuration. The data acquisition along the ring array is carried out identical to that of the 2D-pseudosections along a

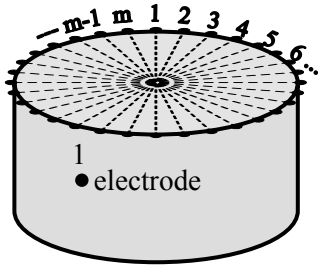

Fig. 8: Multi-electrode ring array for dc resistivity imaging of a tree trunk.

colinear multi-electrode profile. The Wenner pseudosection is collected in all possible electrode spacing and dipole-dipole pseudosections in all possible dipole-dipole offsets with constant dipole spacing.

The measured apparent resistances are inverted using 2D-iterative algorithm which incorporates the cylindrical geometry of the trunk (Geotomo Software, www.geoelectrical.com, s. also Loke and Barker 1995). The inversion is based on a finite element forward modelling subroutine to calculate the electrical response of a 2D cylindrical structure (Silvester and Ferrari 1990; Chambers et al. 2003). Details of the finite element method can be found in Coggon (1971) and Sasaki (1989).

Before starting field experiments we performed first a synthetic modelling with artificial anomalies on a cylinder. After a successful outcome we applied our ring electrodes around a freshly cut trunk (1.5 m length and 0.26 m diameter) in the laboratory and determined its internal resistivity structure ρ. In addition, we extracted samples and determined its fluid content θ in order to correlate ρ to θ (Fig. 9).

Investigating figure 9 shows that the 2D resistivity model displays a concentric ring structure with a radial resistivity decrease and a gravimetric moisture content increase from the centre toward the periphery. The resulting maximum and minimum values of 2000 and 30 Ωm correspond to the moisture values of 42 and 69 %, respectively. This inverse relationship between distributions of both parameters leads us to conclude that the resulting resistivity images can be interpreted mainly by the effect of the moisture distribution within the trunks and less by electrolytic conductivity

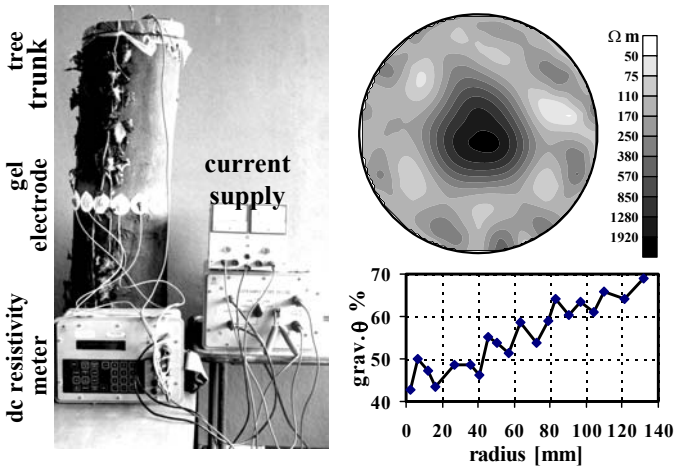

Fig. 9: Resistivity imaging of a cedar trunk (length = 1.5 m, diameter = 0.26 m) in the laboratory with the measurement set up, the 2D inversion model and gravimetric water content θ with radius carried out at core samples of wood. Results show a concentric ring structure with a radial decrease in resistivity and increase in fluid content from the centre outwards.

changes due to variations in ion moisture concentration as measured from samples along the radius of the trunk. This agrees with our electrical and hydrological monitoring survey (for two years using fixed installed arrays at fields of different fertilisation intensities), Hagrey et al. (1998). Most applied agrochemicals (including fertilisers) in agriculture, normally complex compounds, have nearly no effect on the ionic electrolytic conductivity of soil water. This result is supported by monitoring data from chemical analyses and dc conductivity measurements of soil water samples collected from boreholes at the study sites.

More than 100 year old olive trees, supplied mainly by the ground water, were studied at an olive farm in Canosa near Bari. Here we show trunks of two old and two young trees that were imaged using the ring array of 32 and 16 electrodes, respectively. One of the young trees (nearly 7 years old) grows at the roots of an old tree and the second tree (nearly 5 years old) stands alone. The resulting 2D electrical resistivity inversion distribution of all trunks shows generally a ring structure with radial decrease of resistivity from the centre towards the periphery (Fig. 10).

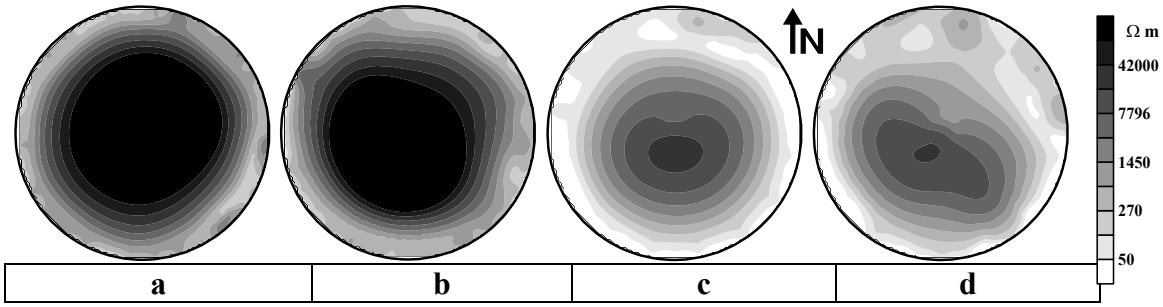

Fig. 10: Resistivity ρ of trunks from olive trees (Canosa, southern Italy), a, b, : two old trunks, ∅ = 26 and 32 cm, (~ 500 years old) with very high ρ in the interior, c, d, : two young trees, (~ 7 years old) with a smaller ρ, not exactly concentric, c: standing isolated, d: growing from the root of an old tree.

Comparing young and old olive trees shows that old olive trunks display much higher resistivity values and more complex and better developed ring structures than young olive trunks. A comparison of young olive trees and of other trees (e.g., oak, beech, peach) in southern and middle European countries shows that the old olive trees are characterized by a relatively dry heartwood (very high electrical resistivities up to 10^6 Ωm). The asymmetry of the ring structure of a young tree on old roots may be related to its position relative to the mother tree and the influence of sun and wind directions.

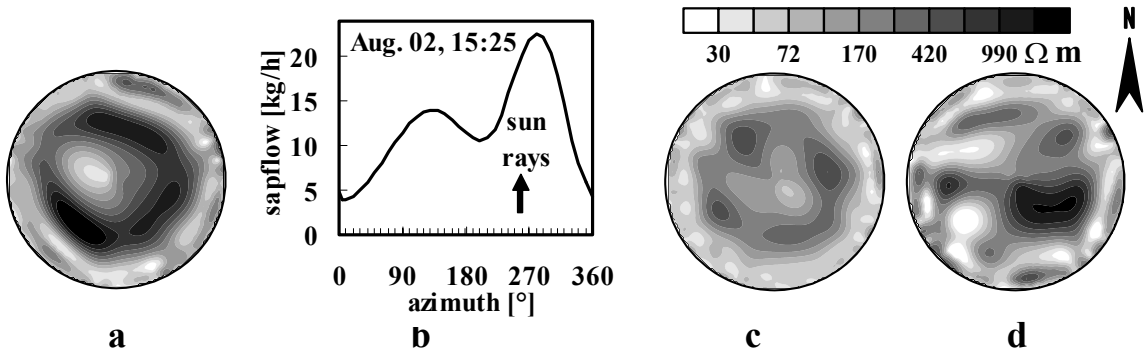

Fig. 11: 2D dc resistivity models and variation in sapflow (Nadezhdina et al., 2001) around tree trunks of a cork oak at Rio Frio, Portugal. At the trunk's circumference, the model (a, radius r=0.22 m) and sapflow (b) carried out simultaneously show a NW disturbance in the ring structure. Models of two more trees image of a normal tree (c, r=0.18 m) and an infected trunk (d, r=0.23 m) where brown outflows were observed at the SW and NW parts.

Nearly 100 year old trees with water supply from rain and ground water were studied by dc resistivity at a cork oak plantation (Montado) in Rio Frio near Lisbon. Trunk images of three different trees are shown (Fig. 10). For one of these the sapflow around the trunk's circumference were measured directly before the dc resistivity model (Fig. 10b,). The sapflow density was measured by one of our EU-partners using the heat field deformation (HFD) technique with sensors installed at different depths along xylem radius in the trunk (Nadezhdina et al. 1998, 2001). The resulting 2D resistivity models show irregularly varying internal structures between the trees, especially in the last tree trunk (Fig. 7d) which seems to be infected, where brown, smelling outflows could be observed. The sap-heartwood-interface is irregular, weakly defined with low resistivity contrast. The resistivity decreases generally from the centre outwards. The 2D resistivity model and sapflow data show disturbances in the ring structure in the WNW direction (Fig. 11a, b). The lowest flow was recorded from North, where a spot with higher resisitivity in sapwood was found. This structural

asymmetry may be attributed to different environmental factors, fracturing that could be observed from the superficial cork layer and infecting bacteria and deceases. Resistivity and sapflow results, verified by taking cores, show that: (a) the heartwood is often wet (may approach similar water content as in the sapwood in some trees), (b) it smells, indicating some infections (e.g. fungi or bacteria), associated with a release of ions and (c) this infection may be one of the reasons of the oak decline in the plantation.

The trunk of a healthy oak tree growing in a small forest near Borken, Germany, has been imaged electrically at different heights (Fig. 8). The resulting 2D resistivity models away from any branch (Fig. 12a) show everywhere a well developed, nearly symmetric ring structure with a central, nearly insulating, dry heartwood (up to $\rho > 10^6$ Ωm). The resistivity decreases outwards where it reaches 25-50 Ωm in the wet sapwood at the outermost zone of 0.02-0.05 m. The ring structure shows gradual changes for measurements directly below a branch, where the outer low resistivity zone becomes thicker at the southern side (Fig. 12).

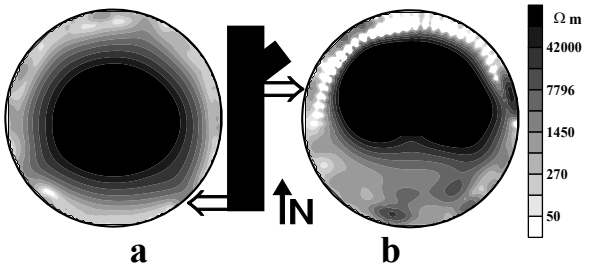

Fig. 12: . 2D resistivity trunk models, rear and near a branch (a, b, respectively), of an oak tree (radius r= 0.31 m), Borken, Germany. The resistivity decreases (moisture increases) from the centre outwards. The trunk (a) shows a well developed, nearly symmetric, ring structure that changes gradually in its southern part with the appearance of a low resistive zone directly below a new branch (b). Other wood tissues grow in this junction zone.

Another example is from eight years old peach trees, diameter 10 cm, within a large orchard in Atalaia, Portugal. After our routine measurements (Fig. 13a) along a fixed ring and longitudinal (parallel to the trunk axis) arrays we cut one of the trees and put the trunk into a container with water. We first applied blue food colour, the trunk getting blue (Fig. 13 b) but not changing its resistivity. We then applied one litre a NaCL solution (3.000 ppm) and observed the resistivity decrease, our electrodes now fixed along the trunk. We obtained resistance pseudosections (Fig. 13c), the first picture showing the situation before the NaCL-injection, the next pictures showing the strong decrease of resistivity which slowly recovers by the injection with fresh water. The experiment demonstrated the different processes due to different solutions applied and provides a first assessment for the sap flow velocities. We conclude that the resistivity imaging technique can also monitor dynamic processes of sapflow if adequate tracers are used.

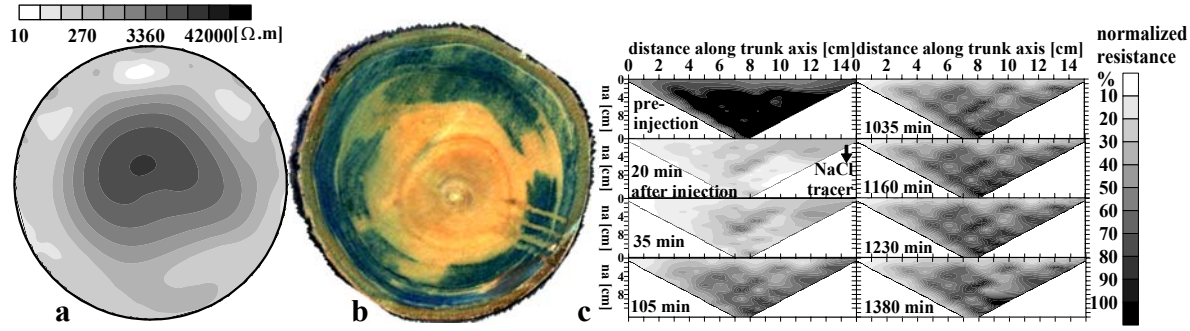

Fig. 13: Dc resistivity experiments at a peach tree trunk with infiltrating coloured water and injecting NaCl tracer that has been washed up with time. (a) 2D inversion trunk model (diameter 0.1 m) resulting from using a ring array before NaCl injection, (b) corresponding stained section, (c) resistance pseudosections resulting from the repeated dipole-dipole measurements (for dipole factor n =1 to n=13) along a longitudinal electrode array parallel to the trunk axis.

Conclusions

In soils and trees, water content, heterogeneities (including root zones) and structures (including internal ring structures of trunks) can be mapped by high-resolution geoelectric techniques. The radar techniques are successfully applied to monitor irrigation, water uptake by roots and their scattering properties. Even processes of the downward water infiltration in soils, upward sap flow in trunks and water uptake by the roots can be monitored under favourable conditions of in-situ repeated time-lapse measurements and using a suitable tracer. Such processes are verified in the laboratory and preferably in our large GeoModel, simulating infiltration and water movement. Our technique of ring electrodes around trunks records the (concentric) resistivity structure which is inversely proportional to their fluid content, the wet and conducting trails, guiding the sap flow, in the young outer layers. Observed deviations from the concentric resistivity (and fluid) content so far were caused by infections. Probably, the ring electrode technique can be used as a fast health inspection of endangered trees.

Acknowledgements
Thanks for Dr J. Michaelsen, former participant of the WATERUSE-Project and now at Water supply authority in Hamburg, Dr A. Thomsen, Danish Institute of Agricultural Sciences Tjele, Denmark, for their help. This work is carried out in the scope of the WATERUSE and GeoModel projects funded by the European Commission and the German Federal Ministry of Research.

References:

Archie, G.E., 1942. The electrical resistivity log as an aid in determining some reservoir characteristics. Transactions of the American Institute of Mining Engineers 146, 54-62.

Chambers, J. E., Loke, M. H., Ogilvy, R. D. & Meldrum, P. I., 2003. Noninvasive monitoring of DNAPL migration through a saturated porous medium using electrical impedance tomography. Journal of Contaminant Hydrology 68, 1-22.

Claerbout, J.F. & Muir, F., 1973. Robust modeling with erratic data. Geophysics, 38, 826-844.

Coggon, J.H., 1971. Electromagnetic and electrical modelling by the finite element method. Geophysics 36, 132– 155.

Davis, J.L. & Annan, A.P., 1989. Ground-penetrating radar for high-resolution mapping of soil and rock stratigraphy. Geophysical Prospecting 37, 531-551.

deGroot-Hedlin, C. & Constable S.C., 1990. Occam's inversion to generate smooth, two dimensional models from magnetotelluric data. Geophysics 55, 1613-1624.

Hanafy, Sh. and Hagrey S.A. al, 2002. GPR tomography for mapping soil moisture and roots. 8th EEGS Meeing, European Section, Aveiro, Expanded Abstracts, 45-48.

Hagrey, S. A. and Müller, C., 2000a. GPR study of pore water content and salinity in sand. Geophyscal Prospecting 48, 63-86.

Hagrey, S. A. al, Nies, M., Frank, A., Heinke, B. & Hartwigsen, H., 1998, Untersuchung zeitlicher Variationen der Bodenfeuchte mit geoelektrischen und bodenhydrologischen Methoden in Hohenschulen (Norddeutschland)- Erste Ergebnisse, *VII Arbeitsseminar „Hochauflösende Geoelektrik“*, Univ. Leipzig, 5p.

Loke, M. H. and Barker, R. D., 1995. Least-squares deconvolution of apparent resistivity pseudosection. Geophysics, 60, 1682-1690.

Loke, M.H., 1999. Time lapse resistivity imaging inversion. Proceedings of the 5th Mtg. of the EEGS Eur. Sec., Budapest, 6-9/9/1999, 4p.

Nadezhdina, N., J. Cermak and V. Nadezhdin. 1998. Heat field deformation method for sap flow measurements. In Proc. 4th International Workshop on Measuring Sap Flow in Intact Plants, Zidlochovice,Czech Republic, Oct.3-5, 72-92.

Silvester, P.P. and Ferrari, R.L., 1990. Finite Elements for Electrical Engineers. Cambridge University Press, Cambridge, 344 p.

Sasaki, Y., 1989. Two-dimensional joint inversion of magnetotelluric and dipole– dipole resistivity data. Geophysics 54, 254–262.

Schön J.H., 1997. Physical Properties of Rocks: Fundamentals and Principles of Petrophysics, Handbook of Geophysical Exploration. Elsevier Science Ltd, Amsterdam.

Silvester, P.P. and Ferrari, R.L., 1990. Finite Elements for Electrical Engineers. Cambridge University Press, Cambridge, 344 p.

Topp, G.C., Davis and J.L.,Annan, A.P., 1980. Electromagnetoc determination of soil water Content. Measurements in coaxial transmission lines. Water Resources Research 16, 574-582.

Wensink, W.A., 1993, Dielectric properties of wet soils in the frequency range 1-3000 MHz. *Geophysical Prospecting* 41, 671-696.

SOUND TOMOGRAPHY FOR STEM INVESTIGATIONS PROVIDING STRUCTURAL INFORMATION FOR STEM WATER/SAP FLOW MEASUREMENTS AND ANALYSIS

Susanne Lorra, Andreas F. Kathage[1]

[1] *GeoHiRes International Ltd., Borken, Germany*

ABSTRACT

During the European Union funded project WATERUSE different elastic waves methods were investigated in order to find a way for non-destructive investigation of the stem structures. It has been the aim in this project to provide structural information of the stems for the sap flow measuring and sap flow modelling scientists.
Ultrasonic measurements did not fulfil the requirements, neither in propagation nor in reflection experiments.
A tomographic approach using a hammer as energy source for sound waves and 12 accelerometers as receivers turned out to be a suitable method for the non-destructive measurement of the stem structure. Using this method it was possible to image the structural defects in the living wood like cavities, rot or other significant changes of the elastic properties of the stems. As soon as this method became available it was used to guide the selection of sample trees for the sap flow measurement teams. This procedure assured that no sap flow sensors were placed on trees or positions on stems where abnormal structures would have caused non-representative modelling results.

The non-destructive determination of the relevant wood structure leads to a considerably better modelling and prediction of the sap flow in the soil – plant continuum. The non-destructive methods offer a much better cost-/performance ratio than invasive methods do.
The understanding of the tree architecture and the corresponding transport mechanism is of great importance for future agriculture and forest planning. Furthermore the non-destructive detection of structural stem defects will be a significant help for the identification of risks for human beings due to potentially dropping trees.

Keywords: Sonic Tomography, Stem Structure, Elastic Properties, Sap Flow

1. INTRODUCTION

The objectives in the EU funded project WATERUSE were the development and test of novel integrated techniques appropriate to describe and quantify water flow through the continuum soil-plant-atmosphere (SPA) suitable for use in heterogeneous stands. The sound tomography method has been identified to be a suitable non-destructive method for the investigation of the stem structure of living trees.

2. MATERIALS AND METHODS

Different tasks had to be carried out in order to find a suitable method for the non-destructive investigation of living tree stems. X-rays were not considered for safety and economical reasons. Methods like GPR and ultrasonic measurements were tested intensively but finally discarded. Only the sonic or sound tomography could be identified as suitable approach for that task.
The applied sound or sonic tomography method uses a device consisting of mainly four components. A small hammer used as energy source, 12 accelerometers as receivers for the elastic sound waves, a control unit taking care of signal processing and a computer for the calculation of the tomograms as well as the data storage.

Figure 1 – The sound tomography method. Receivers and pre-amplifiers are attached to the bark. The case contains the control unit. Data storage, tomogram calculation and visualisation is carried out by a hand held PC.

The sound waves generated with the hammer propagate the wood and arrive at the receivers. The device measures the one-way traveltime of the elastic waves and calculates based on the geometrical data of the stem the corresponding velocities. Low velocities indicate cavities, rot or soft wood, while high velocities correspond with hard wood. Sapwood shows lower velocities than the heartwood (see figure 2).
During the time of this project the software as well as the sensors and the trigger mechanism were improved so that finally a reliably working measurement device became available.

3. RESULTS AND DISCUSSION

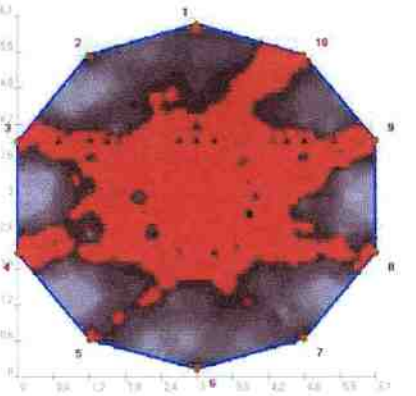

Figure 2 – Tomogram of a beech stem. The red coloured area corresponds with higher velocities than the grey area. The red zones which are extending from the centre to the positions of some sensors on the bark are artefacts, which are caused by the differences in the coverage of calculated wave travel paths.

Figure 3 – Fungus on a beech. The device was attached in order to test if the fungus could be detected.

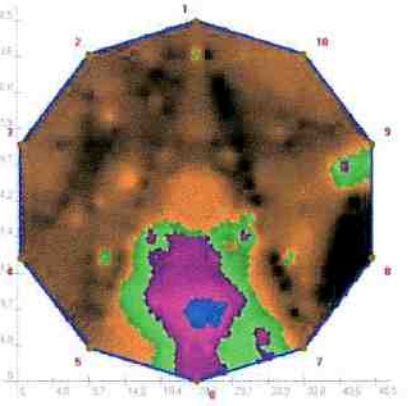

Figure 4 – Locally low velocities indicated by blue, pink and green colour are caused by the presence of fungus in the beech stem.

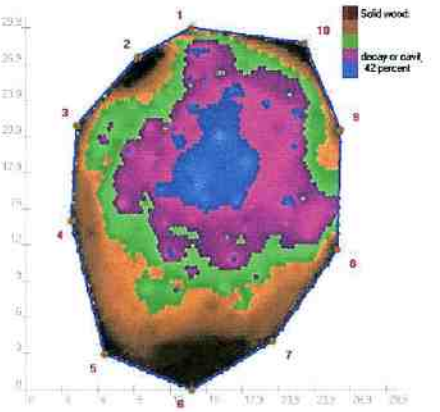

Figure 5 -Tomogram of an Olive stem, measured near Canosa di Puglia. Blue, pink and green regions indicate cavity, rot and soft wood.

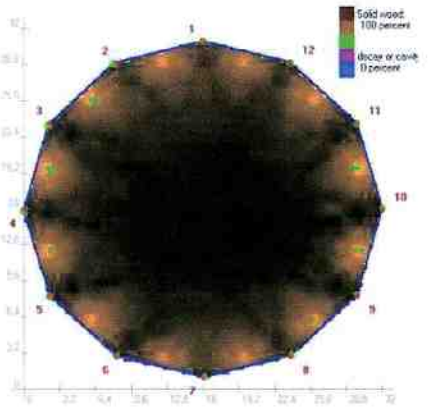

Figure6 – Tomogram of a healthy oak stem at Rio Frio. No low velocities indicate rot or cavities. The small areas of low velocities close to the bark (green dots) are an artefact and caused by the low coverage of travel path rays between the sensors.

The final proof of usefulness was carried out in the cork oak stand at Rio Frio, Portugal. Here the tomograph was used for preselecting sample trees of healthy stem structure. This work was needed to avoid the selection of unsuitable trees for the following long term sap flow measurements. The application of the sound tomographic method saved time and money for the partner team from Brno.

4. CONCLUSIONS

It could be proven during common field experiments that the employed sound tomographic method provides information, which is useful and supporting the teams working on sap flow measurements and models. The developed method is practically and reliably working in the field, which could be shown on the different test site locations.

5. ACKNOWLEDGEMENTS

The demonstrated results have been funded by the European Union under the project "Evaluation of alternative techniques for determination of water budget components in water-limited, heterogeneous land-use systems - WATERUSE (EVK2-CT2000-00079)"

18

USE OF GROUND, AIRBORNE AND SATELLITE REMOTE SENSING FOR ESTIMATING EVAPORATION

Nicole ARCHER and Hamlyn JONES

Plant Research Group, University of Dundee at SCRI, Invergowrie,

Dundee DD2 5DA, Scotland, UK

narche@scri.sari.ac.uk

h.g.jones@dundee.ac.uk

---

1. INTRODUCTION

Remote sensing of canopy temperatures provides probably the most important tool for the remote estimation of evapo-transpiration (E) rates. As shown in a review by Jones *et al*. (2004), there are many algorithms using different variables to estimate E. The choice of algorithm using remotely sensed data to estimate E depends mainly on three factors: 1) The frequency (hourly, daily or less frequent intervals) and scale (leaf, canopy or a whole region) of observations; 2) The type of canopy (homogeneous as for many crops, or heterogeneous; 3) The available variables to input to the energy balance, especially the ground-based meteorological data.

In our study we use surface temperature and image classification techniques (based on hypoerspectral imagery) to identify the different surface components (e.g. different types of vegetation, soil and water) as the main inputs for estimation of E. We therefore must ensure that surface estimates derived from thermal wavelengthes are precise, the classification method is effective in identifiying the surface components of interest and that our methods of extraction of temperature from different surface components are correct.

Following from the theoretical approaches presented by Professor Hamlyn Jones, this presentation will describe the procedure for estimating and extracting surface temperature of different types of surfaces at different scales and using different algorithms to estimate E.

2. MATERIALS AND METHODS

The test site was located on the Mitra Farm of the University of Évora, in the Alentejo Region of Portugal. Measurements were centred on a 25 m meteorological tower erected in an area of low density evergreen oak woodland/pasture consisting primarily of *Quercus rotundifolia* Lam. with some *Quercus suber* L. and an under-storey of mixed grasses and small shrubs including *Cistus* and *Lavendula* spp.. The average tree density for the scene studied was between 35 and 45 trees per hectare with an average cover of 25 %. The area has a typical Mediterranean climate, i.e. hot dry summers and a cool wet winter. Mean annual air temperature has been estimated at 15°C, ranging from 8.6 C in January to 23.1 °C in August (David, et al., 2004). Mean rainfall has been estimated over 1951-1980 to be 665 mm per year and open water evaporation is 1760 mm (INMG, 1991).

Ground measurements were made between 28th June 2001 and 7th July 2001, with overflights of DAIS and ROSIS hyperspectral scanners on 29th June 2001 between 11:17 to

11:56 UTC. Imagery from NOAA-AVHRR 16 and Landsat 5 were acquired on 29th June 2001 13:41 UTC and 28th June 2001 10:48 respectively.

Ground measurements included standard meterorological data from instruments located on the tower (net radiation, solar radiation (Kipp & Zonen CM6b solarimeter), air temperature, atmospheric humidity, wind speed) together with measurements at 2 m (solar radiation, net radiation, air temperature and humidity, windspeed logged at five minute averages). Water temperature was obtained for one reference lake using a fine-wire thermistor floating within 2 cm of the surface. Thermal images were obtained on the ground or from the tower using an Infrared Solutions SnapShot 225 camera (Infrared Solutions, Inc, Plymouth, USA). This camera consists of an uncooled long-wave (8 – 14 μm) Honeywell thermoelectric array detector with 120 × 120 pixels and has 16 bit resolution giving temperatures to better than 0.1 °C. The normalised vegetation index (NDVI) was estimated from the red and near infra-red channels of an Agricultural Digital Camera (Dycam, Woodland Hills, California). Stomatal conductances were measured using either a LiCor 1600 steady-state porometer (Li-Cor Inc., Lincoln, Nebraska) or a ΔT-Devices AP4 automatic porometer (ΔT-Devices, Burwell, Cambs, UK).

The DAIS instrument provided hyperspectral images including thermal data at a resolution of 3.3 m for each pixel, while the ROSIS instrument gave higher resolution (1.2 m) of the visible and near infra-red wavelengths. Reservoirs, bare soil and road areas were included in each image for calibration purposes. All images were atmospherically corrected using the ATCOR4 model. The terrain around the site of interest was relatively flat so no DEM correction was employed. Further analysis was in ENVI (Research Systems Inc., USA) software.

Several different ways of classification in ENVI was checked for accuracy by comparing manually classified pixels, with automated classified pixels. The best classifiers were estimated to be either spectral angle mapping or minimum distance. The ROSIS hyperspectral data at 1.2 m (which included wavelengths between 486 and 874 nm), was used to classify the field area, as this was the highest available resolution for the area. Estimation of the characteristic patch sizes of different classes of land cover was achieved by analysing the frequency distributions of the number of contiguous pixels of each cover type. This determined the size of vegetated component areas within a scene. Images taken by the hand-held camera were also analysed to verify the heterogeneity of surface components within small areas.

Eight different methods were compared for determining the temperatures of the five main component surfaces: tree, shrub, grass, soil and water. The first four use temperature data at the observed resolution, while the remaining four attempt to derive information for smaller areas than the observed individual temperature pixels.

An alternative approach to the estimation of tree and grass temperatures made use of the two or three angles of view possible with the three DAIS flights. The temperatures observed for each flight were corrected for the temporal drift in air temperature recorded at the tower. For the solar zenith angle of 21^o, we have image areas around the meteorological tower at three view angles ($+21^o$, -21^o and 0^o). The total area of common image was ascribed to trees, visible shade and the remaining visible sunlit ground (mostly grass) using the formulae given by Irons *et al*. (1992) which are based on the assumption that the canopy can be represented by a series of spheres resting on the ground. From the mean temperature observed for an area at each of these angles, together with the nadir tree fraction (estimated using the image classification) we estimated the tree temperature and the ground temperature

for the area. These temperatures were used to estimate E using various algorithms. The theory of these algorithms will be explained by Hamlyn Jones in his theoretical presentation.

3. RESULTS

Figure 1 shows the frequency distribution of the linear dimensions of homogeneous vegetation patches averaging results for both the east-west and north-south directions. Bare soil areas tended to have the smallest characteristic size (modal dimension = 2.4 m) followed by trees, shrubs and grass (all with modal dimensions = 8.4 m). Water had a bimodal frequency (modal dimensions were at 10.8 m and 37.2 m), which showed the linear dimensions of two small lakes. Bare soil occurred mainly as tracks in the field site. Both shrubs and grass had additional smaller peaks at 2.4 m which represented patches between trees. Grass areas had the greatest variability of patch size. For all classes the modal size was greater than the pixel size, suggesting that the ROSIS imagery available is of an appropriate scale for this scene.

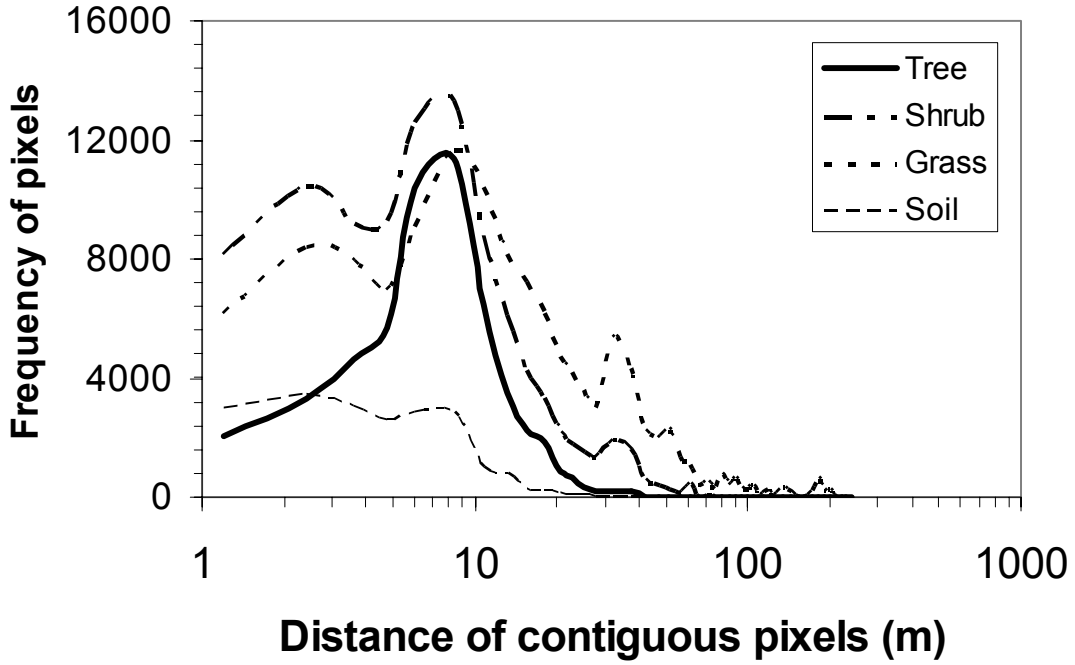

Figure 1 - Frequency of contiguous pixels of ROSIS 1.2 m SAM classification of the main cover types. The highest frequency for tree, shrub and grass occurs at 8.4 m, for soil it is 2.4 m.

For small homogeneous areas viewed from the tower (mostly less than 1 m^2), the mean hand-held temperature estimates were 34.4°C (±0.36) for shaded areas, 49.9 °C (±4.04) for grass and 56.7 °C (±3.46) for soil. The temperature range measured at the airborne level was smaller than at ground level. Within a 3.3 m area on the ground, areas around the tower which were considered to be soil or grass at the DAIS level contained small shrubs, grass, shade and soil, thus lowering the temperature as compared with pure areas. These areas had particularly high temperature ranges ranging from 57.3 °C (pure soil area) to 32.2 °C (shrubs in shade). The average temperatures estimated by DAIS for larger areas which relate to the

hand-held camera images are 33.9 °C (± 0.51) for tree areas, 42.4 °C (±2.68), for shrub areas, 46.8 °C (±1.26) for grass areas and 47.1 °C (±1.48) for soil areas.

Figure 2 a) shows an example of a classified ROSIS image using the spectral angle mapper classifier. As trees, shrubs and grass areas are generally bigger than 1.2 m, these areas were precisely classified using the spectral angle mapper classifier. Figure 4 b) shows the corresponding temperatures derived from the DAIS thermal bands indicating a particularly hot area in the south west corner which was found to be a grazed area.

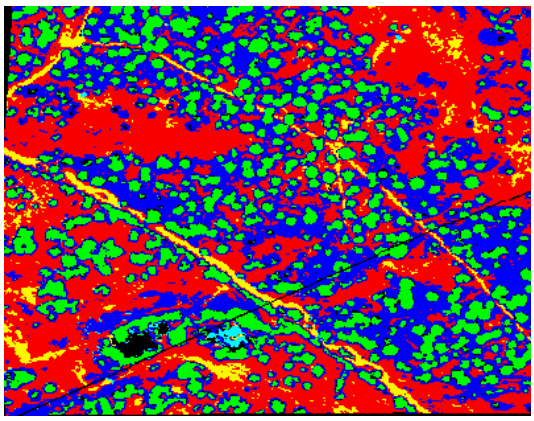

a)

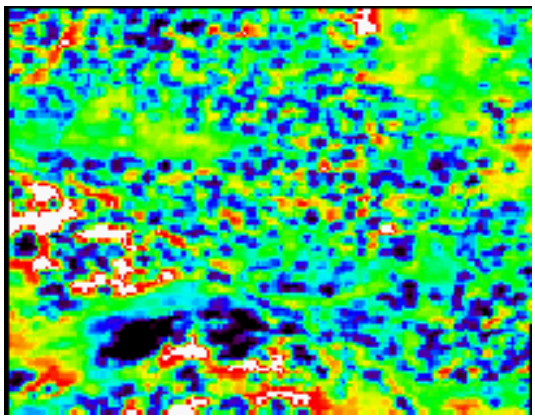

b)

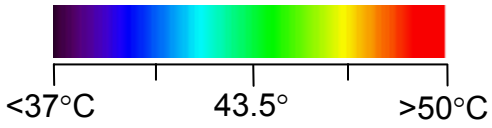

Figure 2 - Use of SAM classifications to extract component temperatures. a) shows the SAM classification of ROSIS (1.2m). For the classifications: Light grey is trees, Black is shrubs, Mid grey is grass, white is soil, Dark black is water. b) shows the temperatures derived from DAIS thermal bands at 3.3 m.

Table 1 shows some examples of estimates of E using different algorithms. The temperatures given in Table 1 were extracted from DAIS 3.3 m pixels representing lakes, well watered trees growing at the margin of the lakes/ponds, trees growing away from water, shrub areas and grassland areas.

	Calibration areas		Test surfaces			
	Lake	Soil	Trees by lake	Trees by tower	Grass	Shrub
Temperature (°C)	30.5	46.1	32.0	37.0	43.4	40.8
Evaporation estimates (W m^{-2})						
1) ATCOR estimate of λE (Richter, 2001)	720	390	721	707	492	541
2) g_{aH} from wet and dry surfaces (Jones, 1992)			691	653	219	326
3) Corrected for Rn (Jones and Archer, 2003)			752	708	221	349
4) CWSI (Inoue *et al*. 1994)			706	378	55	151

Table 1 - Evapotranspiration estimates (λE, W m^{-2}) for different vegetation at the Mitra site. Air temperature and air humidity at 10 m at the time of flights was 30.2 C and 1542 Pa, respectively. g_{aH} is boundary layer conductance, Rn is net radiation, CWSI is crop water stress index. The four different algorithms are: 1) The ATCOR model, 2) Uses boundary layer conductance and wet and dry references, 3) corrects Rn by removing soil heat flux from Rn and 4) uses a vegetation index to estimate absorbed radiation and CWSI.

Overall there was good agreement between the rates of evapotranspiration estimated by the different methods, except for ATCOR, which appeared to significantly overestimate E from the grass/shrub areas, while the CWSI method underestimates E.

4. DISCUSSION AND CONCLUSION

Differences between estimates of component temperatures using ground and airborne sensors are related to differences in the measurement scale. As the pixel area decreases the chance of detecting pure extreme pixels (soil or water, sun or shade) increases, significantly affecting the derived temperature distributions of different surfaces. The use of a hand-held thermal IR camera allows one to obtain temperature information at much higher resolution than does the airborne imagery, and shows the real range of extreme temperatures within a 3.3 m pixel.

The estimation of the surface component scales using SAM classification at 1.2 m resolution gave an indication of whether the pixel sizes used when extracting temperatures were sufficient to classify most surface components adequately, given the fact that there will

always be some mixed pixels. As the 3.3 m pixels are larger than the dominant scale for soil, it is clear that they are too large to separate soil and grass correctly. This caused underestimation of soil temperatures when soil was classified at 3.3 m resolution. The choice of method for extracting temperature depends on whether a surface temperature distribution of each surface component is required or simply the average of an area.

The use of a simple shadow model assuming that the tree canopies could be represented by spheres, combined with temperature estimates from contrasting view angles gave a valuable approach to the automated estimation of the temperatures of specific scene components such as trees and grass/soil areas. The use of reference dry and/or wet pixels for estimation of boundary layer conductance and for estimation of potential evaporation rates appeared to give reasonable estimates of evaporation from the various surfaces, and certainly for the mixed grass-shrub areas seemed likely to be much more reliable than the values derived from ATCOR. The temperature of the dry reference surfaces is a critical requirement for effective use of the algorithms presented above, and it may be that the pixels chosen for this were unrepresentative of either the radiative or aerodynamic properties of the transpiring pixels. The ATCOR algorithms, however, did attempt to estimate the differences in radiative properties of the different surfaces. A further key assumption is that the apparent thermal time constant should be similar for all surfaces (as temperatures were changing significantly over the period of measurements and just prior to them); unfortunately the soil and lake surfaces have different temperature dynamics than do the various types of vegetation. These differences remain to be quantified for the particular area used for this study.

The presentation will also discuss how this procedure for estimating E can be scaled to satellite images and how these values relate to estimated ground values of E.

REFERENCES

Archer, N. A. L., Jones H. G. (Submitted Feb. 2004). Integrating hyperspectral imagery at different scales to estimate component surface temperatures. submitted for Special Issue in *International Journal of remote sensing*.

Irons, J. R., Campbell, G. S., Norman, J. M., Graham, D. W., and Kovalick, W. 1992: Prediction and measurement of soil bidirectional reflectance. *IEEE Trans. Geosci. and Remote Sens*. 30, pp. 249-260.

Inoue, Y., Moran, M. S., Pinter Jr., P. J. 1994. Remote sensing of potential and actual daily transpiration of plant canopies based on spectral reflectance and infrared thermal measurements – Concept with preliminary test. Journal of Agricultural Meteorology. 49 (4), 237-246.

Jones, H. G. & Archer, N. A. L. 2003. Airborne imaging spectrometry (DAIS/ROSIS) for estimation of evaporation from heterogeneous *Montado* vegetation in Portugal. In: *Proceedings of the 3rd European Association of Remote Sensing Laboratories Workshop on Imaging Spectroscopy.* 13 – 16th May 2003. Oberpfaffenhofen, Germany.

Jones, H.G., 1992. Plants and microclimate. Cambridge University Press, Cambridge.

Richter R., 2001: Value adding products derived from the ATCOR models. Paper DLR-1B 564-01/01, DLR, Oberpfaffenhofen, Germany.